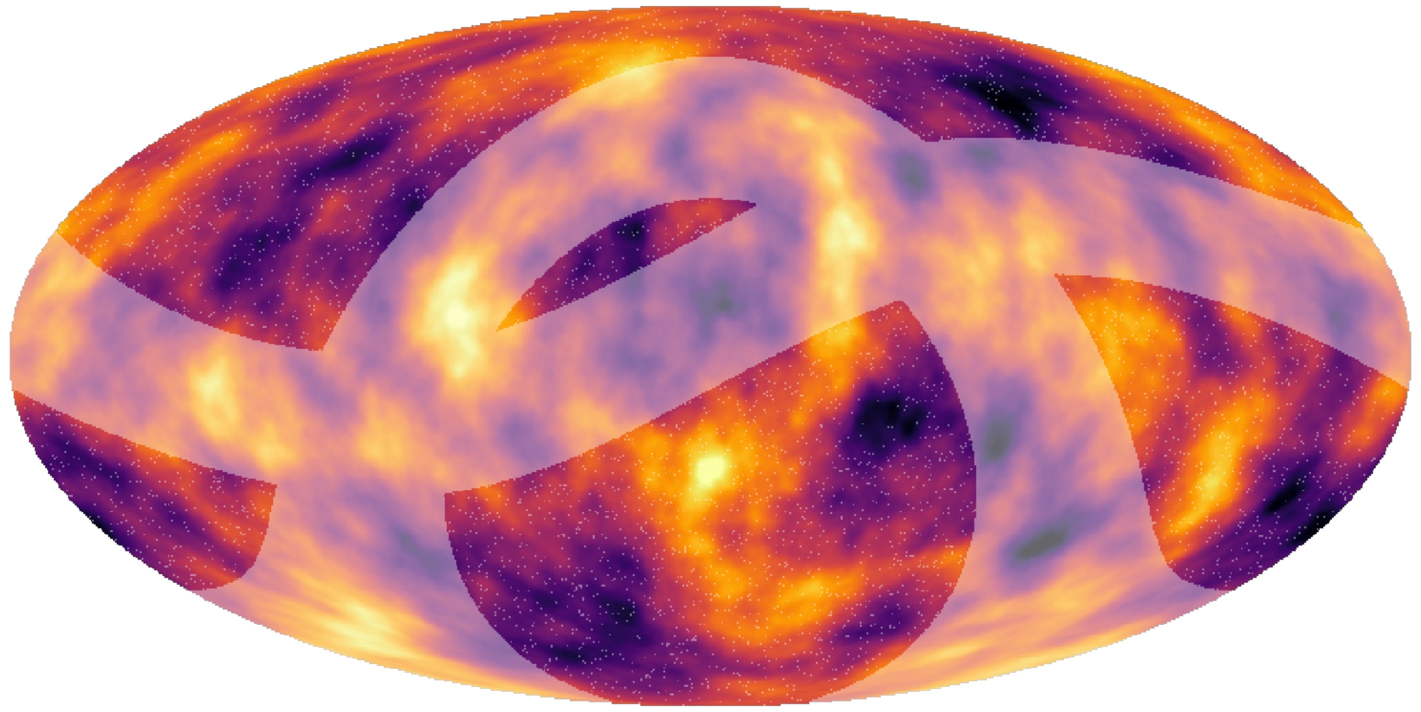

Almanac

Generic Field Level Inference for Full-Sky Cosmological Fields and Angular Power Spectra

Dr. Arthur Loureiro @ German Centre for Cosmological Lensing
(Oskar Klein Centre, Stockholm University & Imperial College London)

The Almanac Team

Dr Arthur Loureiro

Prof. Alan Heavens

Dr. Elena Sellentin

Dr. Lorne Whiteway

Prof. Andrew Jaffe

+ Javier S. Lafaurie

1. Observational Cosmology

Where are we, and where are we going?

The Era of Stage III Cosmological Surveys is almost over

Stage III Surveys

“It’s ΛCDM whether you like it or not…”

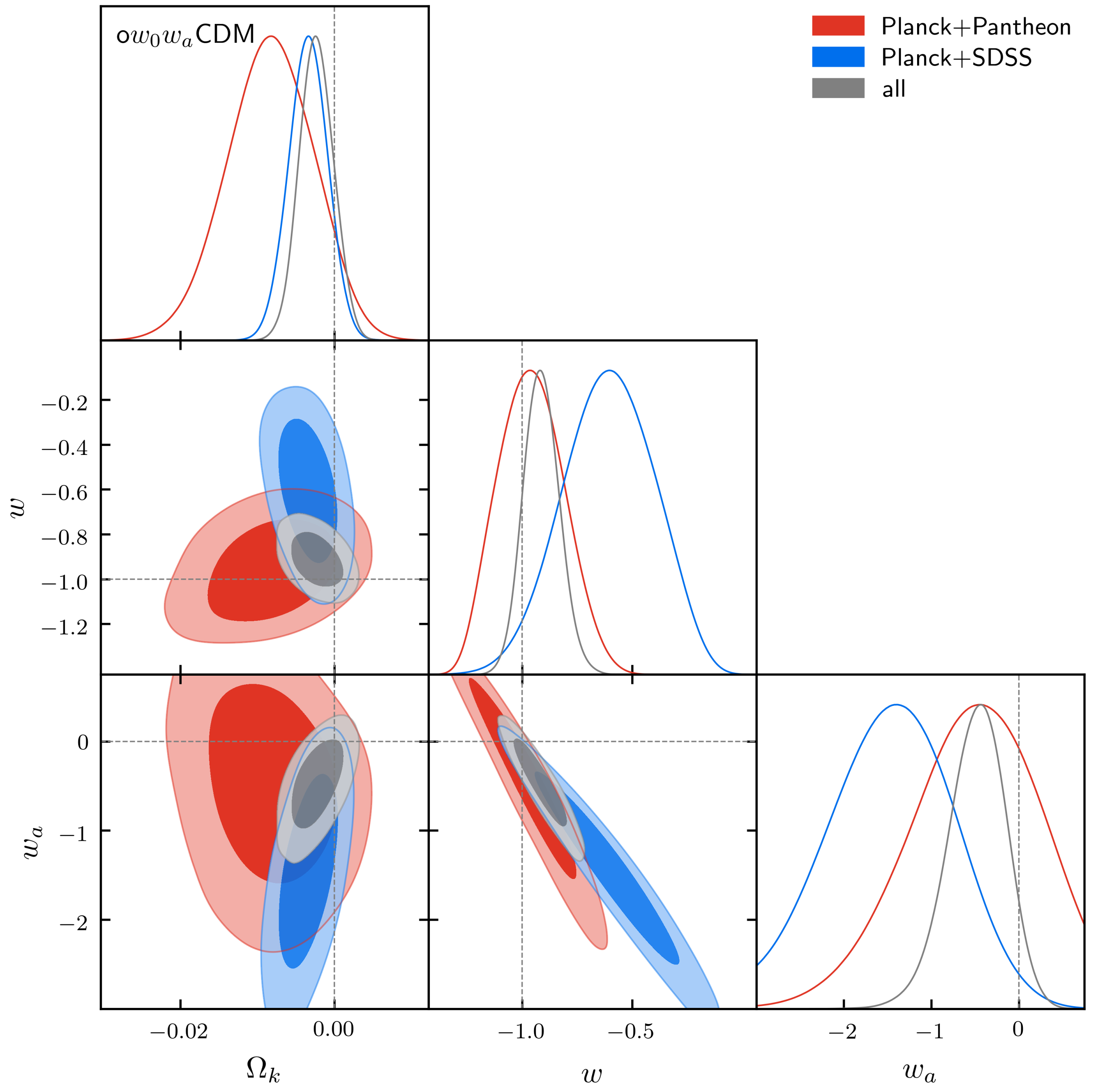

eBOSS Collaboration
(Alam et al. 2021)

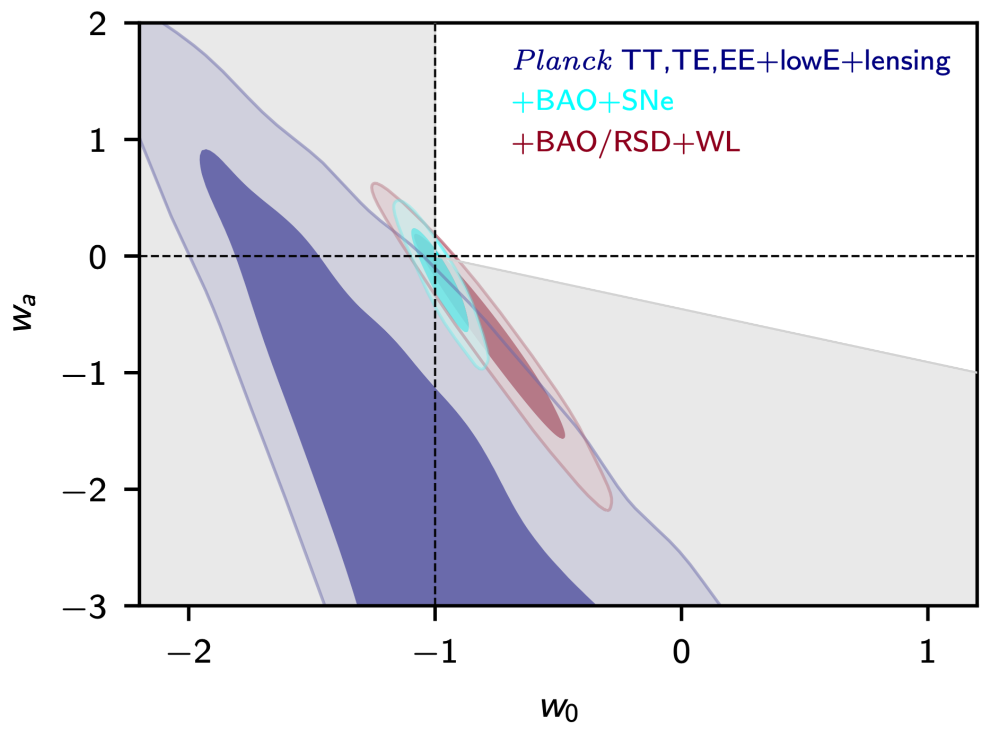

Planck Collaboration, 2018

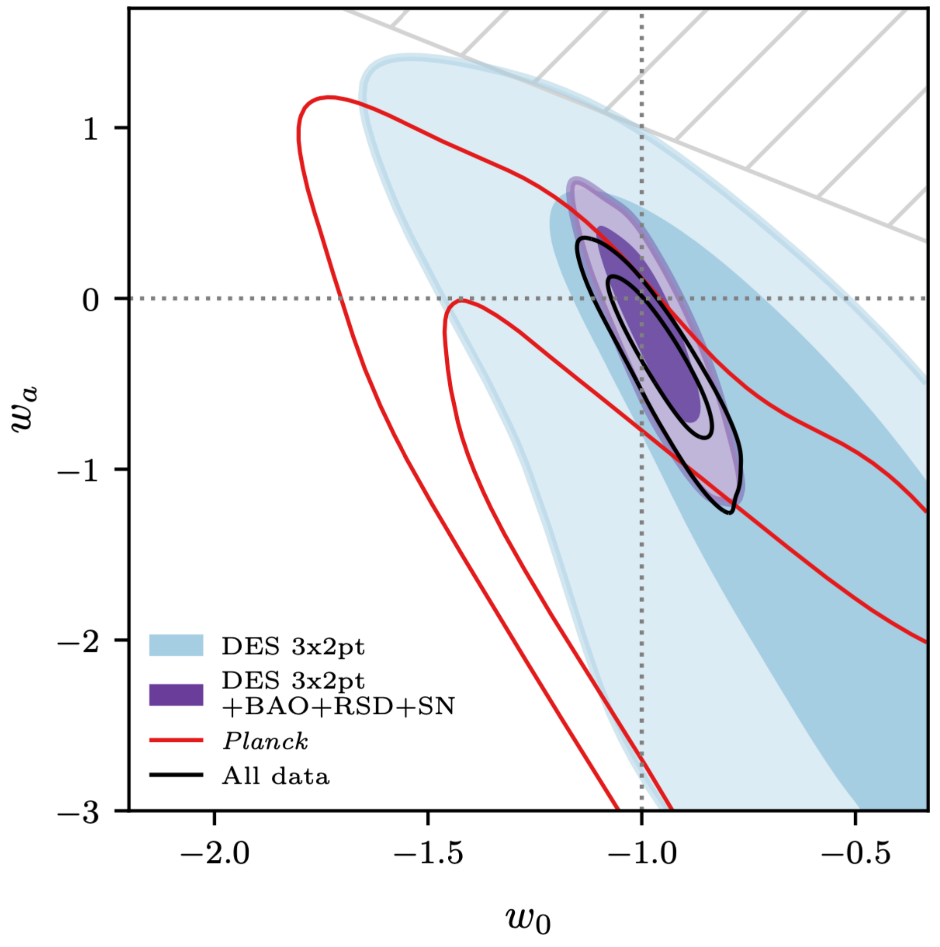

Dark Energy Survey, 2022

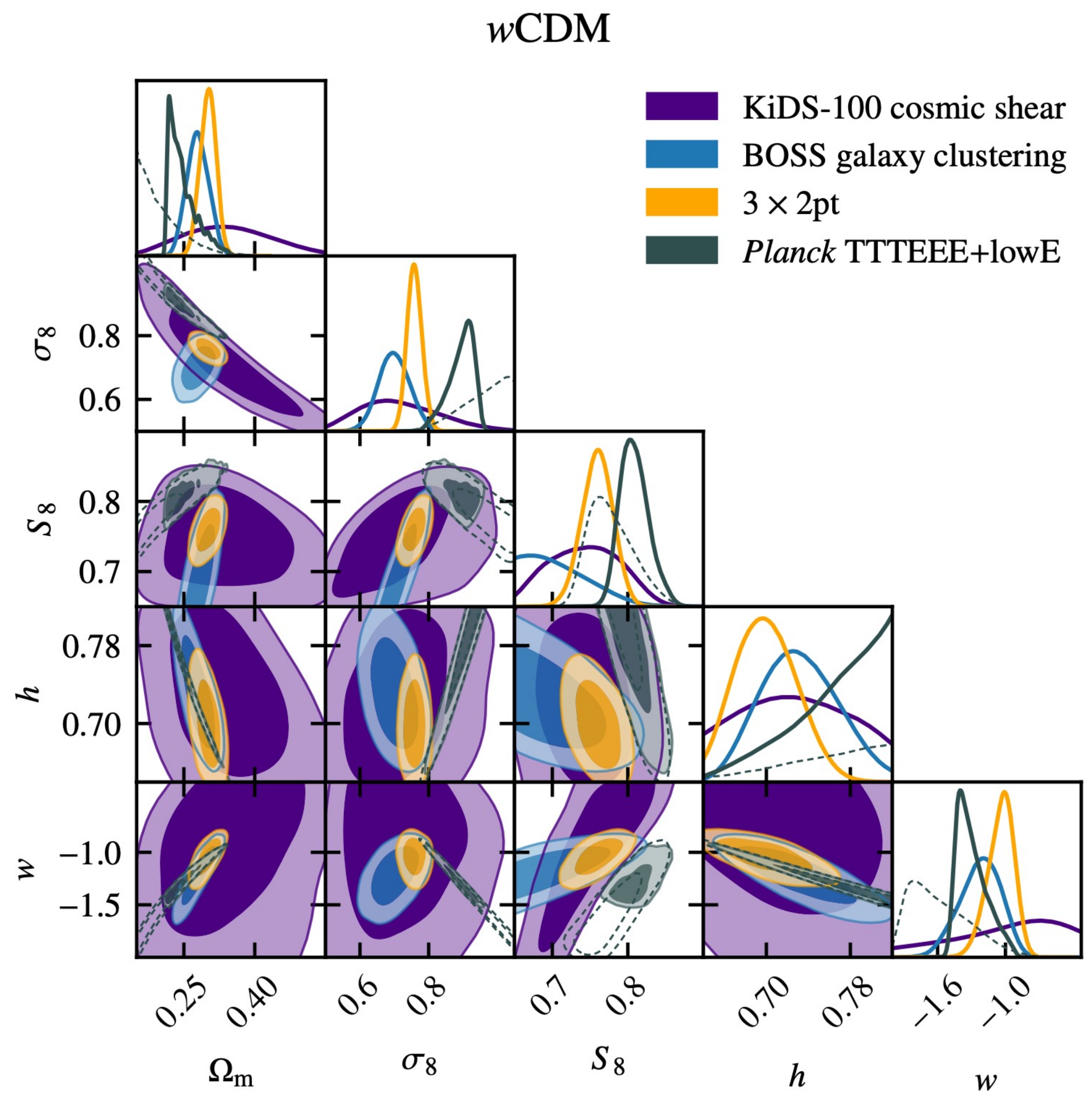

KiDS Collaboration
(Tröster et al., 2020)

Stage III Surveys

“It’s ΛCDM whether you like it or not…”

OR NOT

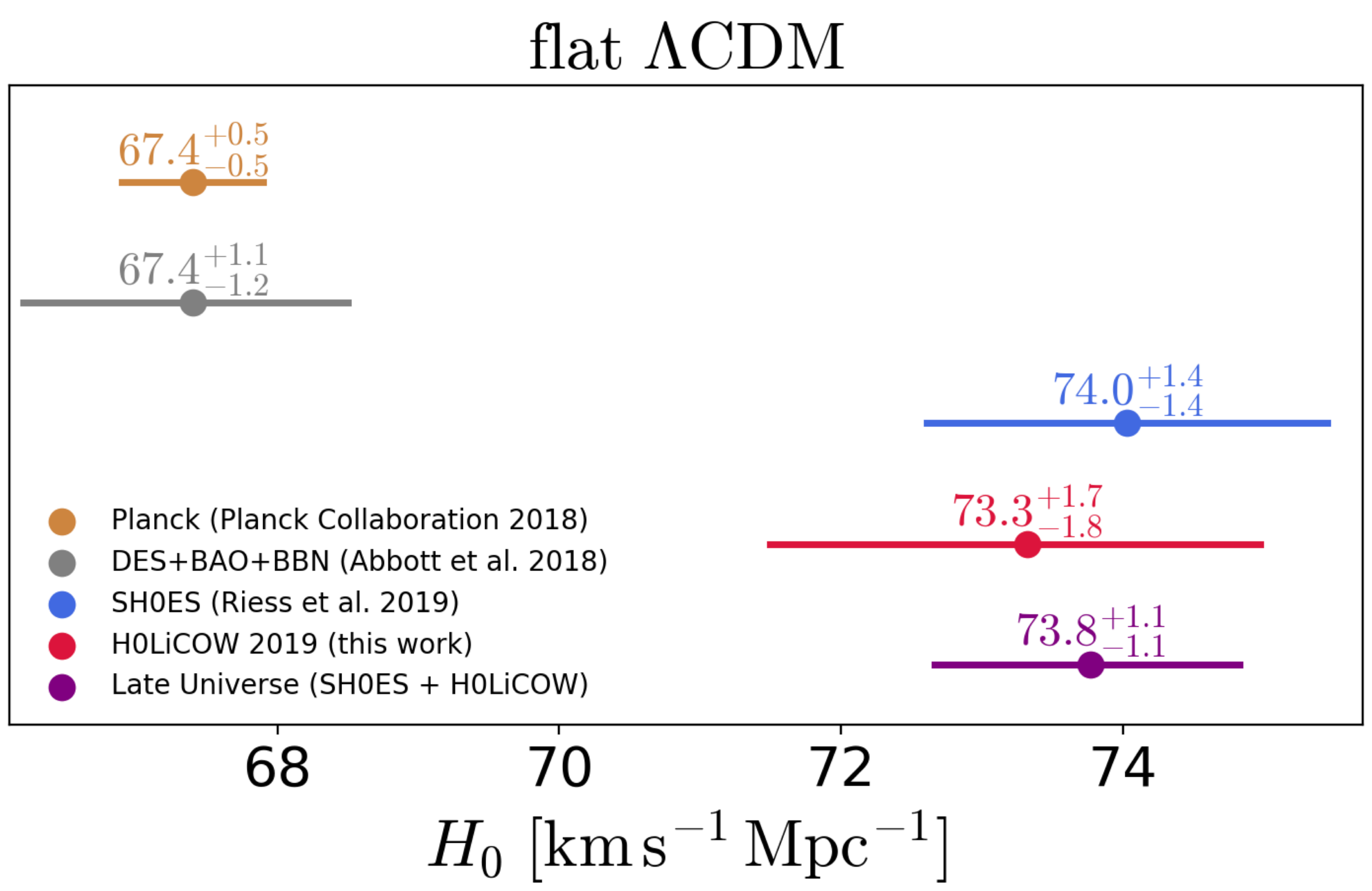

Wong et al. 2019

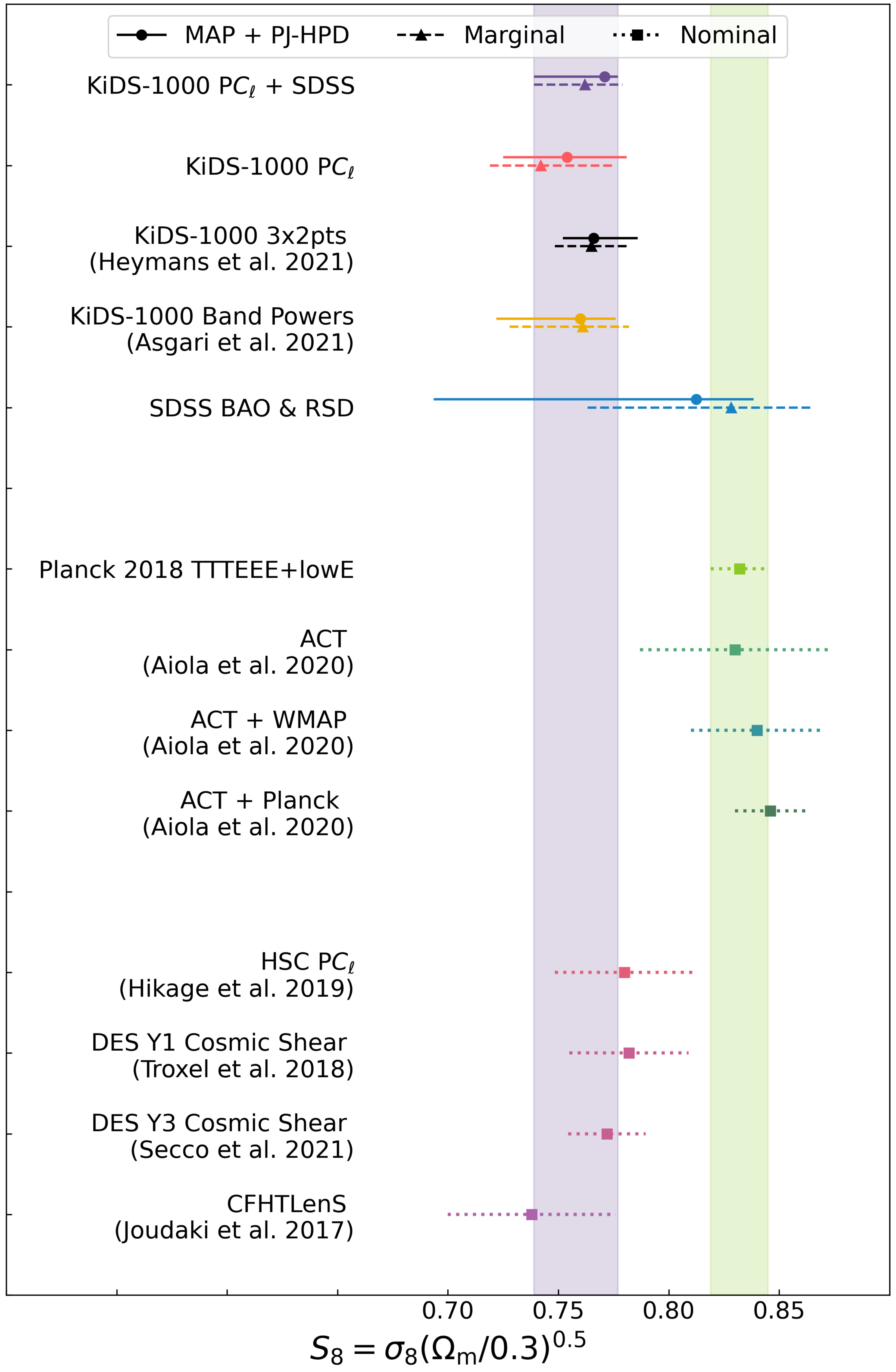

Loureiro et al., *A&A* (2022)

Stage III Surveys

"It's ΛCDM whether you like it or not…"

OR NOT

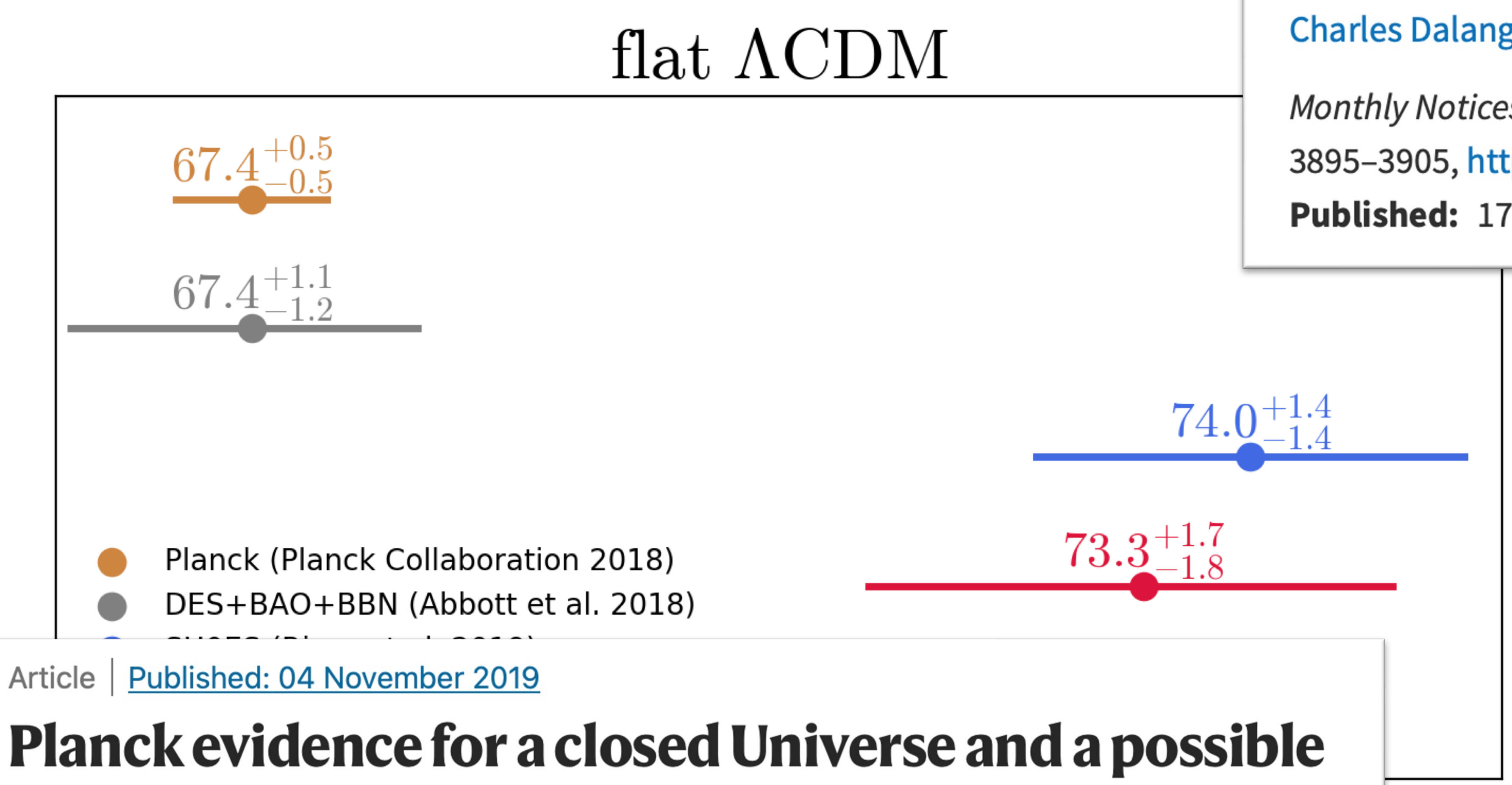

Wong et al. 2019

JOURNAL ARTICLE

On the kinematic cosmic dipole tension

Charles Dalang, Camille Bonvin

Monthly Notices of the Royal Astronomical Society, Volume 512, Issue 3, May 2022, Pages 3895–3905, https://doi.org/10.1093/mnras/stac726

Published: 17 March 2022 **Article history ▾**

Article | Published: 04 November 2019

Planck evidence for a closed Universe and a possible crisis for cosmology

Eleonora Di Valentino, Alessandro Melchiorri & Joseph Silk

Nature Astronomy **4**, 196–203 (2020) | Cite this article

A&A 597, A126 (2017)

Relieving tensions related to the lensing of the cosmic microwave background temperature power spectra

F. Couchot, S. Henrot-Versillé, O. Perdereau, S. Plaszczynski, B. Rouillé d'Orfeuil, M. Spinelli and M. Tristram

Received: 13 November 2015 **Accepted:** 24 September 2016

PHYSICAL REVIEW LETTERS **128,** 091302 (2022)

Cosmic Birefringence from the *Planck* Data Release 4

P. Diego-Palazuelos,[1,2,*] J. R. Eskilt,[3,†] Y. Minami,[4] M. Tristram,[5] R. M. Sullivan,[6] A. J. Banday,[7,8] R. B. Barreiro,[1] H. K. Eriksen,[3] K. M. Górski,[9,10] R. Keskitalo,[11,12] E. Komatsu,[13,14] E. Martínez-González,[1] D. Scott,[6] P. Vielva,[1] and I. K. Wehus[3]

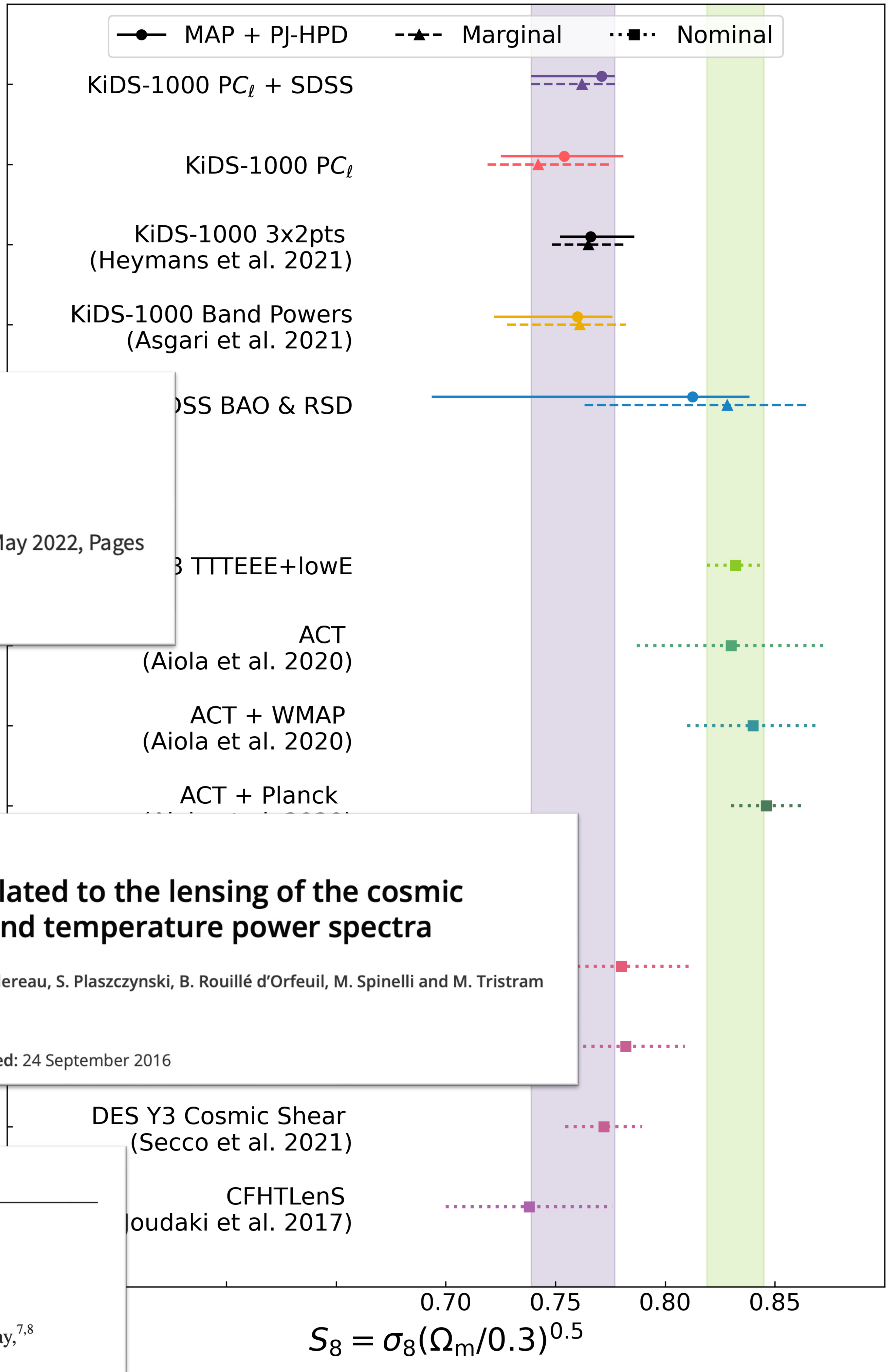

Loureiro et al., *A&A* (2022)


Stage IV Surveys
are just around the corner!

- ~ 2 Billion galaxies for Weak Lensing
- ~ 50 Million galaxies for Galaxy Clustering
- Photometric and Spectroscopic
- 15 000 deg^2
- Up to redshift of ~ 2
- Launch: 2023

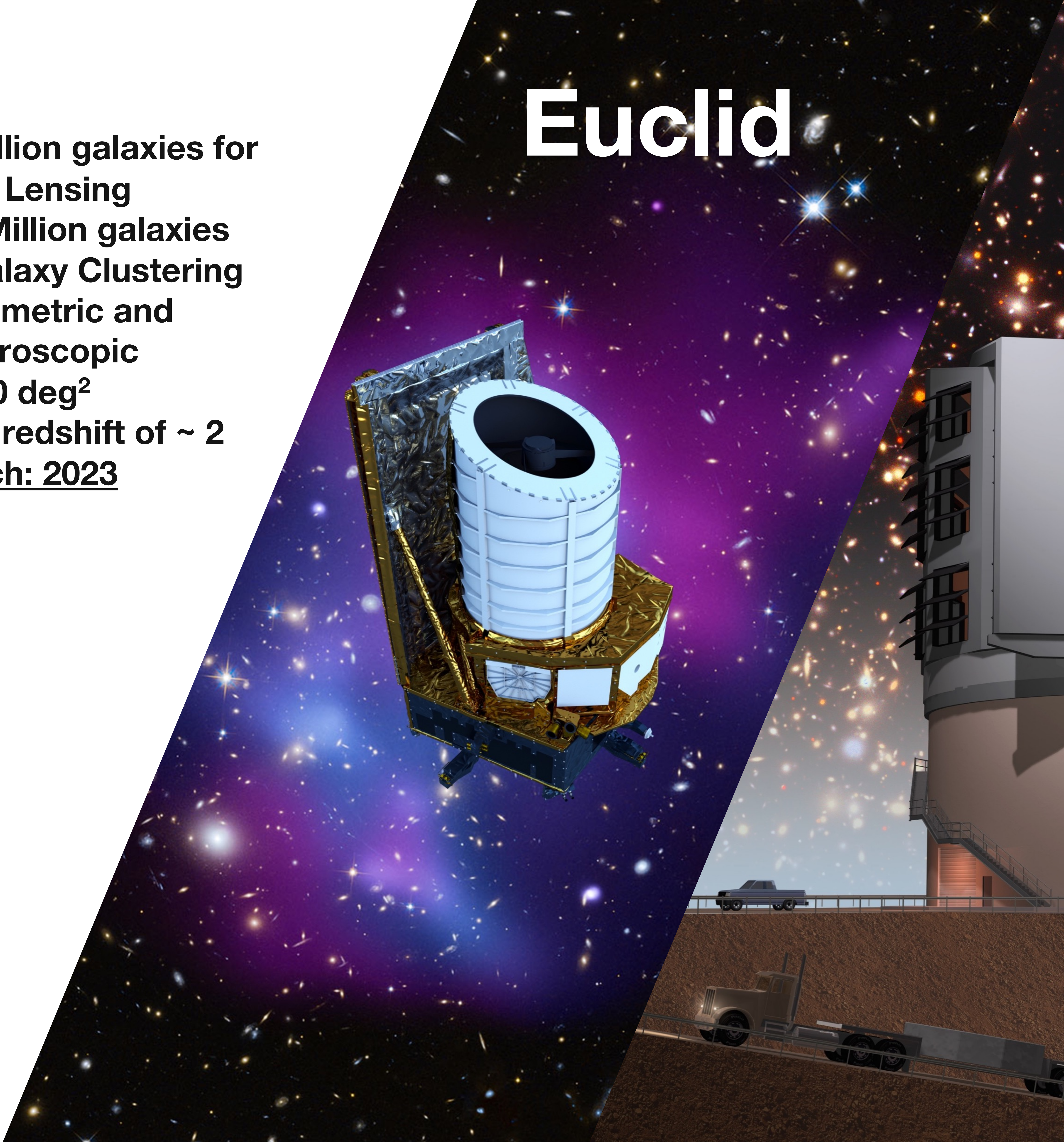

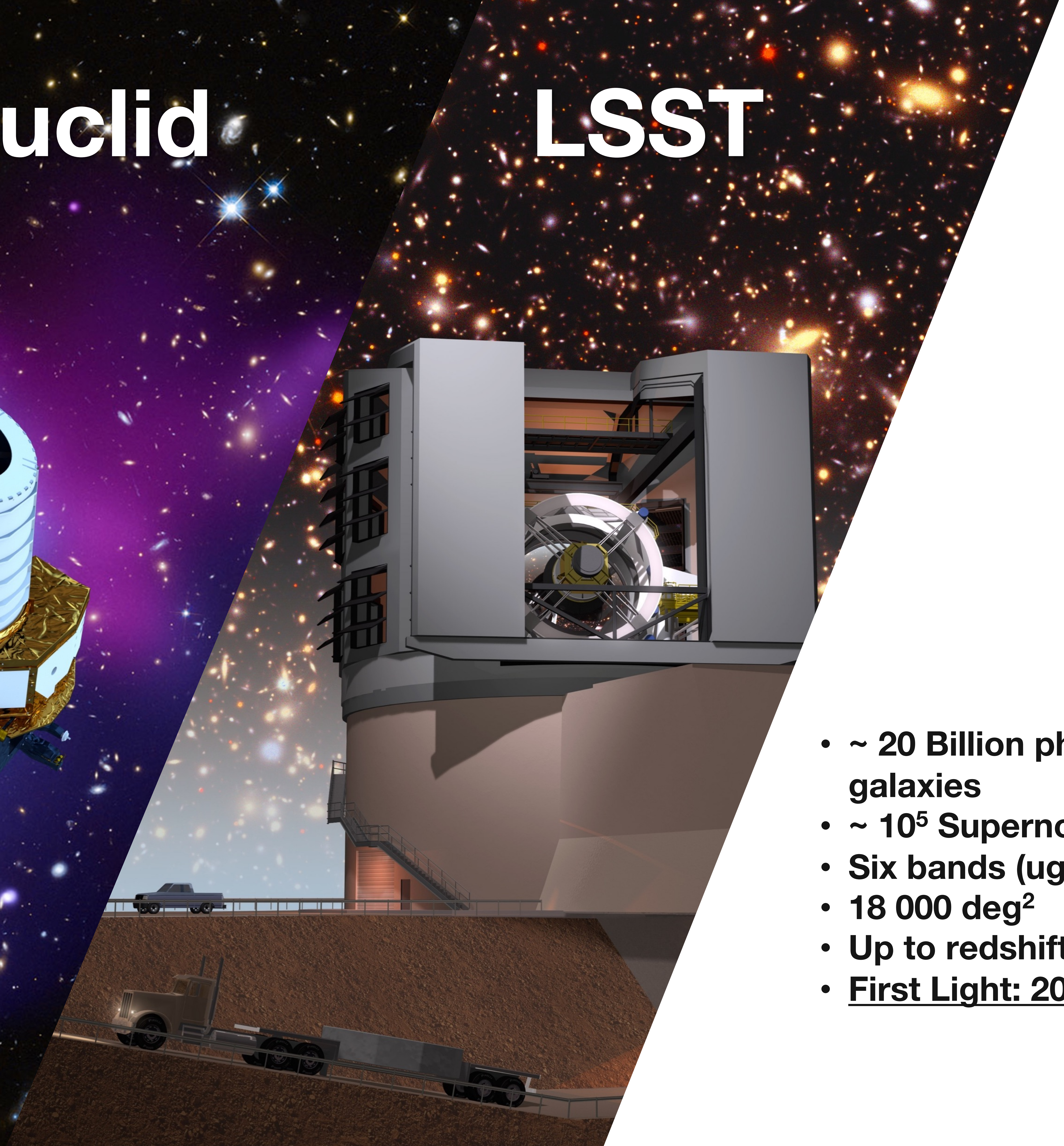

- ~ 20 Billion photometric galaxies
- ~ 10^5 Supernovae
- Six bands (ugrizy)
- 18 000 deg^2
- Up to redshift of ~ 1.2
- First Light: 2023

- ~ 2 Billion galaxies for Weak Lensing
- ~ 50 Million galaxies for Galaxy Clustering
- Photometric and Spectroscopic
- 15 000 deg^2
- Up to redshift of ~ 2
- Launch: 2023

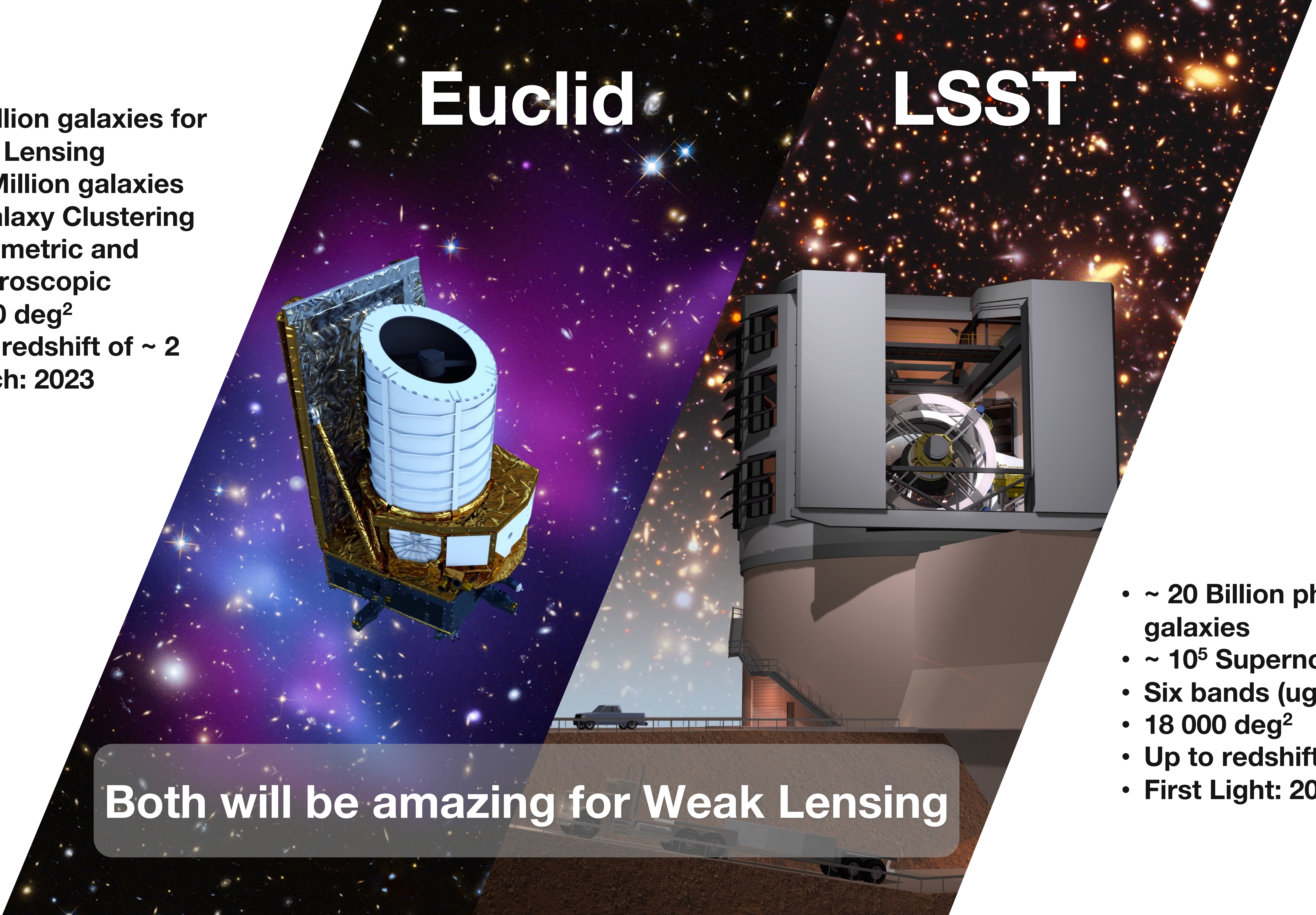

- ~ 20 Billion photometric galaxies
- ~ 10^5 Supernovae
- Six bands (ugrizy)
- 18 000 deg^2
- Up to redshift of ~ 1.2
- First Light: 2023

Exploring Stage-IV data will require the next generation of data analysis techniques, breaking away from outdated assumptions such as sky-flatness, gaussianity, etc.

1. Weak Lensing

A speed-run

Weak Lensing

(mandatory slide!)

We can probe the growth of structures in the universe using weak gravitational lensing

$$S_8 = \sigma_8 \left(\frac{\Omega_m}{0.3}\right)^{1/2}$$

as well as the distribution of matter along the line-of-sight.

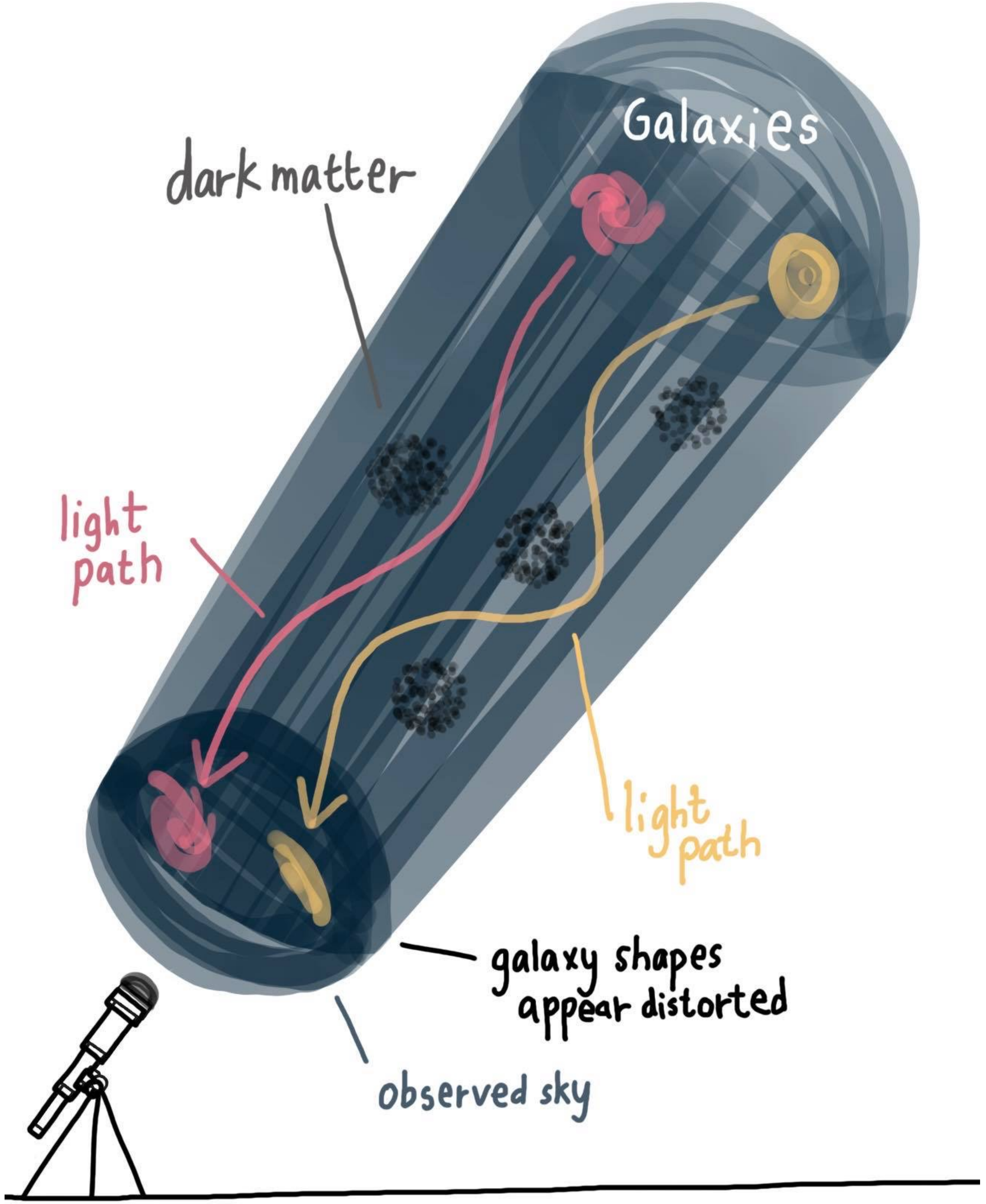

Image Credit: Elin Blomberg

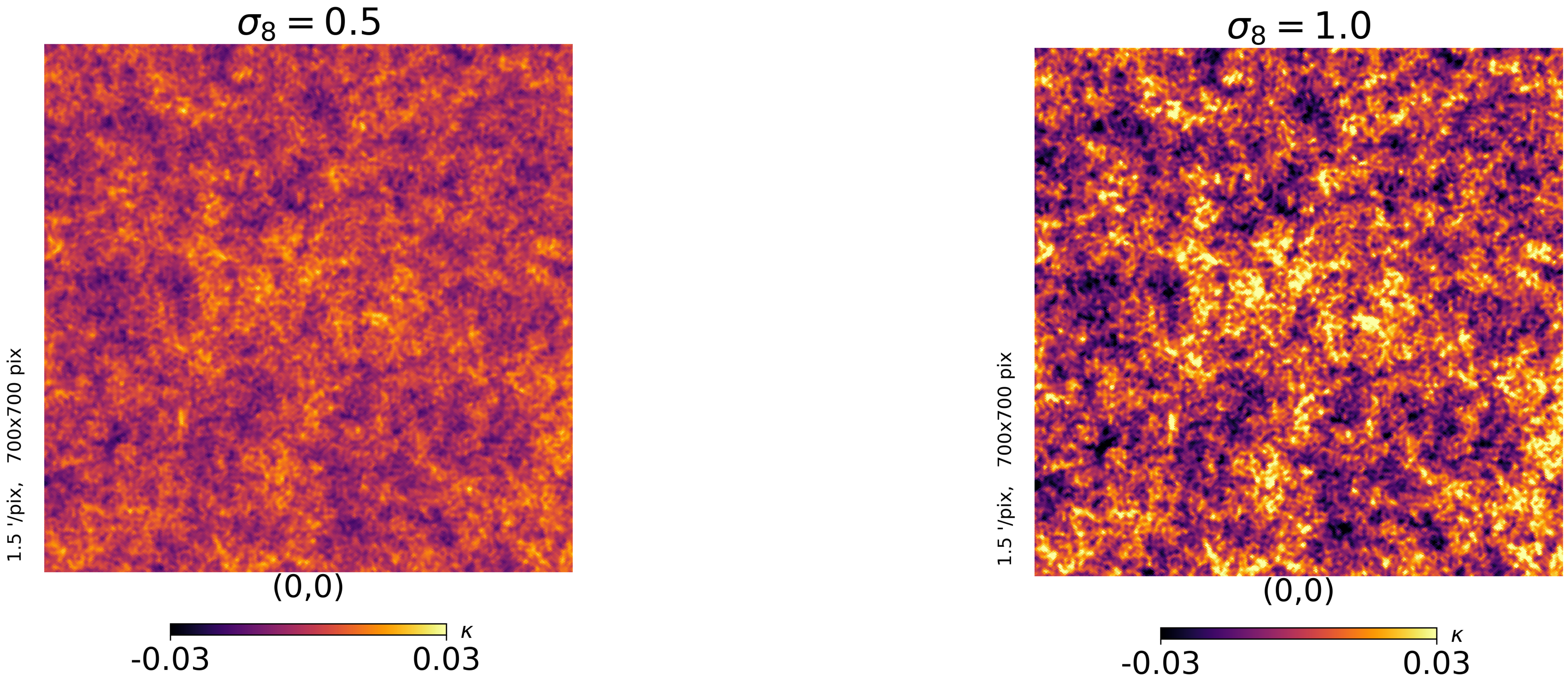

The amplitude of matter density fluctuations

Weak Lensing Theory Speed-run

- The mapping between the lensing source's true angular position and the observed angular position is $\theta_{s,i} \approx A_{ij}\theta_{\mathrm{obs},j}$, with

$$A_{ij} = \delta_{ij} - \partial_i \partial_j \tilde{\Psi}$$

where

$$\tilde{\Psi}(\chi_{\mathrm{s}}, \hat{n}) = 2\int_0^{\chi_s} d\chi \frac{f_K(\chi_{\mathrm{s}} - \chi)}{f_K(\chi) f_K(\chi_s)} \Psi(\chi, \hat{n})$$

Newtonian
Grav. Potential

- From these, we can define the Weak Lensing observables (in harmonic space):
  - Convergence:

$$\kappa_{\ell m} = -\frac{1}{2}\ell(\ell+1)\,\tilde{\Psi}_{\ell m}$$

  - Shear:

$$\gamma_{\ell m} = \frac{1}{2}\sqrt{(\ell-1)\ell(\ell+1)(\ell+2)}\,\tilde{\Psi}_{\ell m}$$

- Since shear is a spin-2 field it can be decomposed into *E*- and *B*-modes

$$E_{\ell m} = -\frac{1}{2}\int \mathrm{d}\Omega\,\left[\gamma(\hat{n})\,{}_{+2}Y^*_{\ell m}(\hat{n}) + \gamma^*(\hat{n})\,{}_{-2}Y^*_{\ell m}(\hat{n})\right]$$

and

$$B_{\ell m} = \frac{\mathrm{i}}{2}\int \mathrm{d}\Omega\,\left[\gamma(\hat{n})\,{}_{+2}Y^*_{\ell m}(\hat{n}) - \gamma^*(\hat{n})\,{}_{-2}Y^*_{\ell m}(\hat{n})\right]\,.$$

Weak Lensing Theory Speed-run

- The mapping between the lensing source's true angular position and the observed angular position is $\theta_{s,i} \approx A_{ij}\theta_{\text{obs},j}$, with

$$A_{ij}$$

where

$$\tilde{\Psi}(\chi_{\text{s}}, \hat{n}) = 2$$

WELL, YOU KNOW IT…

Newtonian
Grav. Potential

- From these, we can define the Weak Lensing observables (in harmonic space):
  - Convergence:

$$1)\, \tilde{\Psi}_{\ell m}$$

$$\ell(\ell+1)(\ell+2)\, \tilde{\Psi}_{\ell m}$$

it can be
modes

$$E_{\ell m} = -\frac{1}{2}\int \mathrm{d}\Omega \left[\gamma(\hat{n})\, {}_{+2}Y^*_{\ell m}(\hat{n}) + \gamma^*(\hat{n})\, {}_{-2}Y^*_{\ell m}(\hat{n})\right]$$

and

$$B_{\ell m} = \frac{\mathrm{i}}{2}\int \mathrm{d}\Omega \left[\gamma(\hat{n})\, {}_{+2}Y^*_{\ell m}(\hat{n}) - \gamma^*(\hat{n})\, {}_{-2}Y^*_{\ell m}(\hat{n})\right] .$$

2. Field Level Inference

What is it, and Why do we care?

“Vintage” Cosmology

Ex: Weak Lensing Surveys

Galaxy Shapes

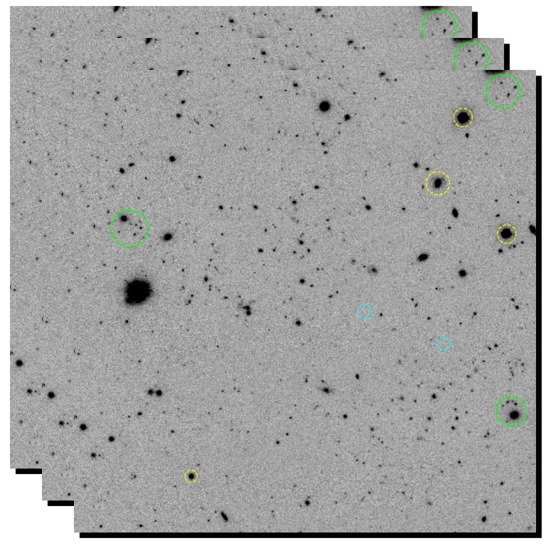

Kannawadi et al. 2018

“Vintage” Cosmology

Ex: Weak Lensing Surveys

Galaxy Shapes

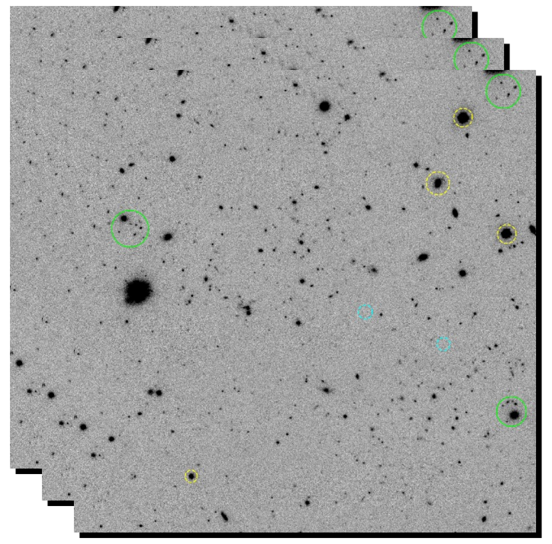

Kannawadi et al. 2018

“Estimator”

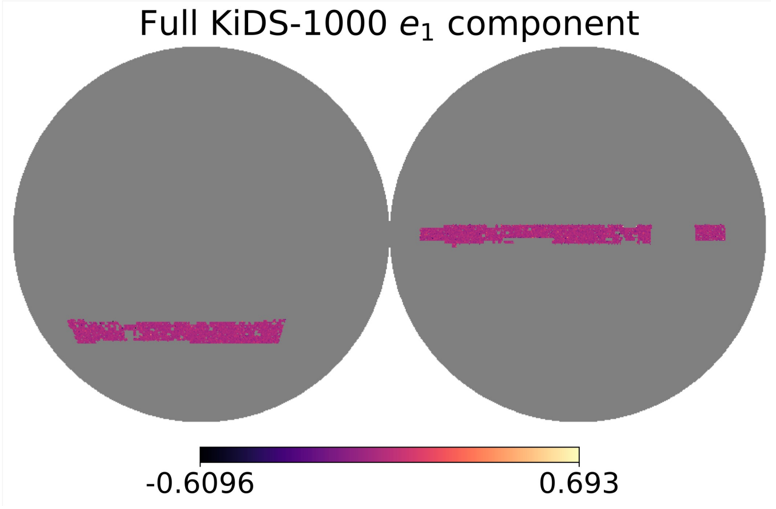

Galaxy shear maps

“Vintage” Cosmology

Ex: Weak Lensing Surveys

Galaxy Shapes

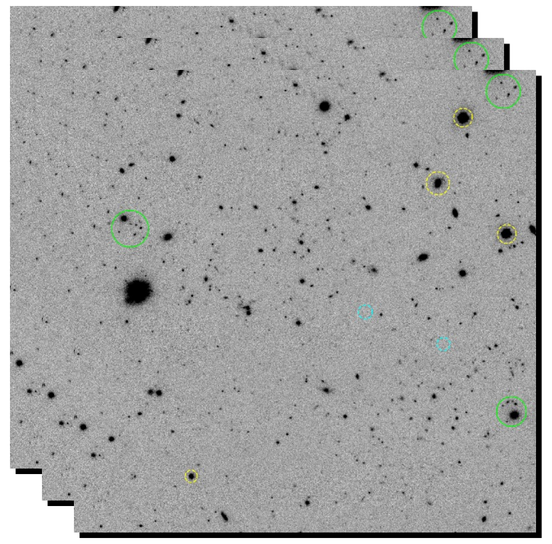

Kannawadi et al. 2018

“Estimator”

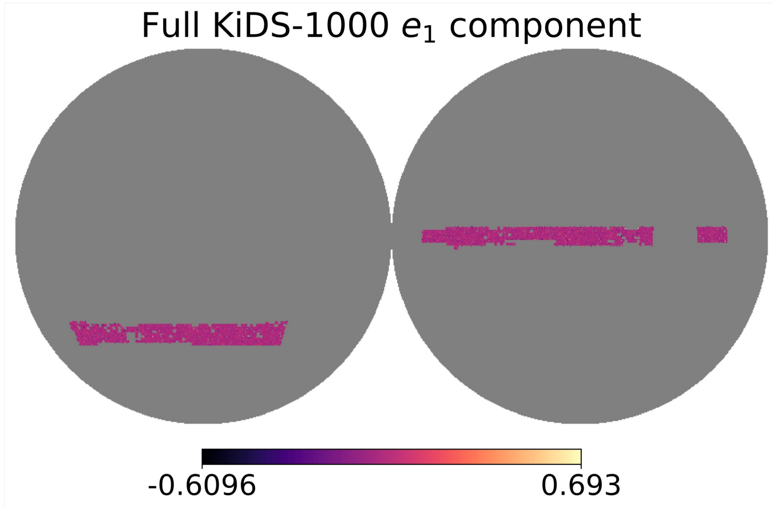

Galaxy shear maps

Estimator

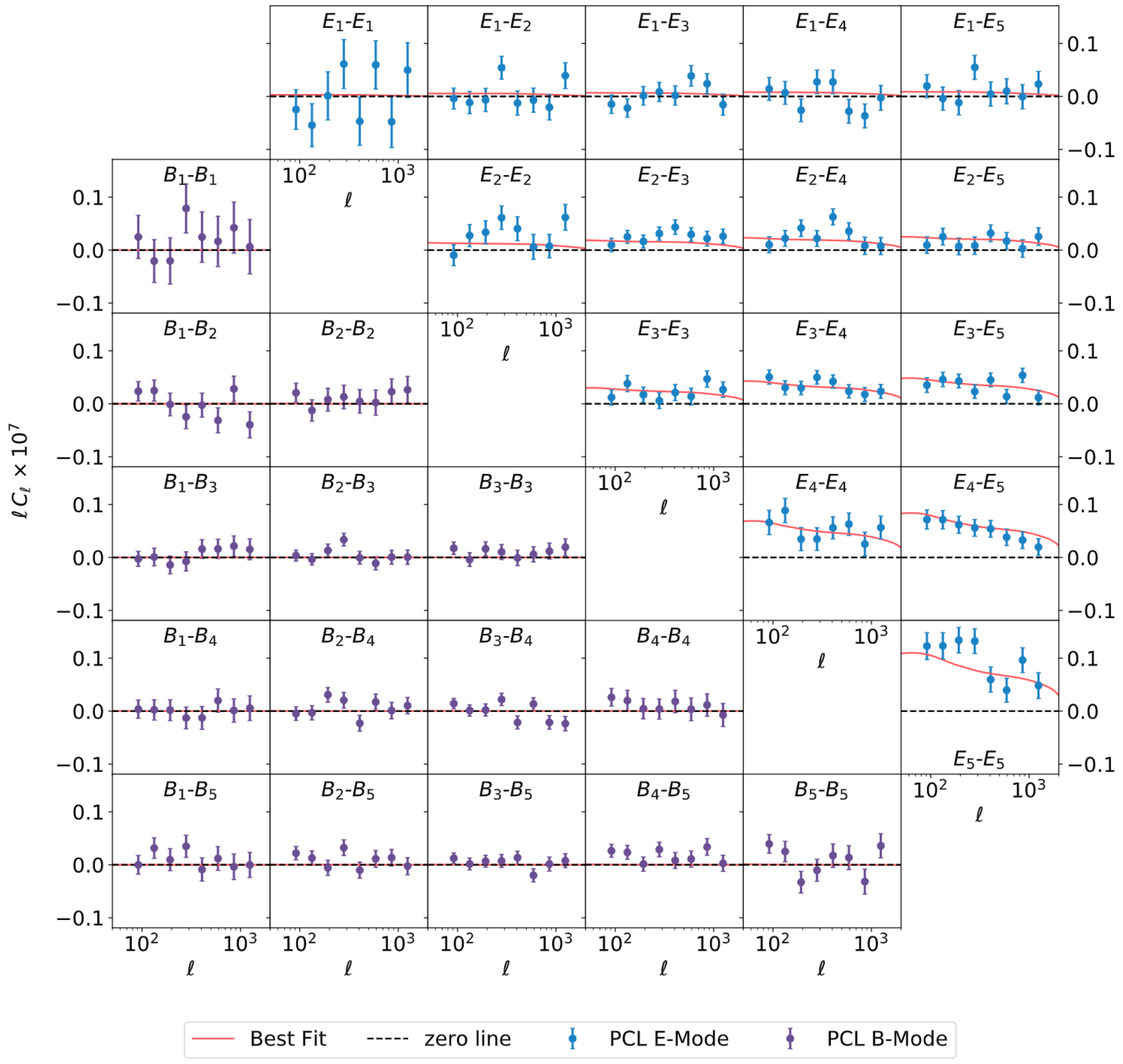

“Vintage” Cosmology

Ex: Weak Lensing Surveys

Galaxy Shapes

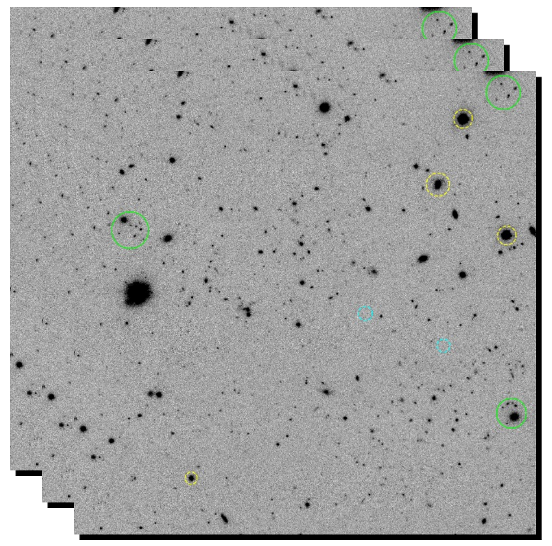

Kannawadi et al. 2018

“Estimator”

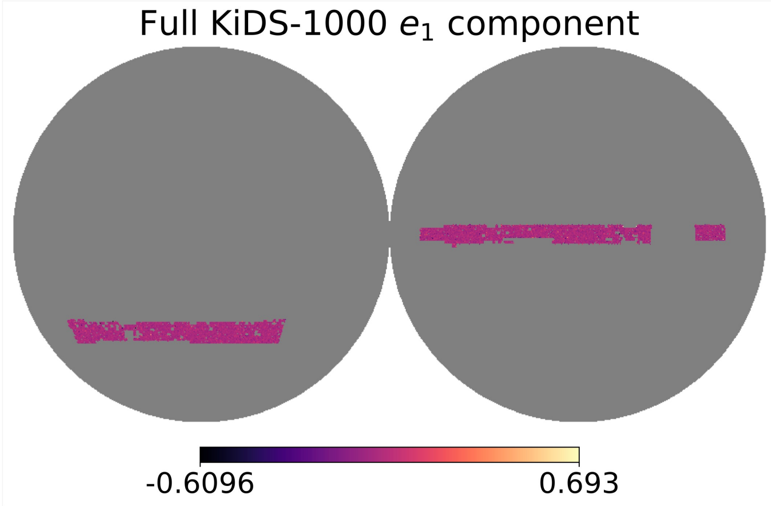

Galaxy shear maps

Estimator

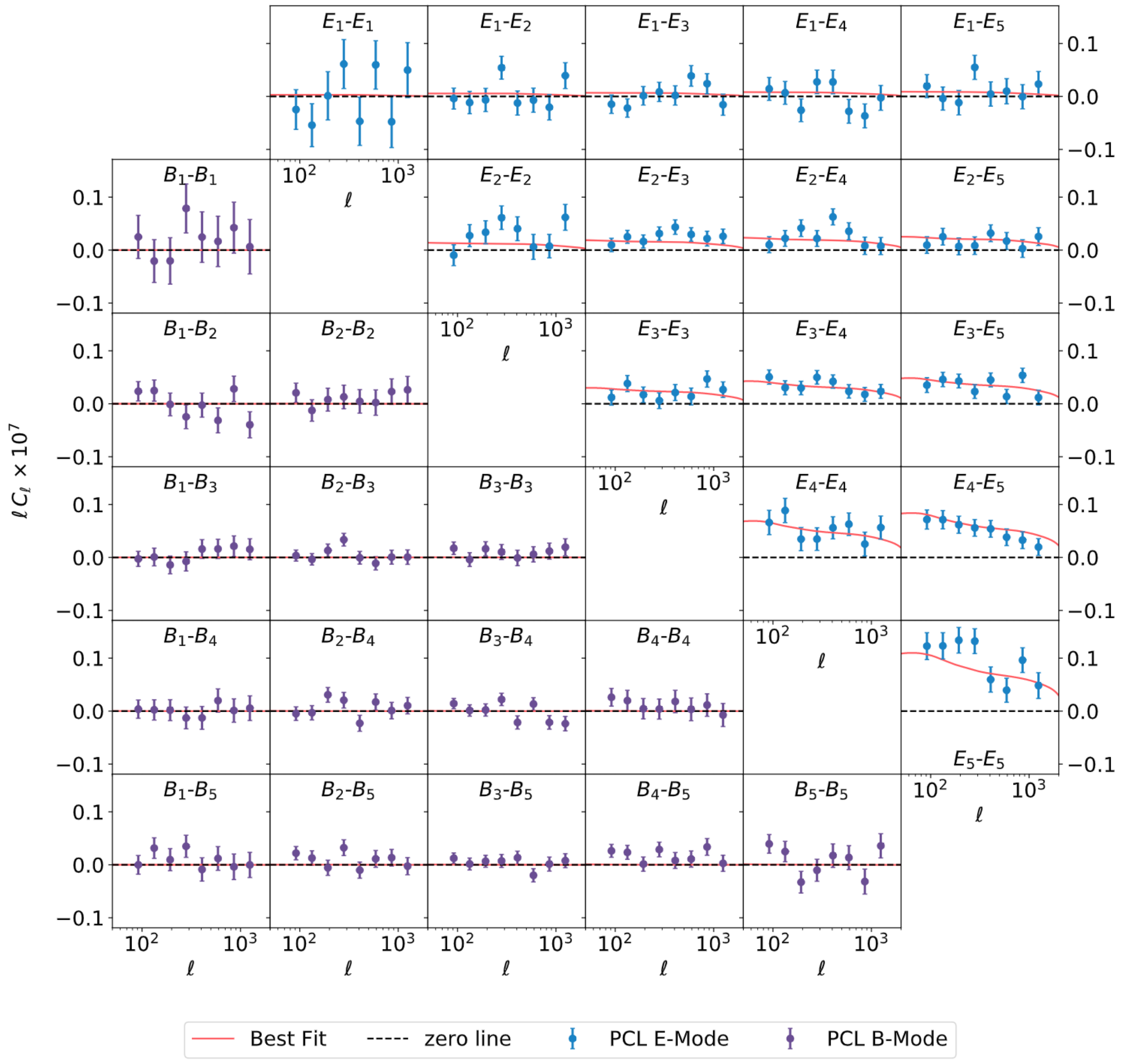

Bayesian Inference

Loureiro et al. 2021 **(2110.06947)**

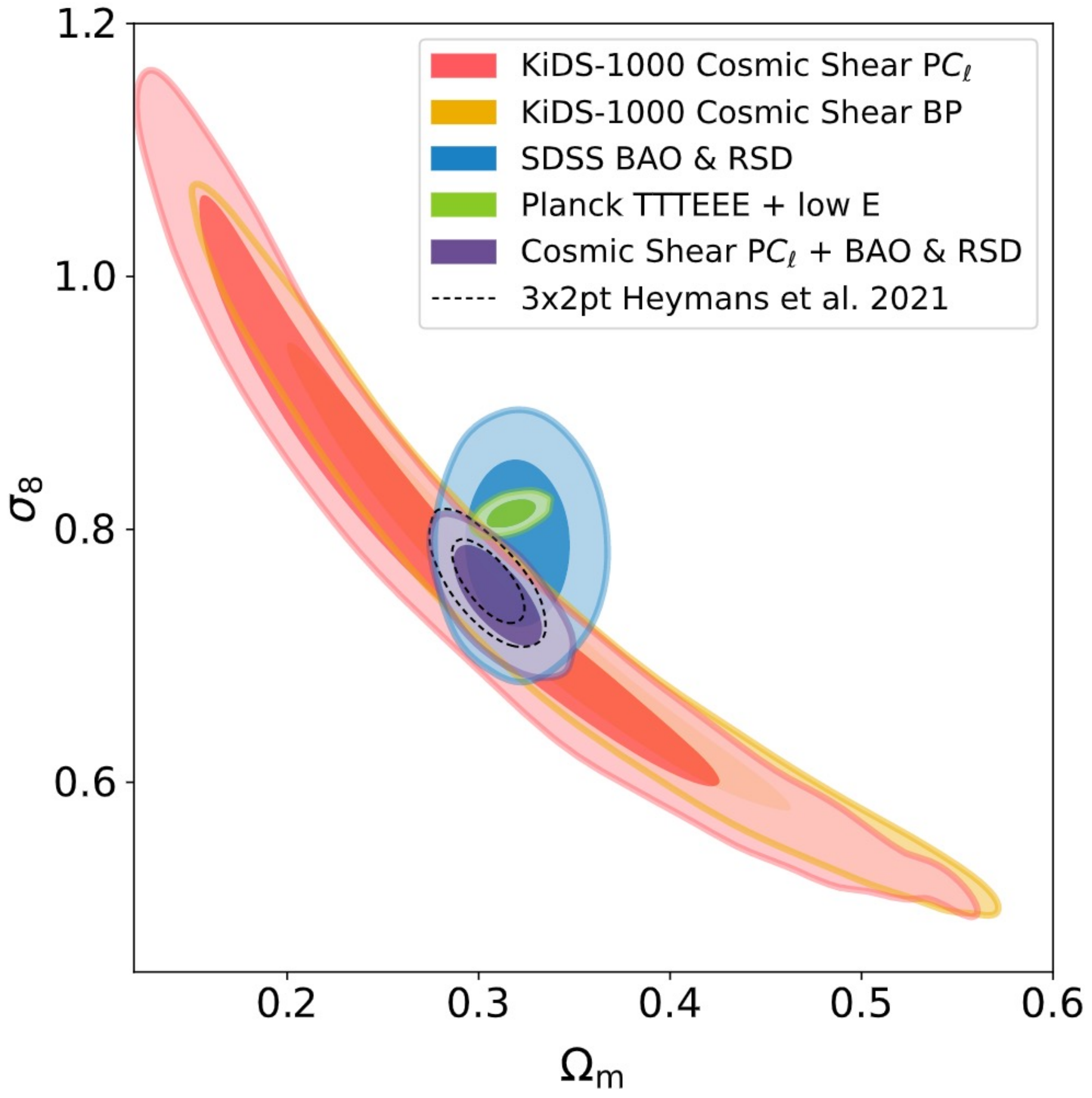

Cosmological Parameters

Bayesian Hierarchical Cosmology

Ex: Weak Lensing

Galaxy Shapes

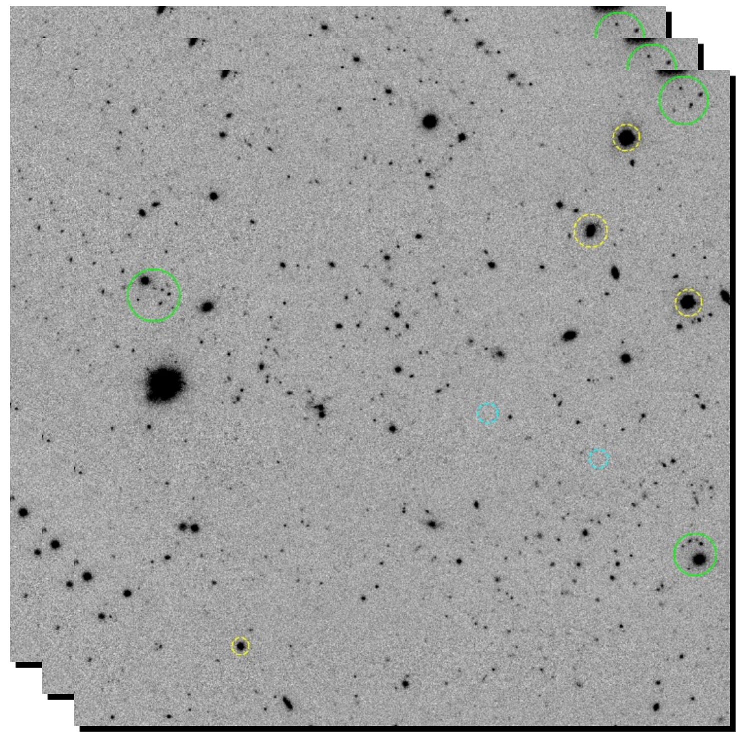

Bayesian Hierarchical Cosmology

Ex: Weak Lensing

Porqueres et al. 2021(**2108.04825)**

Galaxy Shapes

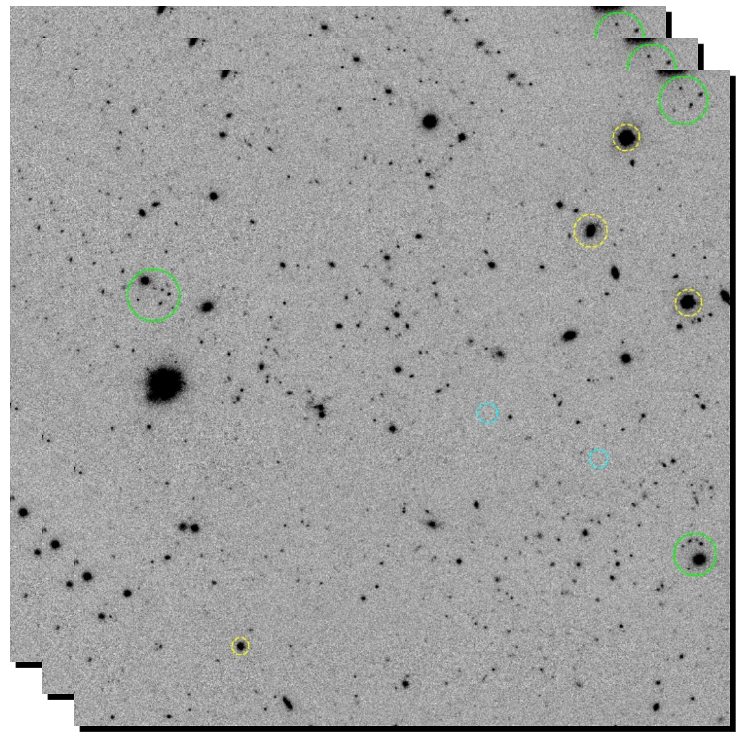

Hierarchical
Model

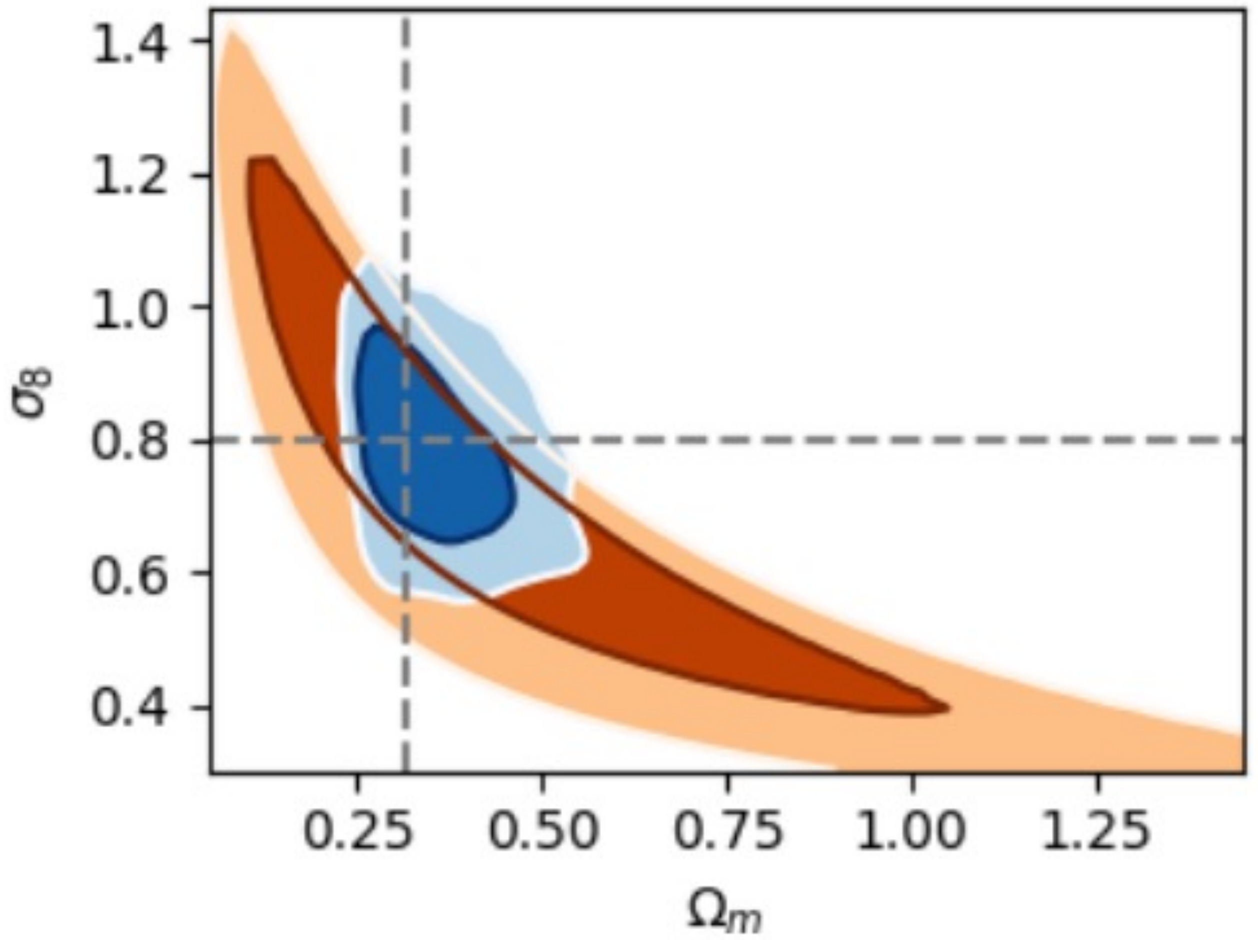

Cosmological Parameters

Bayesian Hierarchical Cosmology

Ex: Weak Lensing

Porqueres et al. 2021(**2108.04825)**

Galaxy Shapes

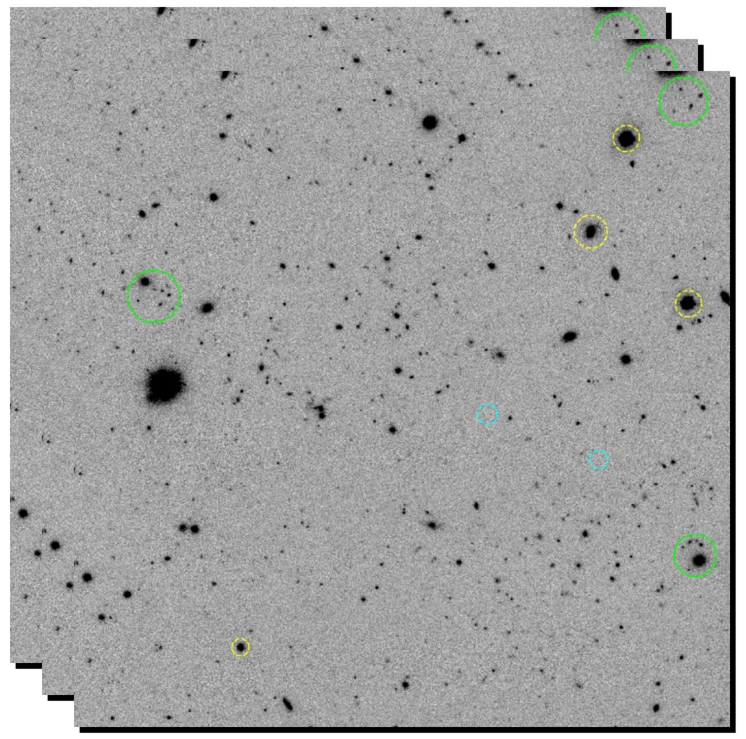

Hierarchical
Model

Intermediate
products

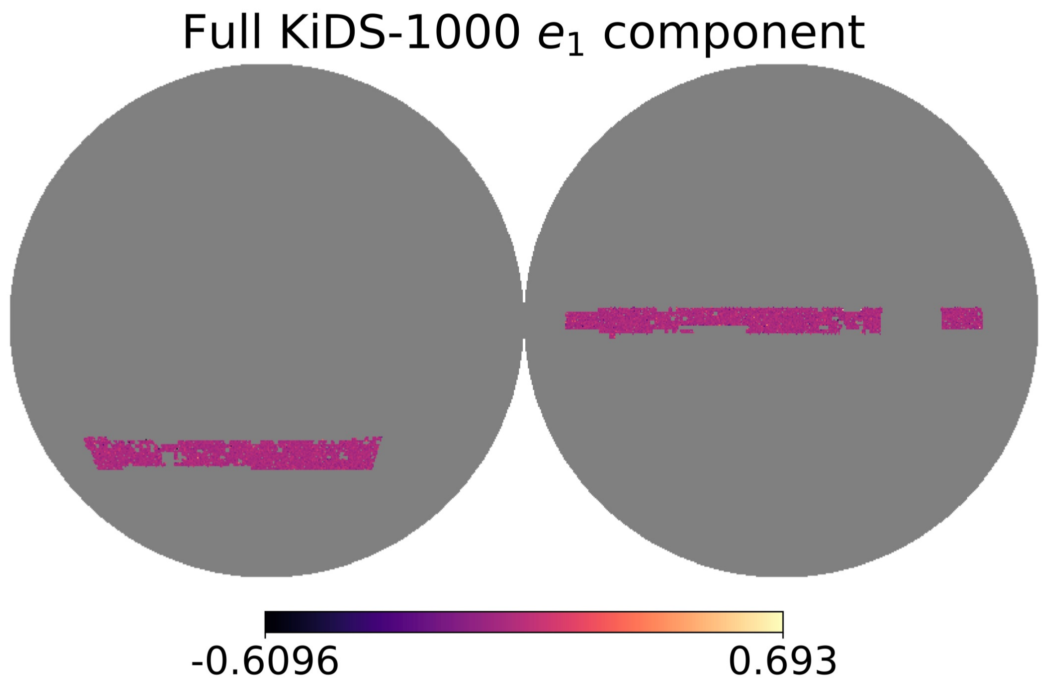

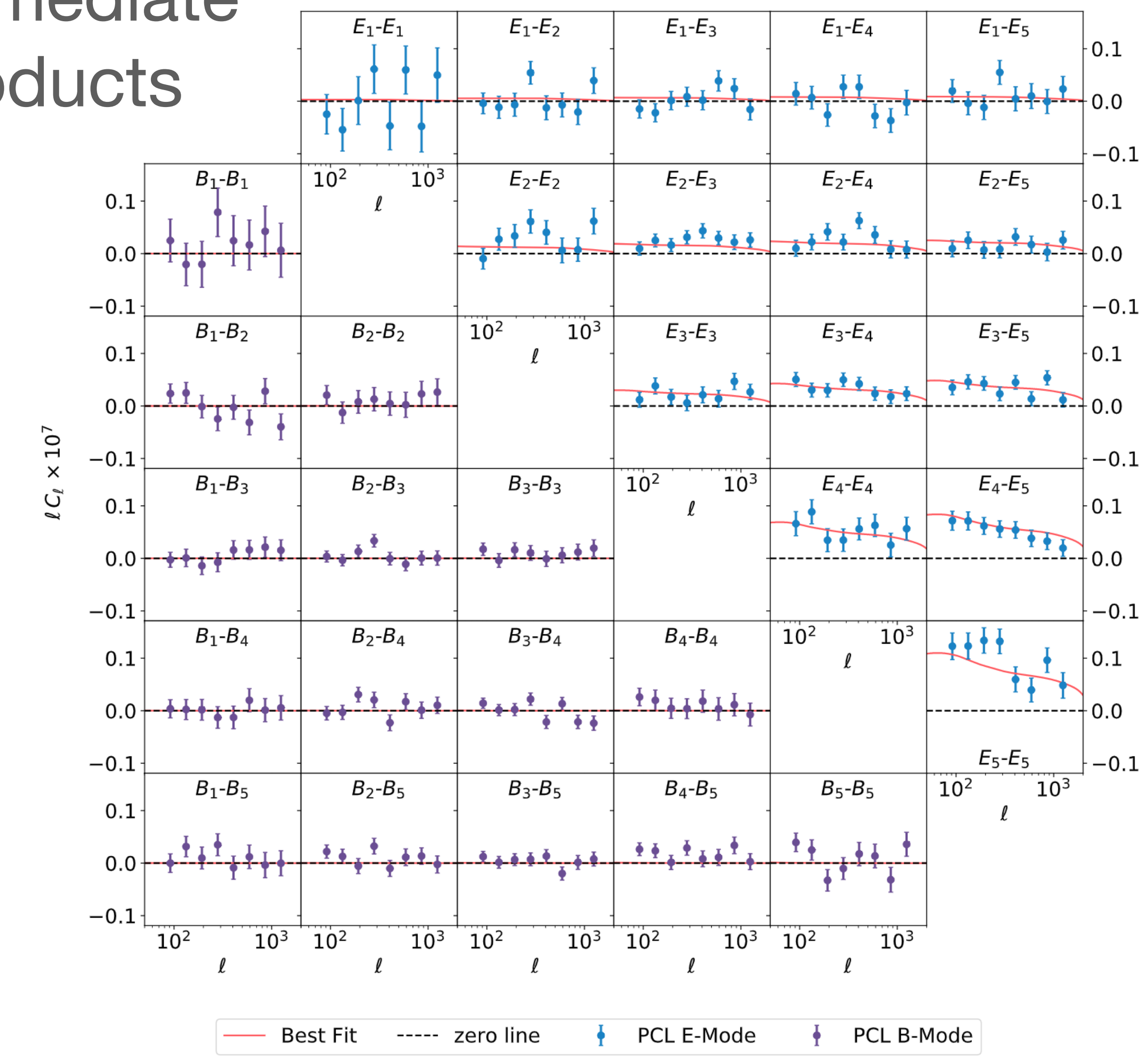

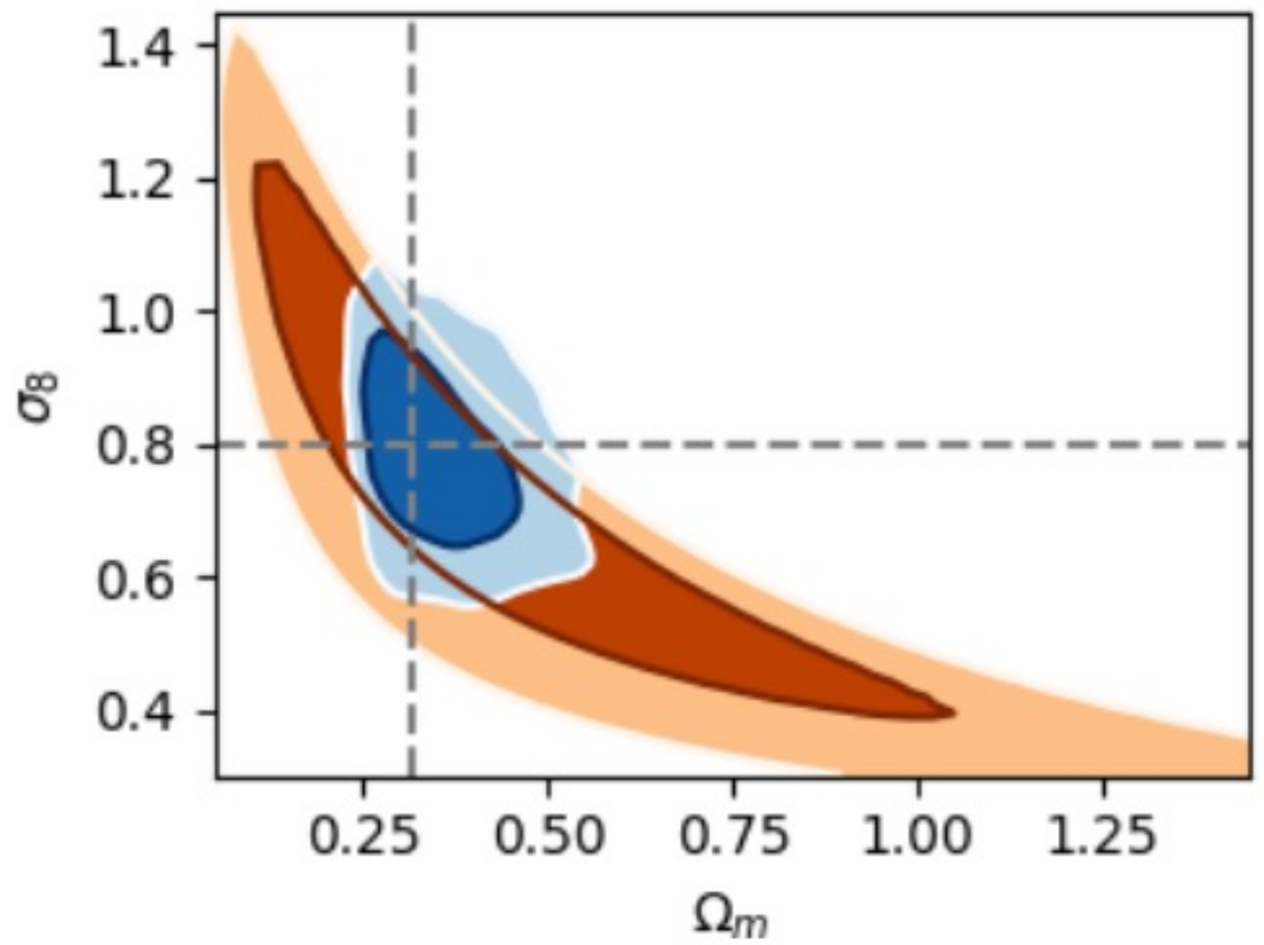

Cosmological Parameters

Field Level Inference

Compared to other methods

Leclercq & Heavens 2021 (2103.04158)

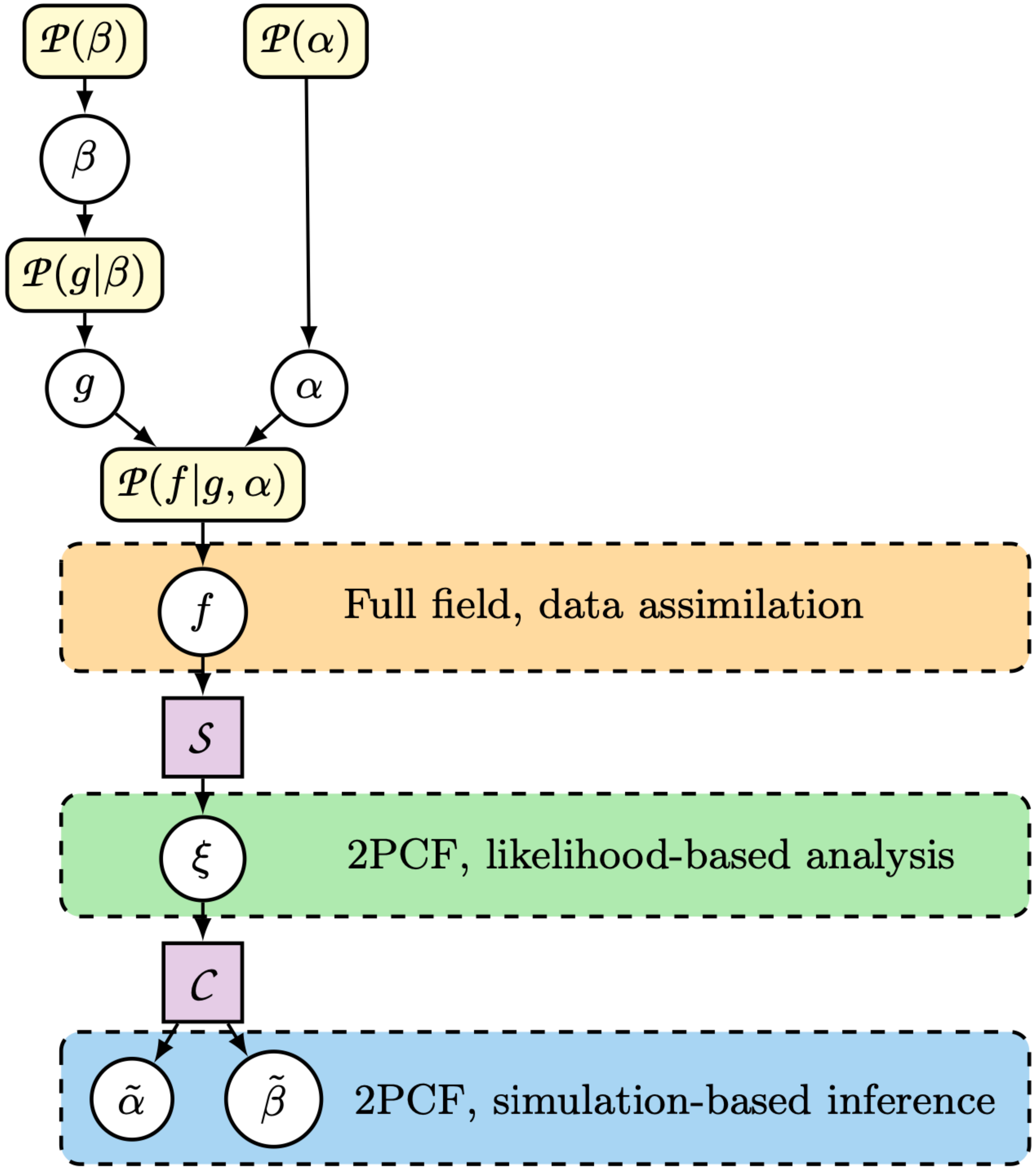

Field Level Inference

Compared to other methods

Leclercq & Heavens 2021 (2103.04158)

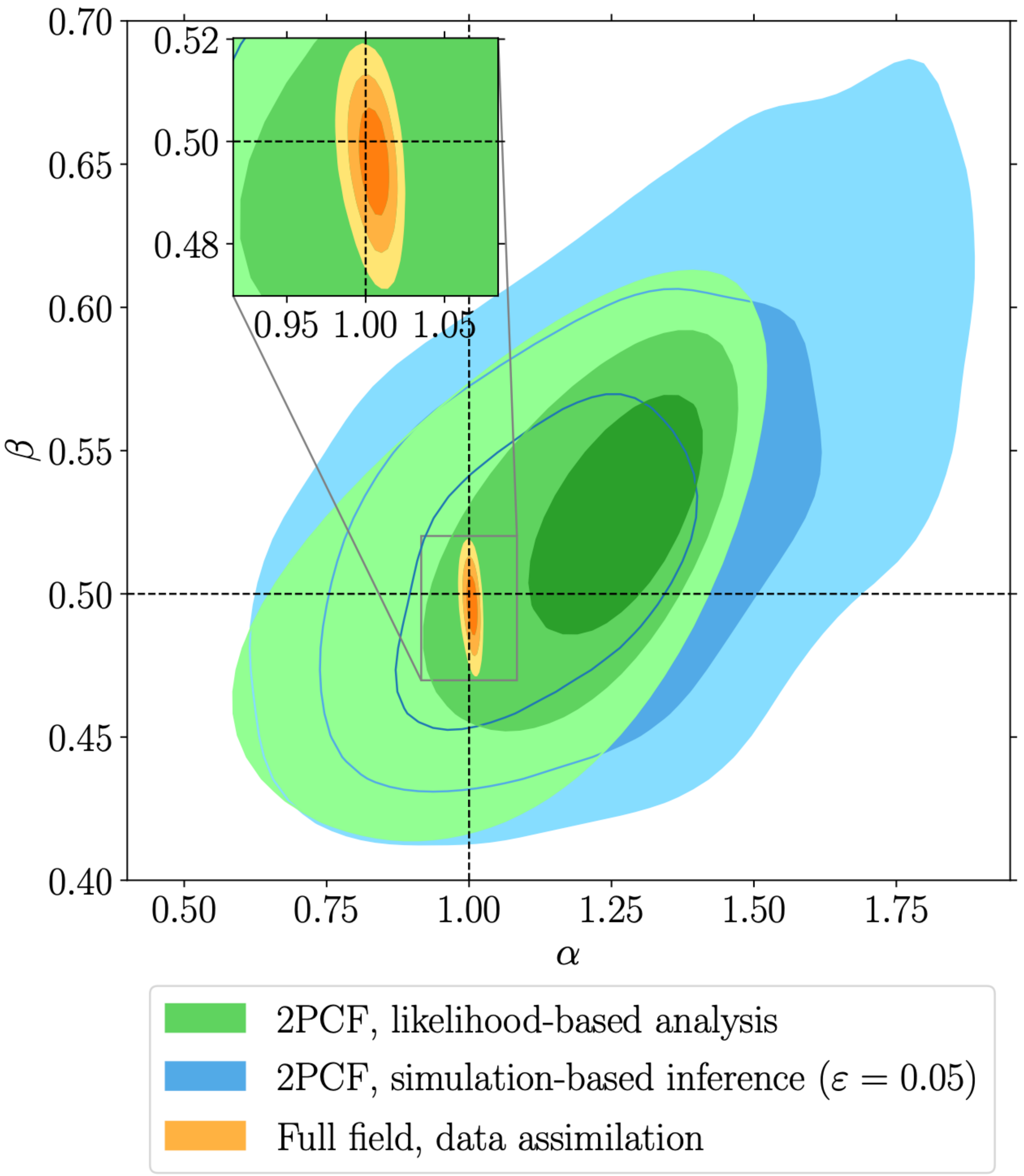

Bayesian Hierarchical Cosmology

Ex: Weak Lensing

Porqueres et al. 2021(**2108.04825)**

Galaxy Shapes

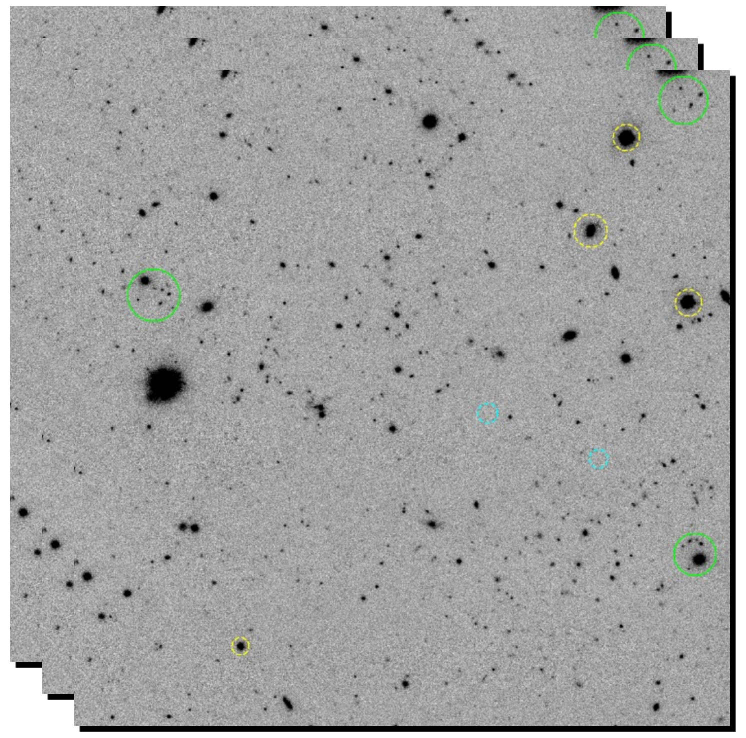

Hierarchical
Model

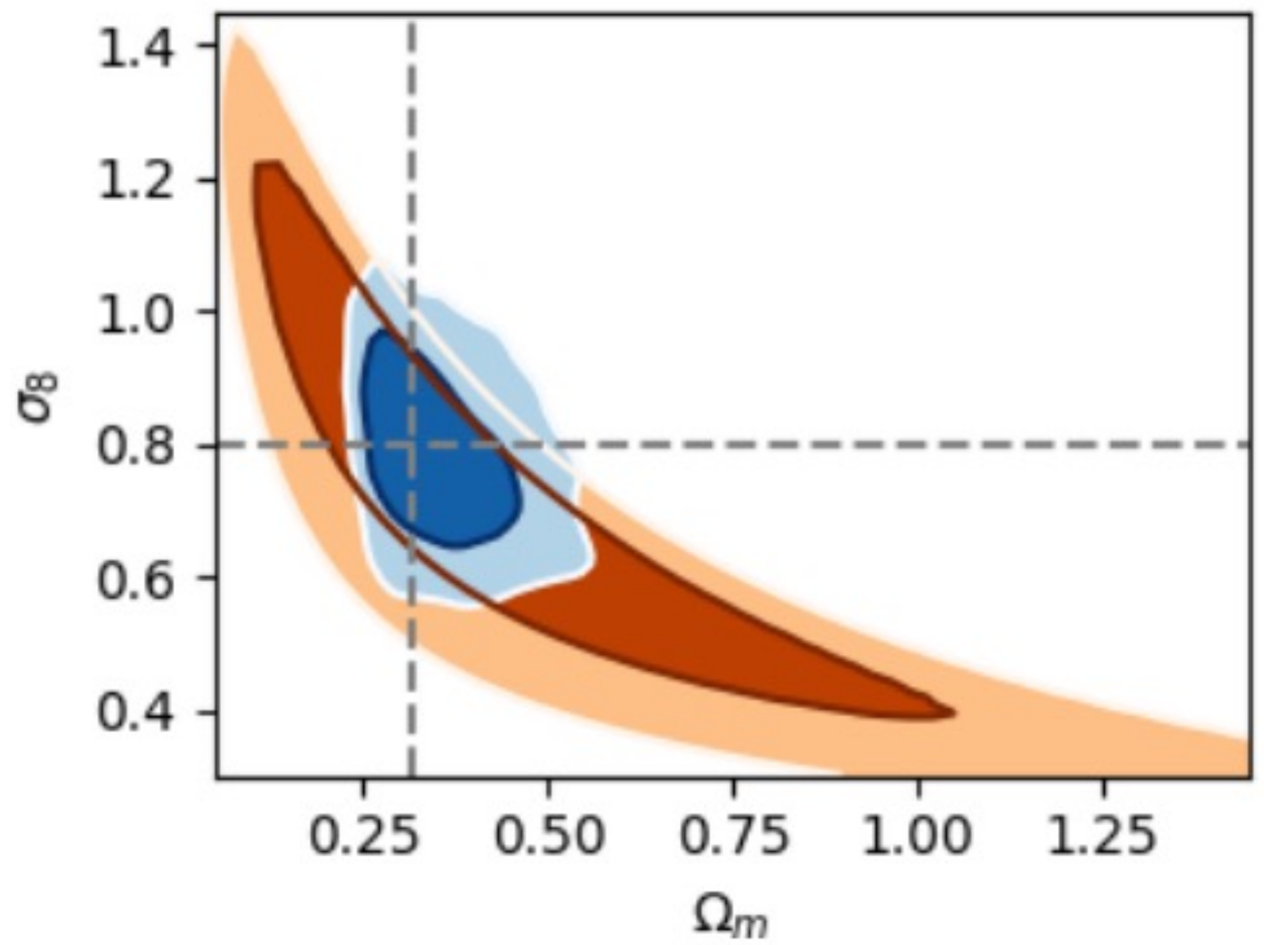

Cosmological Parameters

Intermediate
products

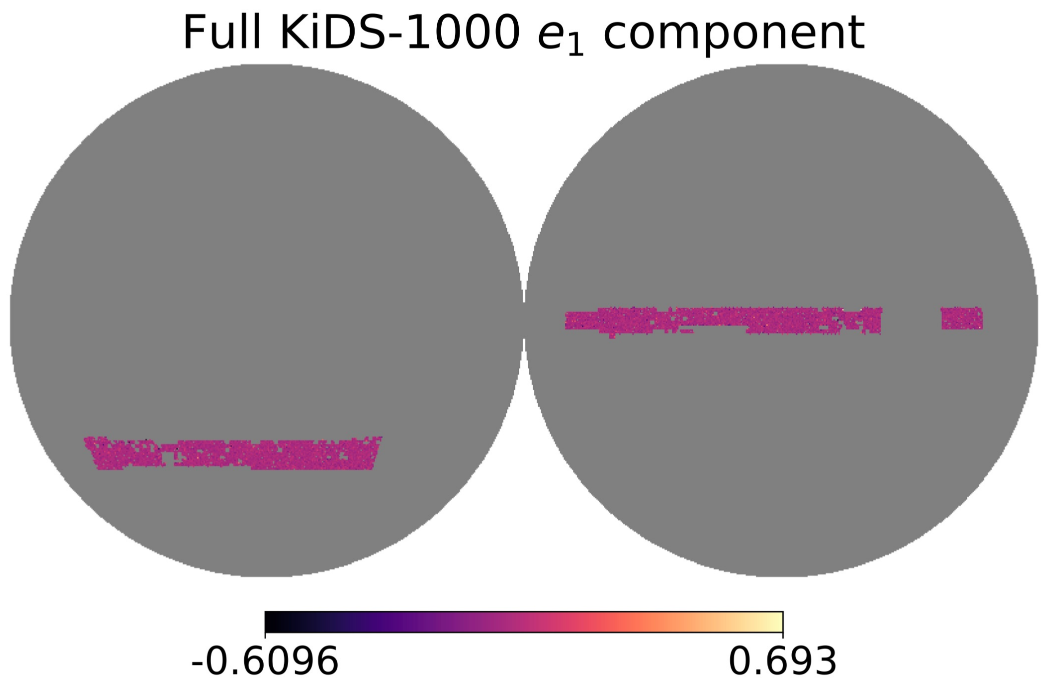

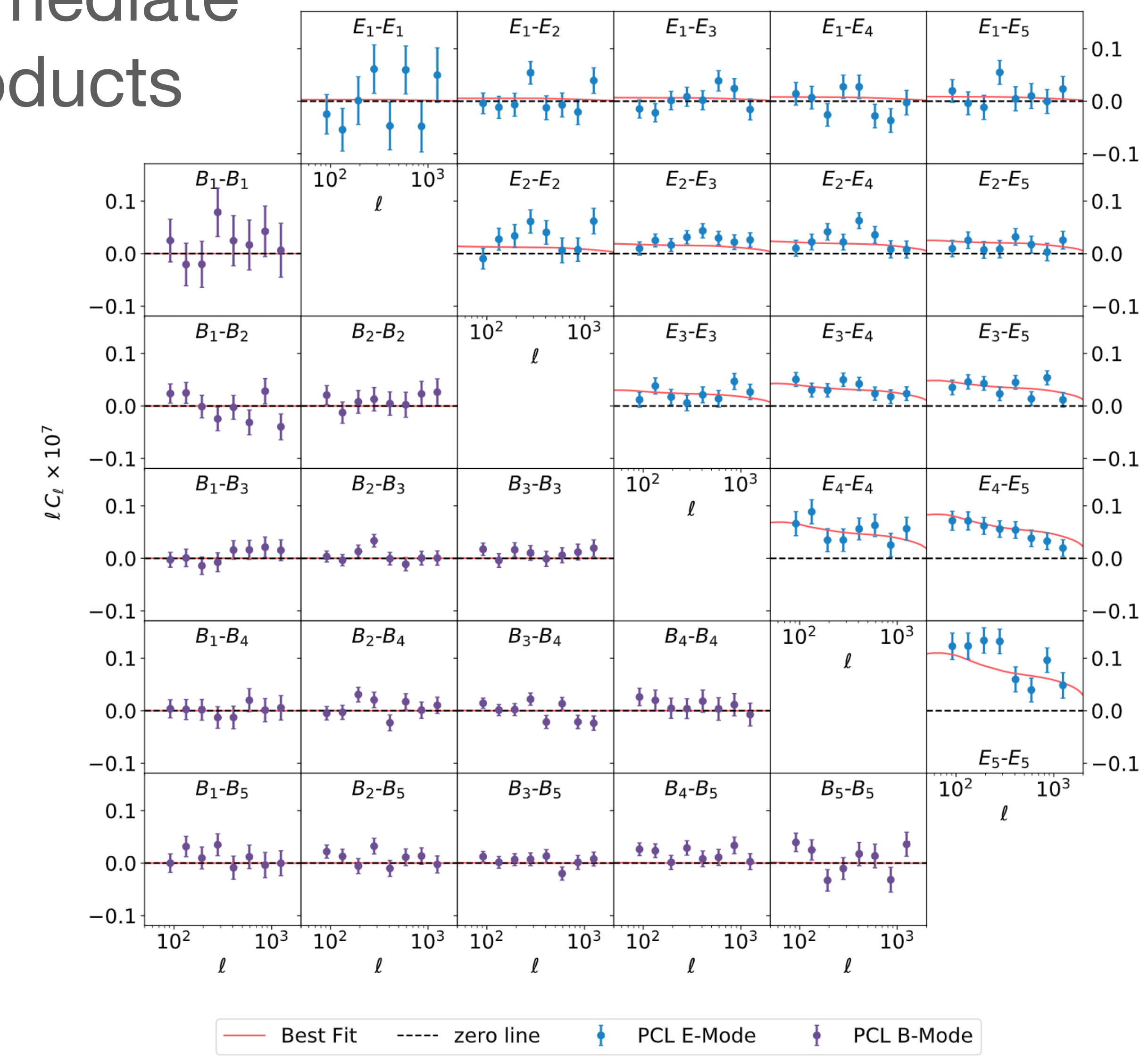

Ideal Bayesian Hierarchical Model

For Weak Lensing Analysis

Alsing et al. 2015 (1505.078400)

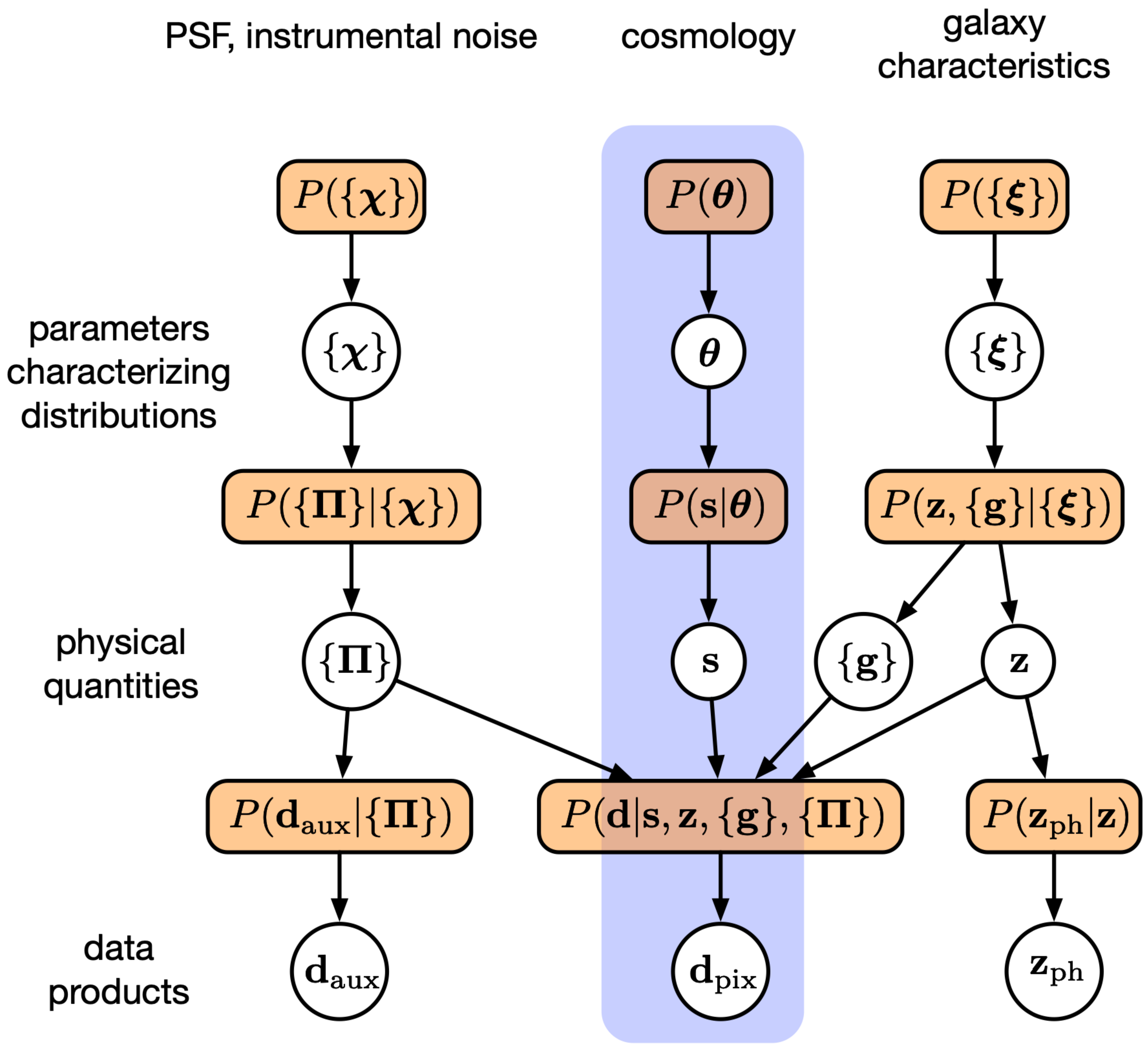

3. Almanac

Sampling full sky cosmological fields and their power spectra

Almanac

Spin-0 and Spin-2 Cosmological Fields

An arbitrary spin-s field can be represented in the basis of spin-s spherical harmonics

$$f(\hat{n}) = \sum_{\ell m} f_{\ell m} \; {}_sY_{\ell m}(\hat{n})$$

With

$$f_{\ell m} = \int d\Omega \; f(\hat{n}) \; {}_sY^*_{\ell m}(\hat{n})$$

And covariance

$$\mathsf{C} \equiv \langle f_{\ell m} f^*_{\ell' m'} \rangle \delta_{\ell\ell'} \delta_{mm'}$$

Figures from Planck Collaboration, SDSS Collaboration & S. Pires et al. 2010

Almanac

Spin-0 and Spin-2 Cosmological Fields

An arbitrary spin-s field can be represented in the basis of spin-s spherical harmonics

$$f(\hat{n}) = \sum_{\ell m} f_{\ell m} \; {}_sY_{\ell m}(\hat{n})$$

With

$$f_{\ell m} = \int d\Omega \; f(\hat{n}) \; {}_sY^*_{\ell m}(\hat{n})$$

And covariance

$$\mathsf{C} \equiv \langle f_{\ell m} f^*_{\ell' m'} \rangle \delta_{\ell\ell'} \delta_{mm'}$$

Spin-0 Fields

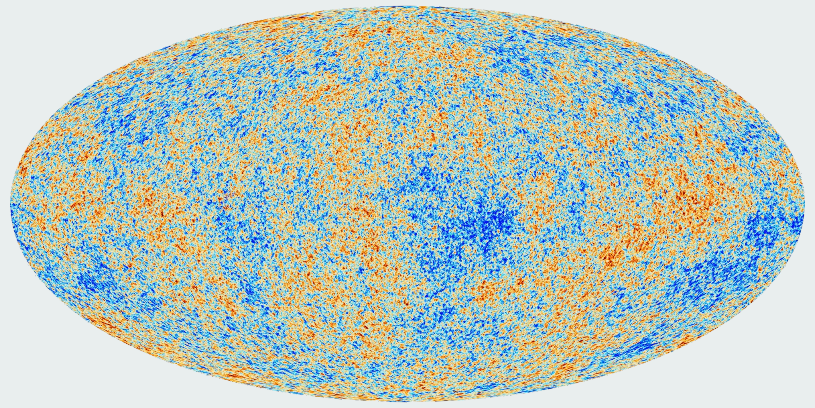

CMB Temperature

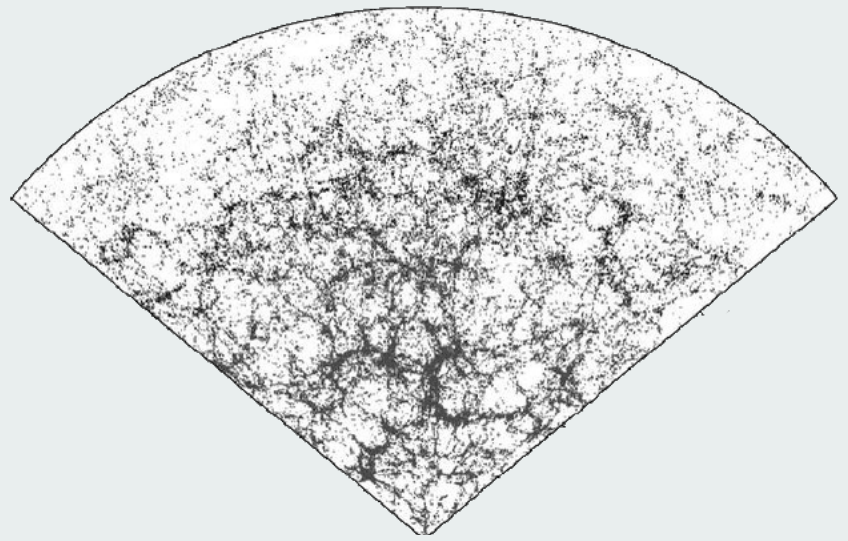

Galaxy Clustering

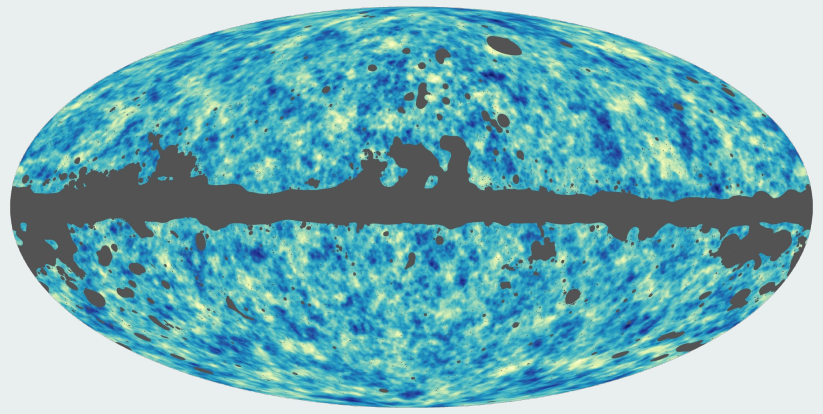

Lensing Convergence

Figures from Planck Collaboration, SDSS Collaboration & S. Pires et al. 2010

Almanac

Spin-0 and Spin-2 Cosmological Fields

An arbitrary spin-s field can be represented in the basis of spin-s spherical harmonics

$$f(\hat{n}) = \sum_{\ell m} f_{\ell m} \; {}_sY_{\ell m}(\hat{n})$$

With

$$f_{\ell m} = \int d\Omega \; f(\hat{n}) \; {}_sY^{*}_{\ell m}(\hat{n})$$

And covariance

$$\mathrm{C} \equiv \langle f_{\ell m} f^{*}_{\ell' m'} \rangle \delta_{\ell \ell'} \delta_{m m'}$$

Spin-0 Fields

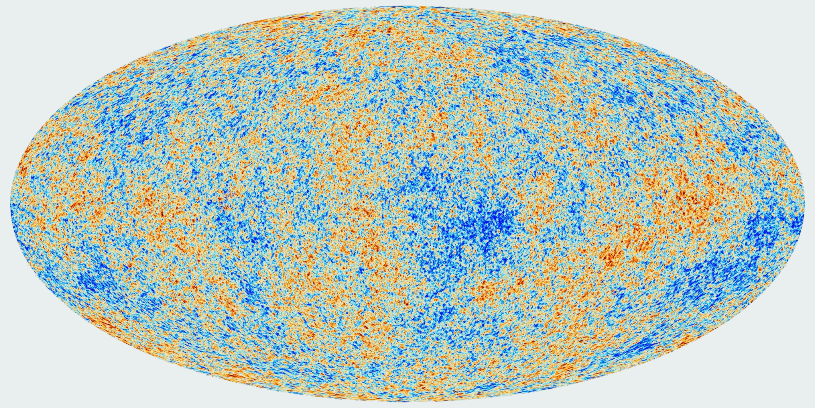

CMB Temperature

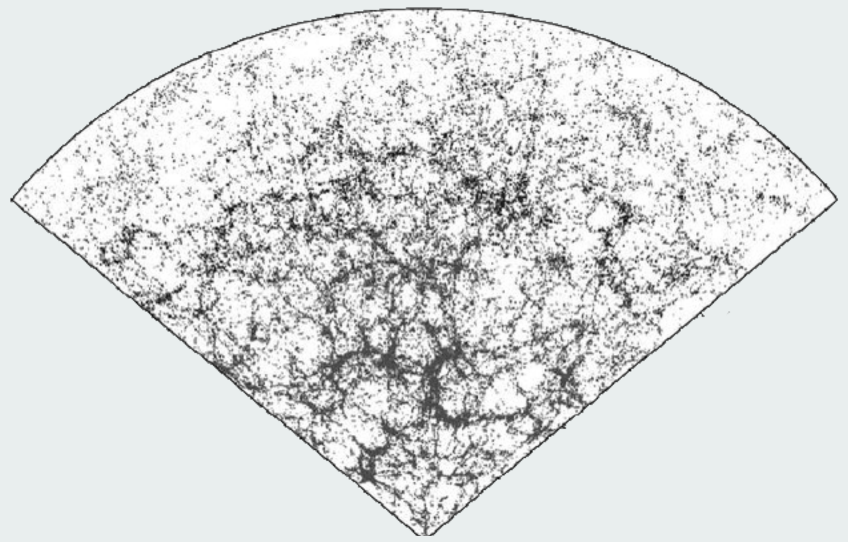

Galaxy Clustering

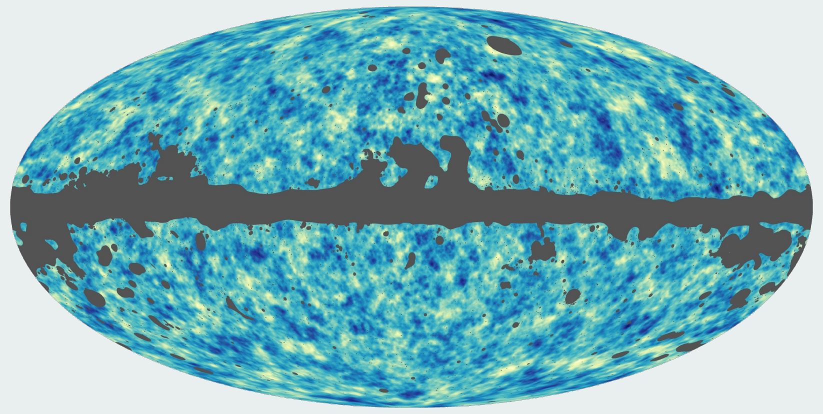

Lensing Convergence

Spin-2 Fields

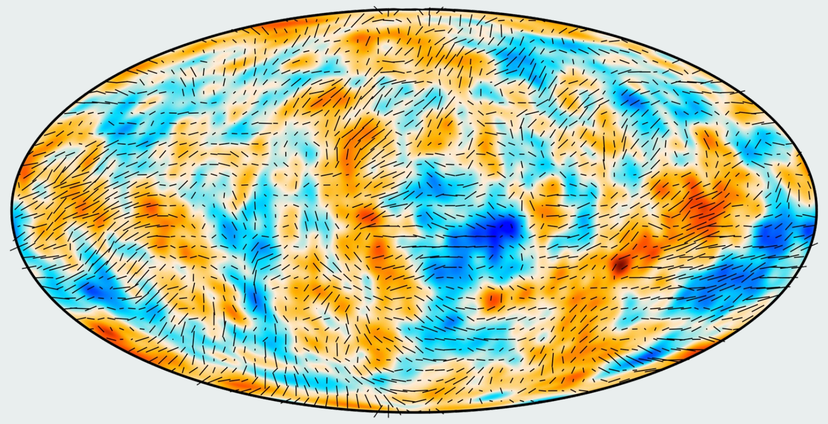

CMB Polarisation

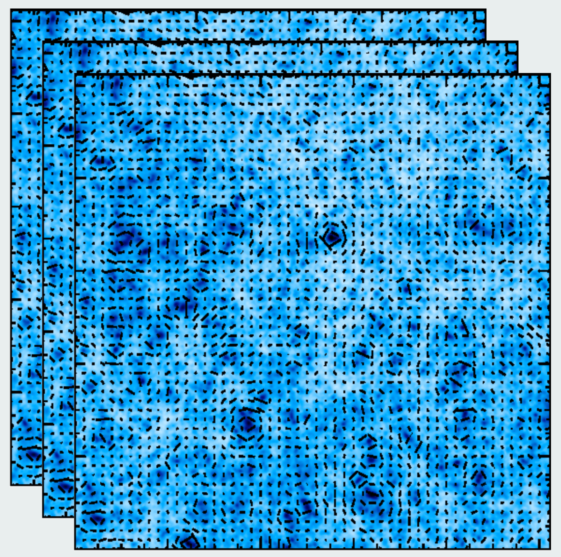

Cosmic Shear

Figures from Planck Collaboration, SDSS Collaboration & S. Pires et al. 2010

Almanac

Directed Acyclical Graph & posterior

$$\mathcal{P}(\mathsf{C}, \boldsymbol{a}|\boldsymbol{d}, \mathsf{N}) \propto \mathcal{L}(\boldsymbol{d}|\boldsymbol{a}, \mathsf{N})\mathcal{G}(\boldsymbol{a}|\mathsf{C})\pi(\mathsf{C})$$

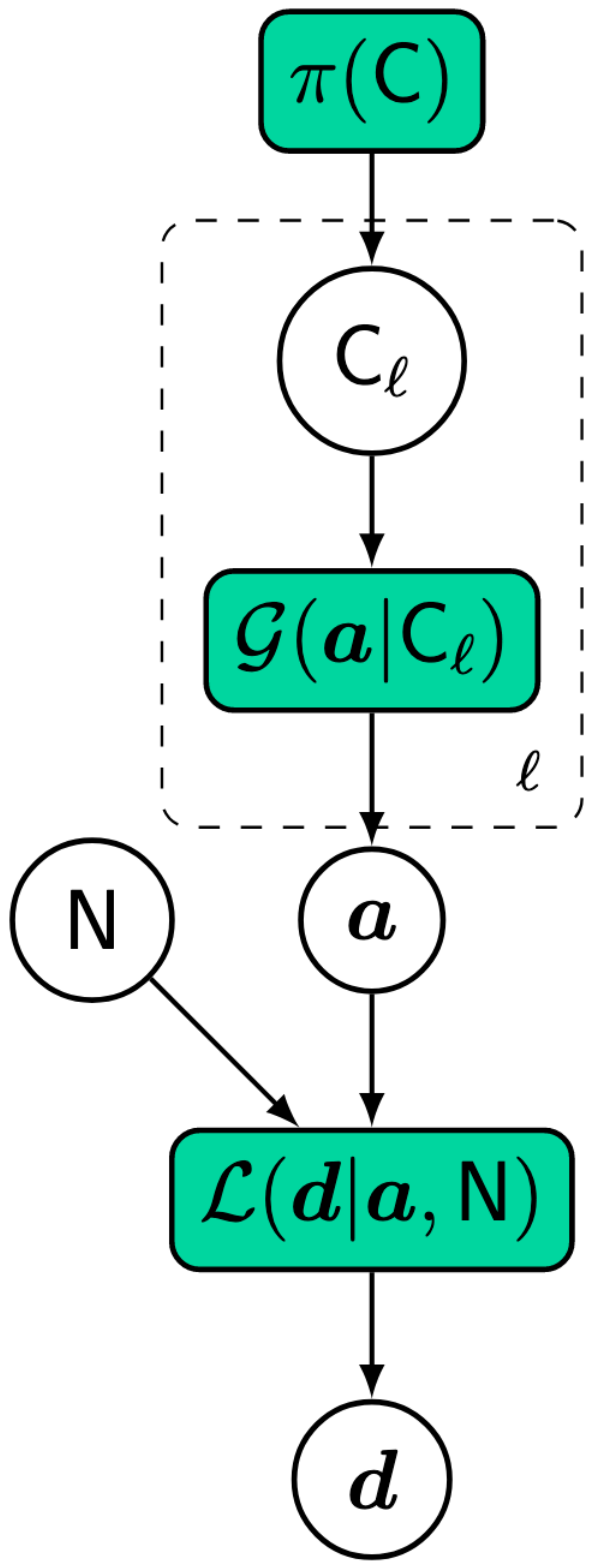

Alsing et al. 2015, Loureiro et al. 2022 (ArXiv:2210.13260), Sellentin, Loureiro et al, *in prep*

Almanac

Directed Acyclical Graph & posterior

$$\pi(\mathsf{C}) = |\mathsf{C}|^q$$

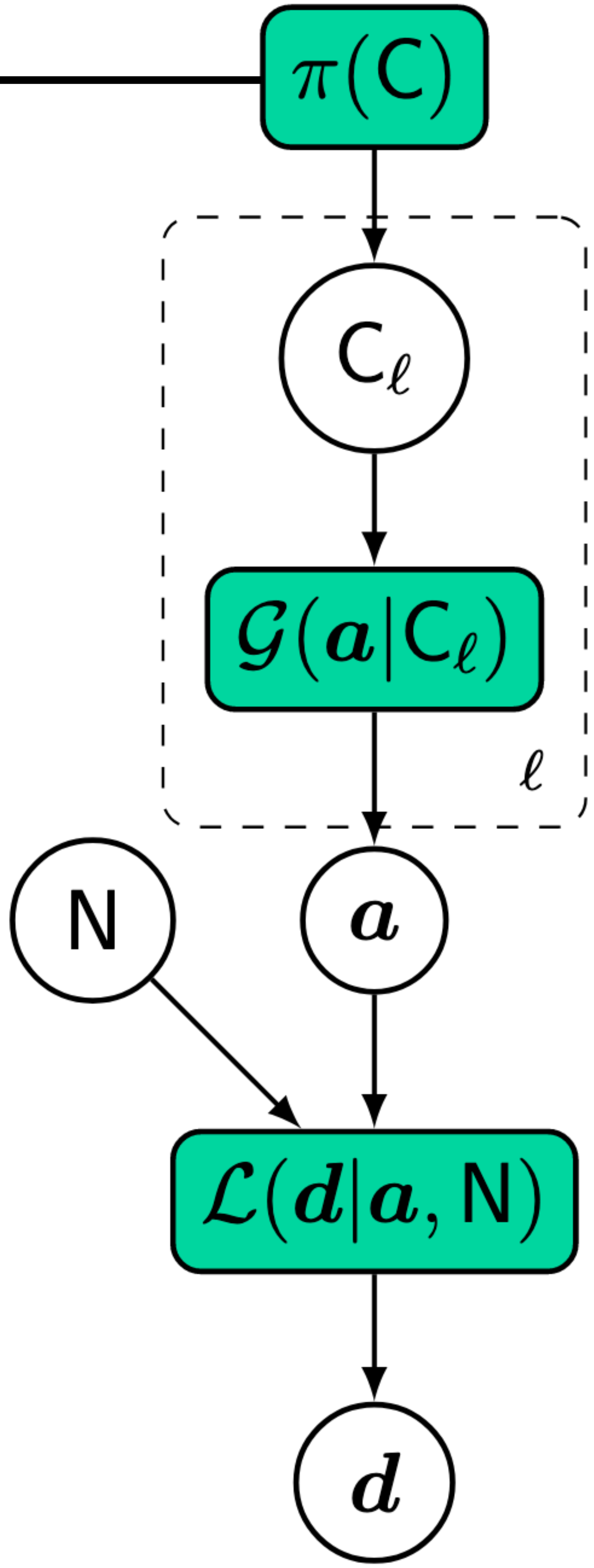

Loureiro et al. 2022 (ArXiv:2210.13260), Sellentin, Loureiro et al, *in prep*

Almanac

Directed Acyclical Graph & posterior

$$\pi(\mathsf{C}) = |\mathsf{C}|^q$$

$$\mathcal{G}(\boldsymbol{a}|\mathsf{C}) = \frac{1}{\sqrt{|2\pi\mathsf{C}|}} \exp\left(-\frac{1}{2}\boldsymbol{a}^{\mathrm{T}}\mathsf{C}^{-1}\boldsymbol{a}\right)$$

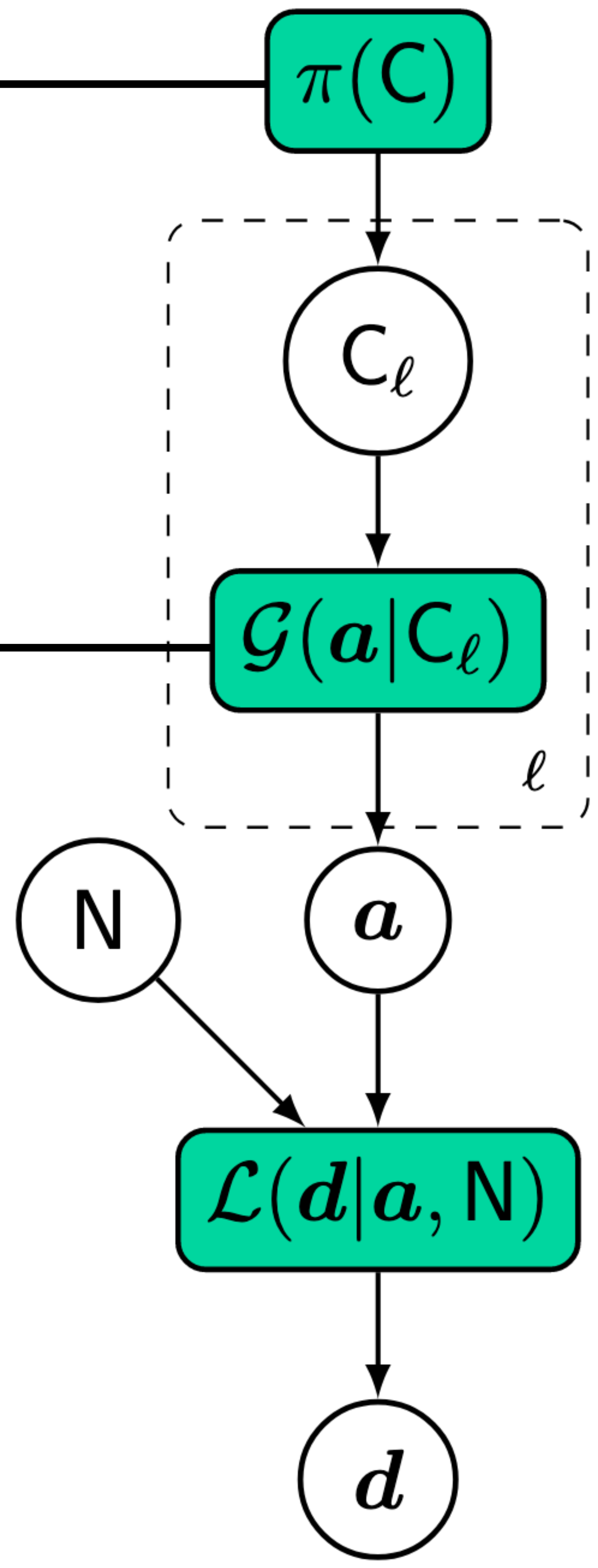

Loureiro et al. 2022 (ArXiv:2210.13260), Sellentin, Loureiro et al, *in prep*

Almanac

Directed Acyclical Graph & posterior

$$\pi(\mathsf{C}) = |\mathsf{C}|^q$$

$$\mathcal{G}(\boldsymbol{a}|\mathsf{C}) = \frac{1}{\sqrt{|2\pi \mathsf{C}|}} \exp\left(-\frac{1}{2}\boldsymbol{a}^{\mathrm{T}}\mathsf{C}^{-1}\boldsymbol{a}\right)$$

$$\mathcal{L}(\boldsymbol{d}|\boldsymbol{a},\mathsf{N}) \propto \exp\left[-\frac{1}{2}(\boldsymbol{d}-\mathsf{Y}\boldsymbol{a})^{\mathrm{T}}\mathsf{N}^{-1}(\boldsymbol{d}-\mathsf{Y}\boldsymbol{a})\right]$$

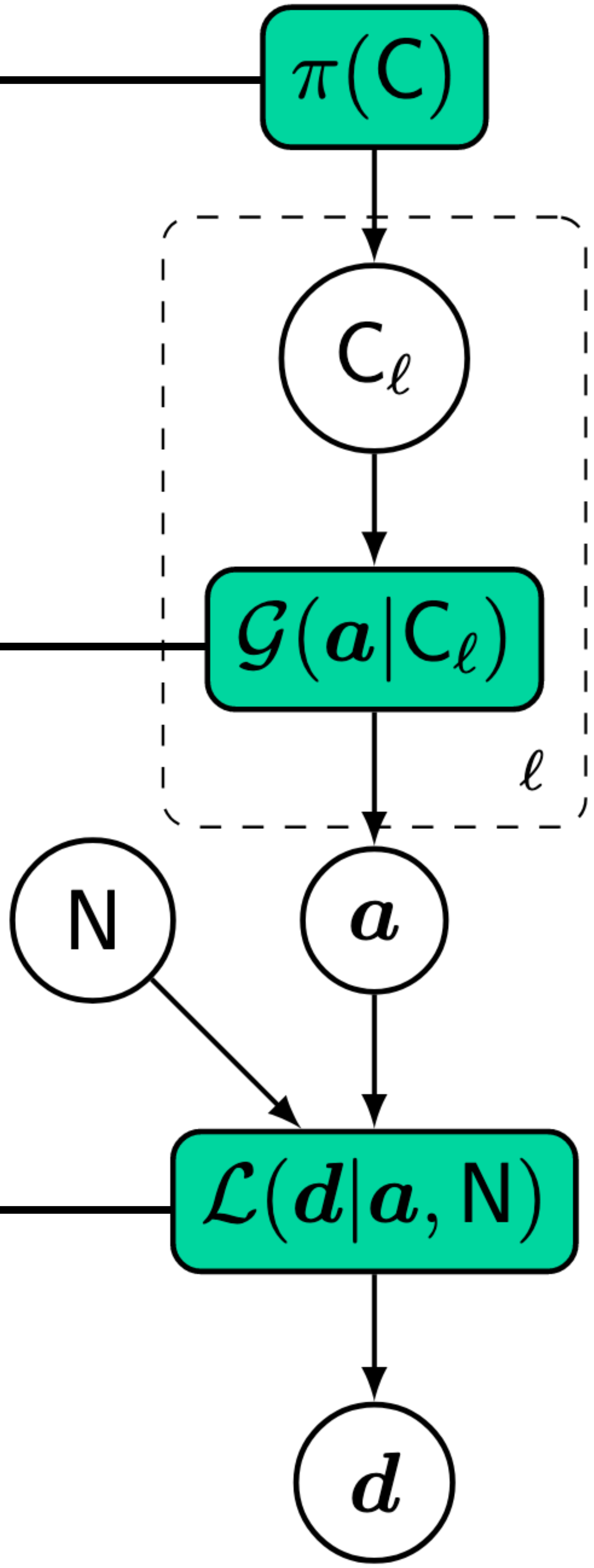

Loureiro et al. 2022 (ArXiv:2210.13260), Sellentin, Loureiro et al, *in prep*

Almanac

Directed Acyclical Graph & posterior

$$\pi(\mathsf{C}) = |\mathsf{C}|^q$$

Gaussian Prior DOES NOT mean a Gaussian posterior!!!

$$\mathcal{L}(\boldsymbol{d}|\boldsymbol{a},\mathsf{N}) \propto \exp\left[-\frac{1}{2}(\boldsymbol{d}-\mathsf{Y}\boldsymbol{a})^{\mathrm{T}}\mathsf{N}^{-1}(\boldsymbol{d}-\mathsf{Y}\boldsymbol{a})\right]$$

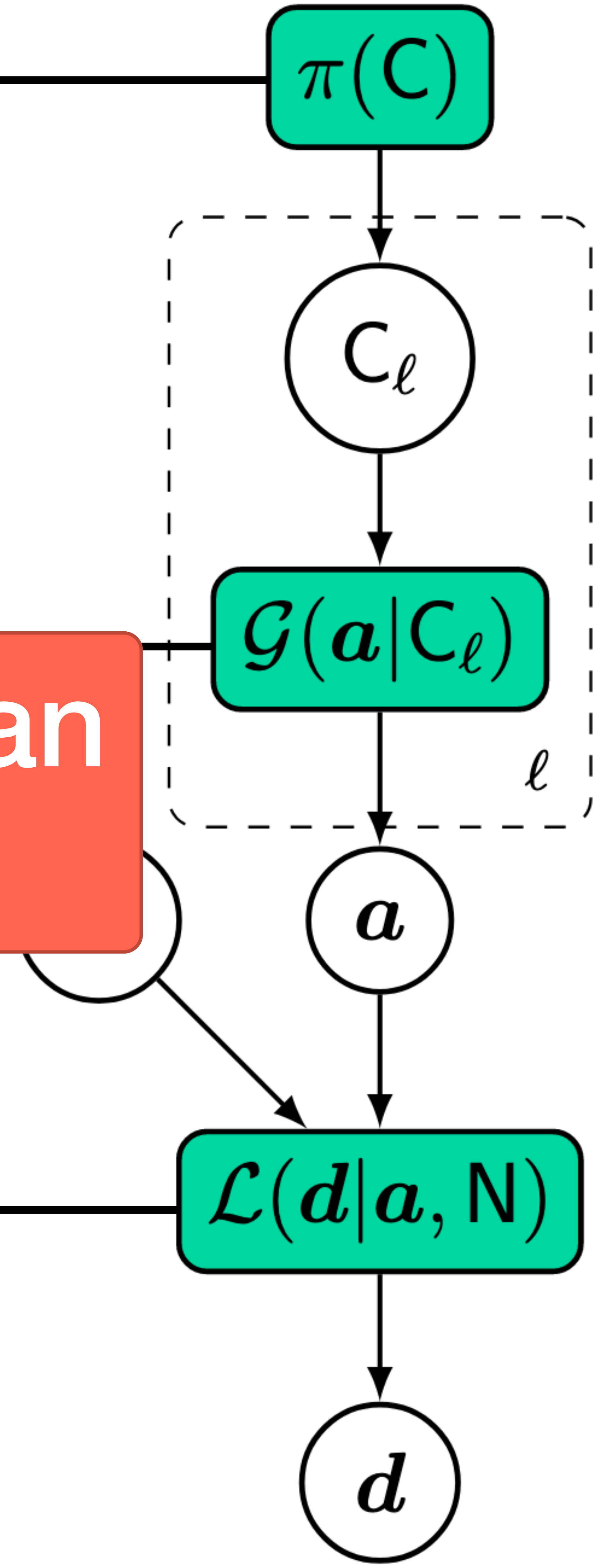

Loureiro et al. 2022 (ArXiv:2210.13260), Sellentin, Loureiro et al, *in prep*

Almanac

Directed Acyclical Graph & posterior

$$\mathcal{P}(\mathsf{C}, \boldsymbol{a}|\boldsymbol{d}, \mathsf{N}) \propto \mathcal{L}(\boldsymbol{d}|\boldsymbol{a}, \mathsf{N})\mathcal{G}(\boldsymbol{a}|\mathsf{C})\pi(\mathsf{C})$$

~ 10^6 - 10^8 parameters

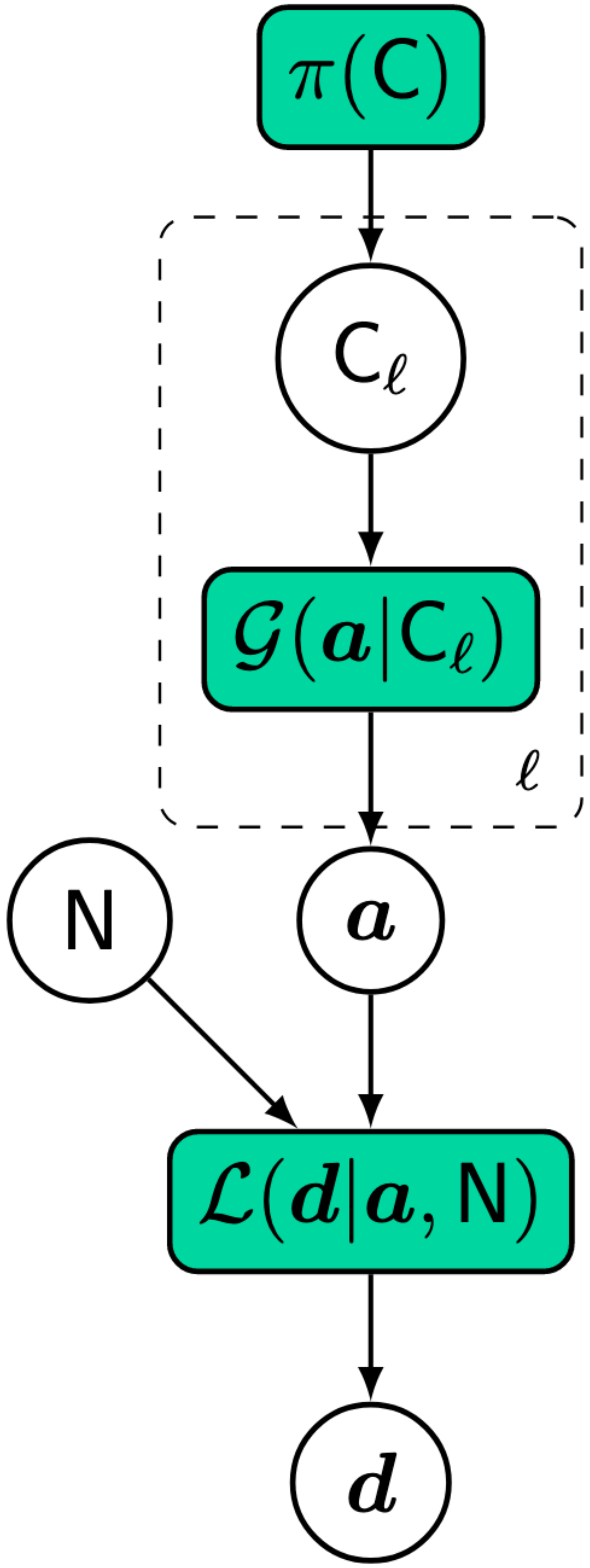

Loureiro et al. 2022 (ArXiv:2210.13260), Sellentin, Loureiro et al, *in prep*

4. Sampling High Dimensional Posteriors

Coordinate Transformations & the Tuned Hamiltonian Monte-Carlo

Hamiltonian Monte Carlo

- Explores the phase space using an analogy with dynamical systems with our parameters being the positions

$$\mathcal{H} = \sum_i^N \frac{p_i^2}{2m_i} + \Psi(\mathbf{a}, \mathbf{C}_\ell)$$

- The potential is related to the posterior:

$$\Psi(\mathbf{a}, \mathbf{C}_\ell) = -\ln p(\mathbf{a}, \mathbf{C}_\ell | \mathbf{d}, \mathbf{N})$$

- Evolves as a dynamical system with the momenta marginalized over

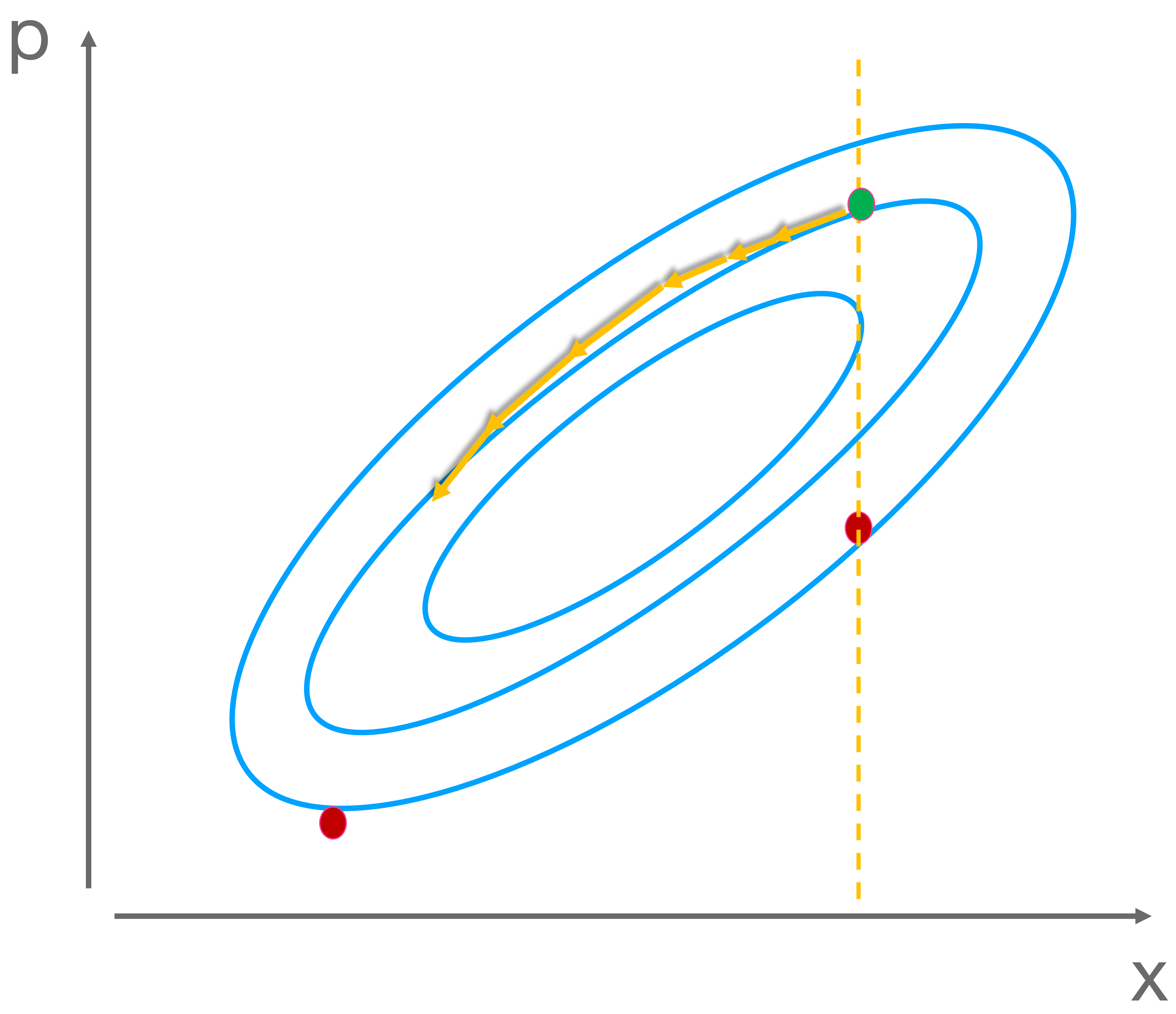

The sting-ray problem

- The C matrix needs to be positive definite

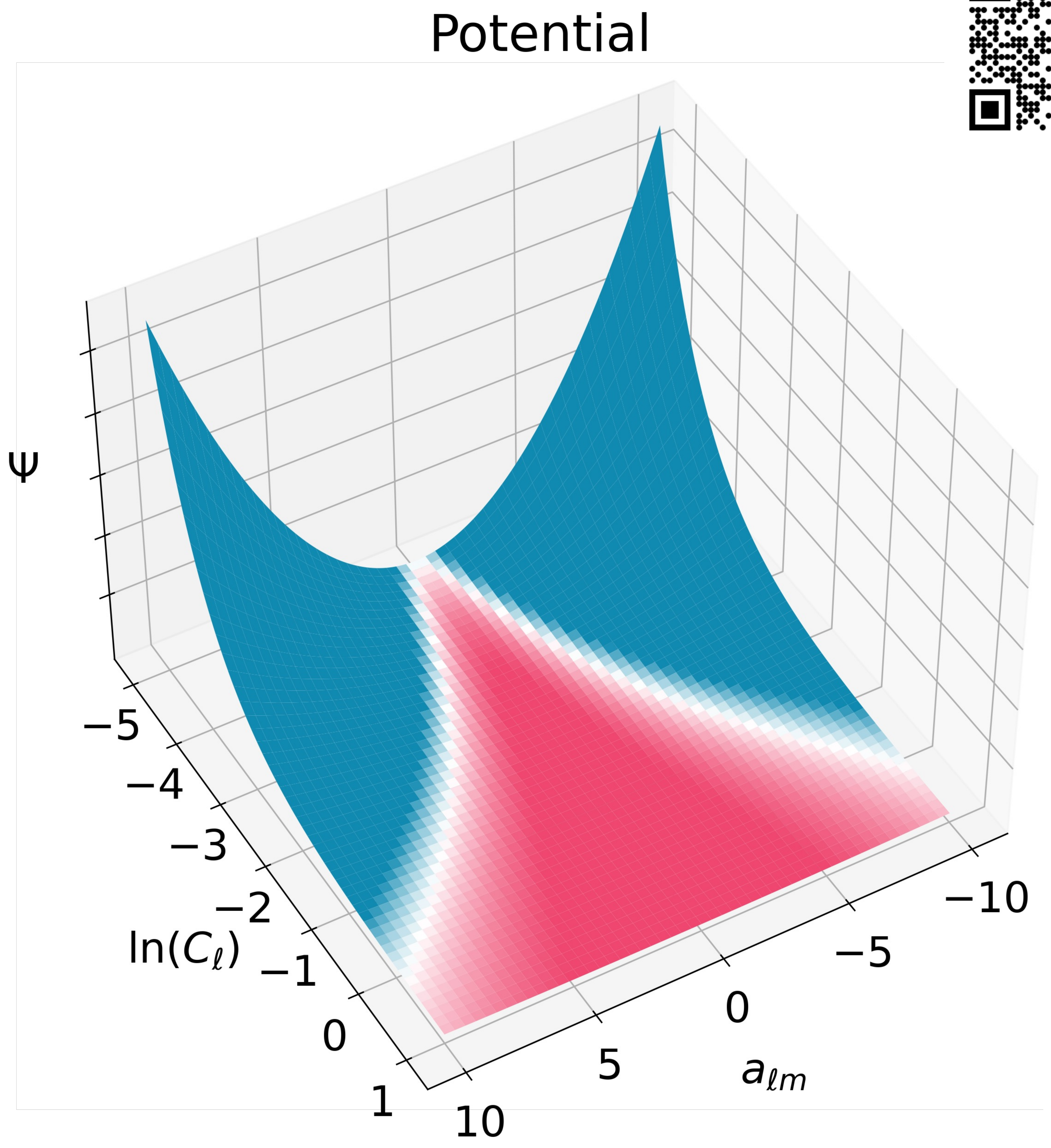

Loureiro et al., OJA,. 2023 (ArXiv:2210.13260)

The sting-ray problem

- The C matrix needs to be positive definite
- The most straightforward coordinate system to ensure this is using **a** and G = ln(C).

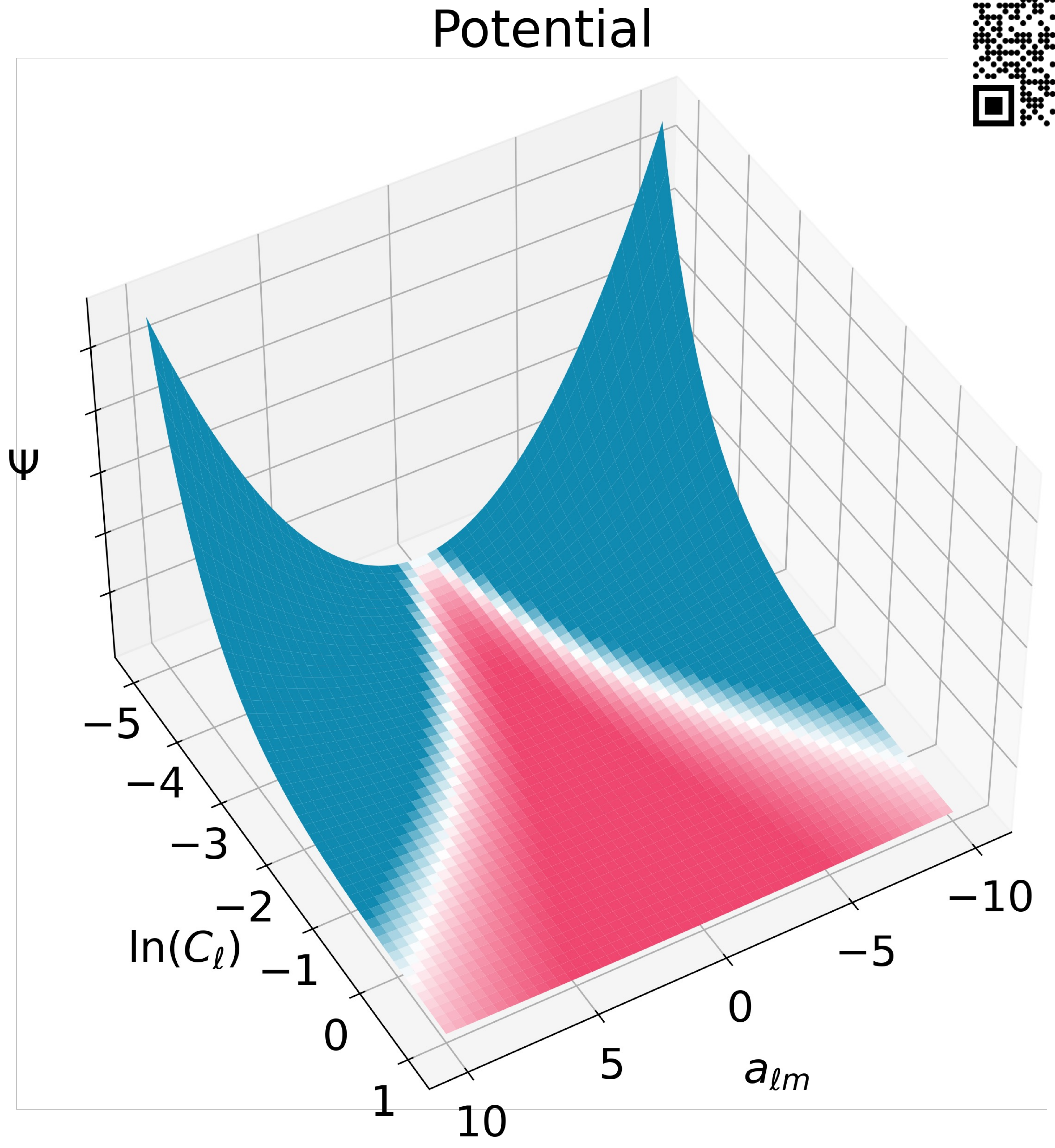

Loureiro et al., OJA,. 2023 (ArXiv:2210.13260)

The sting-ray problem

- The C matrix needs to be positive definite
- The most straightforward coordinate system to ensure this is using **a** and G = ln(C).
- However, we fall into the Sting-Ray (Neil's Funnel) posterior problem

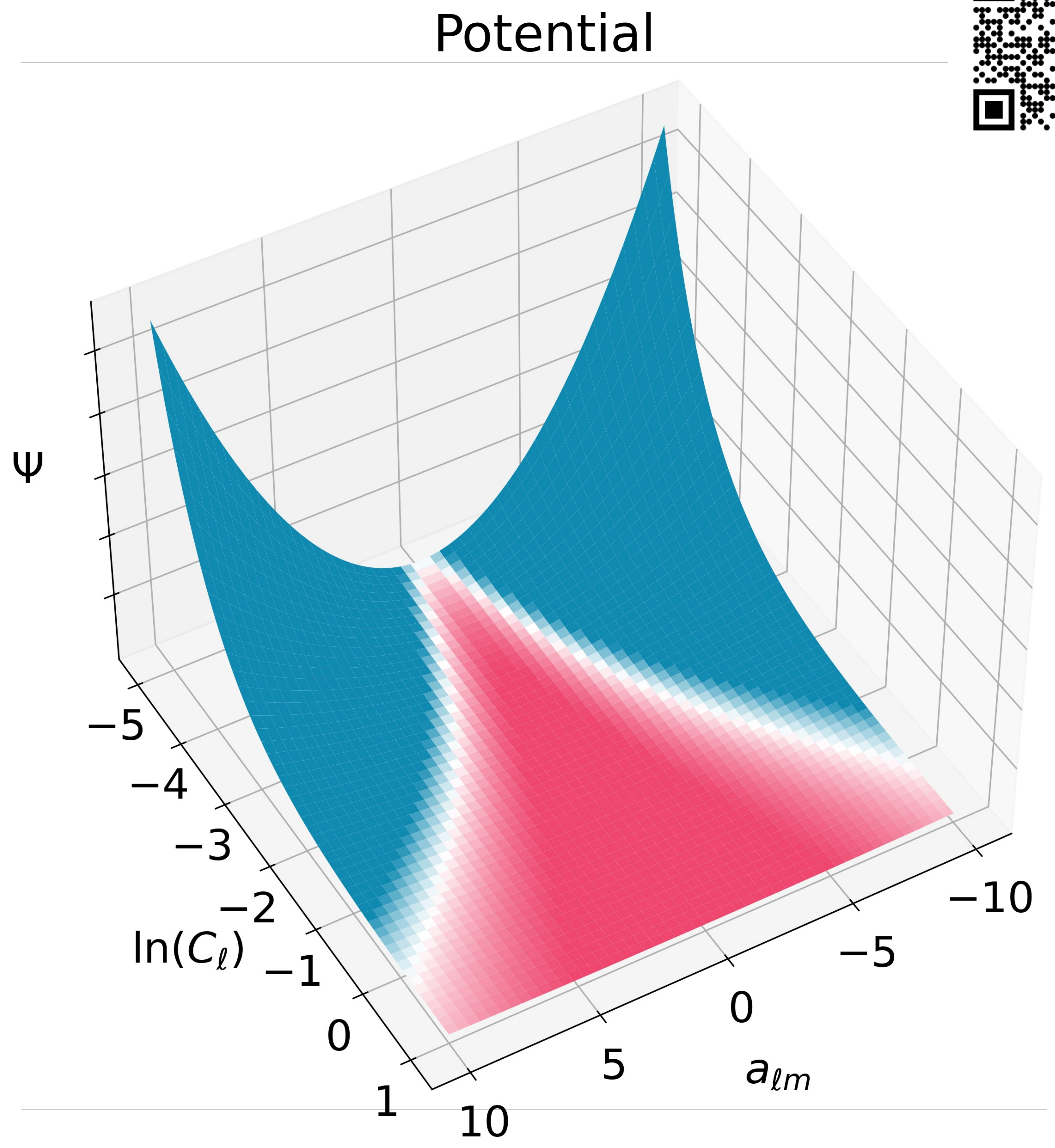

Loureiro et al., OJA,. 2023 (ArXiv:2210.13260)

The sting-ray problem

- The C matrix needs to be positive definite
- The most straightforward coordinate system to ensure this is using **a** and G = ln(C).
- However, we fall into the Sting-Ray (Neil’s Funnel) posterior problem
- Sampler becomes inefficient

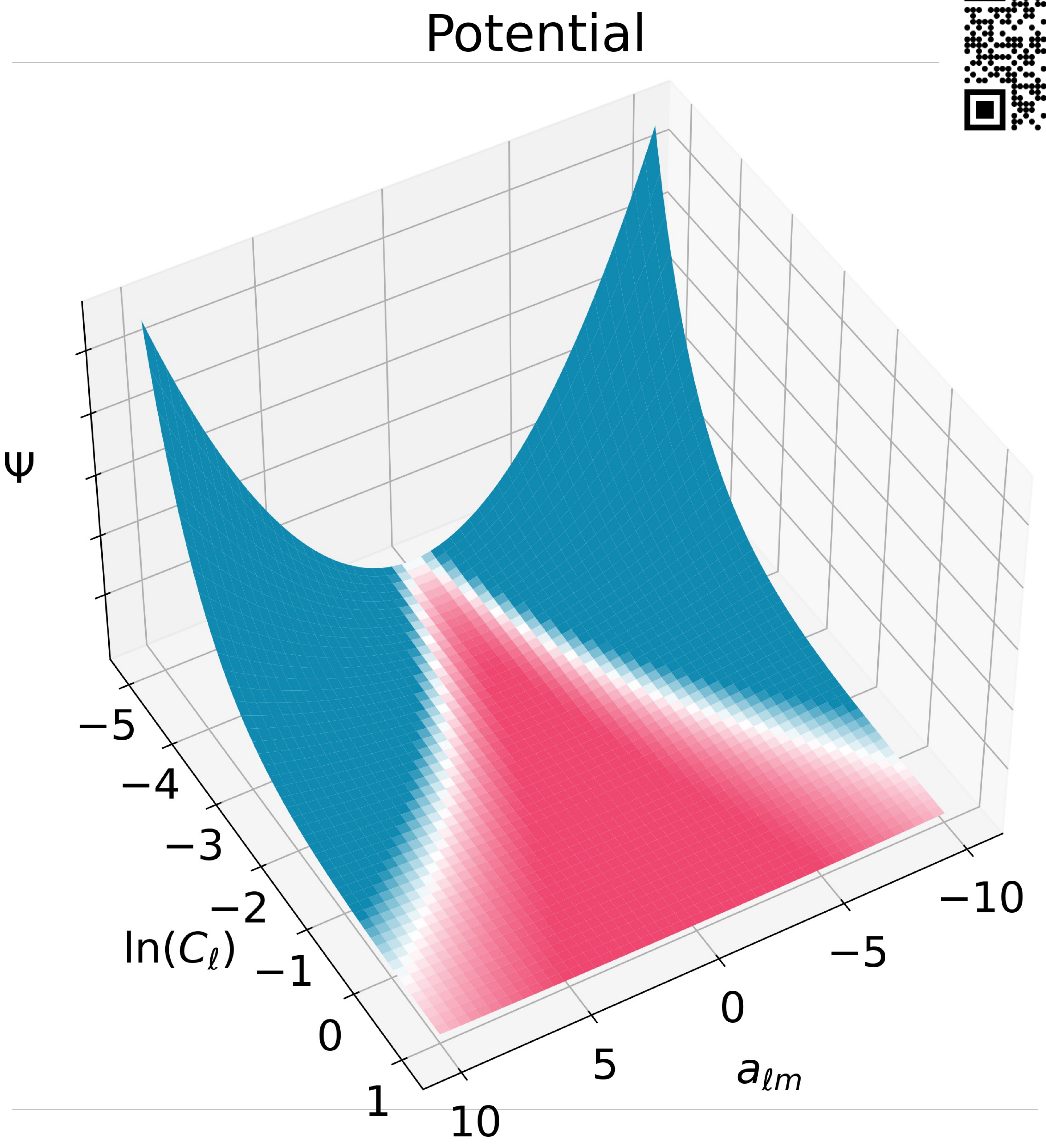

Loureiro et al., OJA,. 2023 (ArXiv:2210.13260)

The sting-ray problem: SOLVED

- Rescaling the fields by their standard deviation

$$\boldsymbol{x} = \mathsf{L}^{-1}\boldsymbol{a}$$

where $C=LL^T$

- Taking the diagonal-log of the Cholesky decomposed covariance

$$K_{\alpha\beta} = \begin{cases} \ln(L_{\alpha\beta}) & \text{if } \alpha = \beta\,, \\ L_{\alpha\beta} & \text{otherwise.} \end{cases}$$

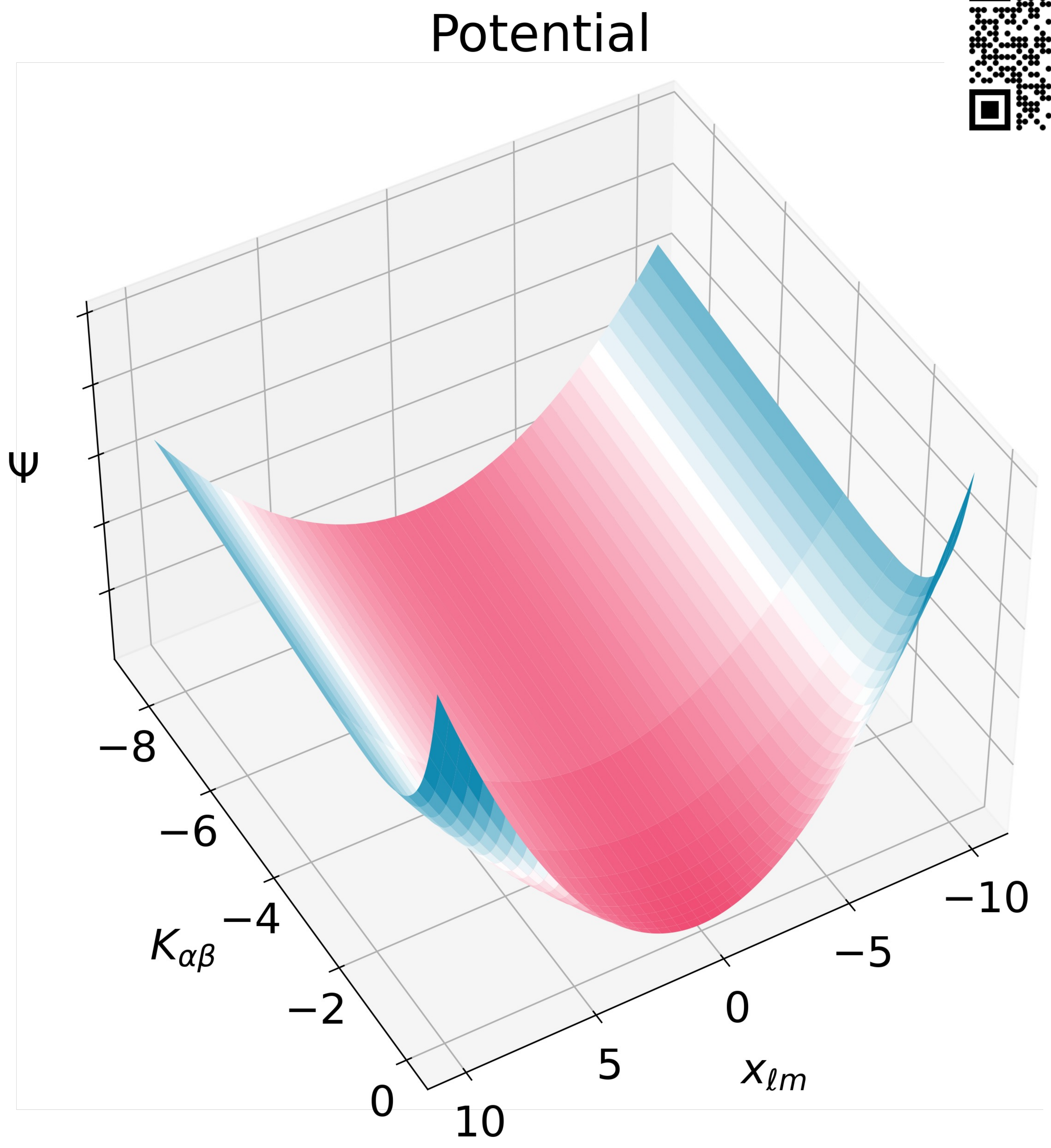

Coordinate System comparison

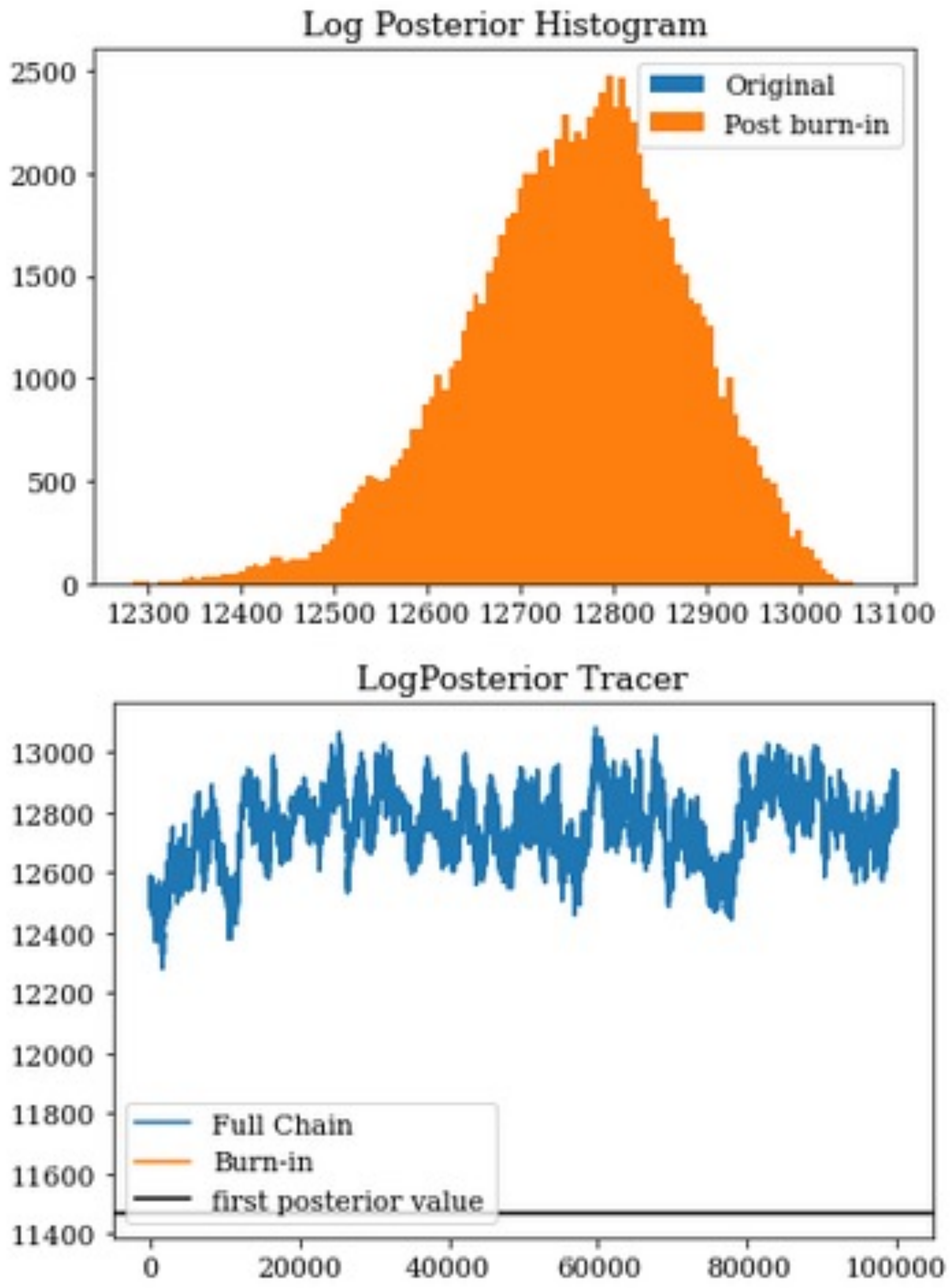

Naïve: $G_\ell = \log(C_\ell)$ & $a_{\ell m}$

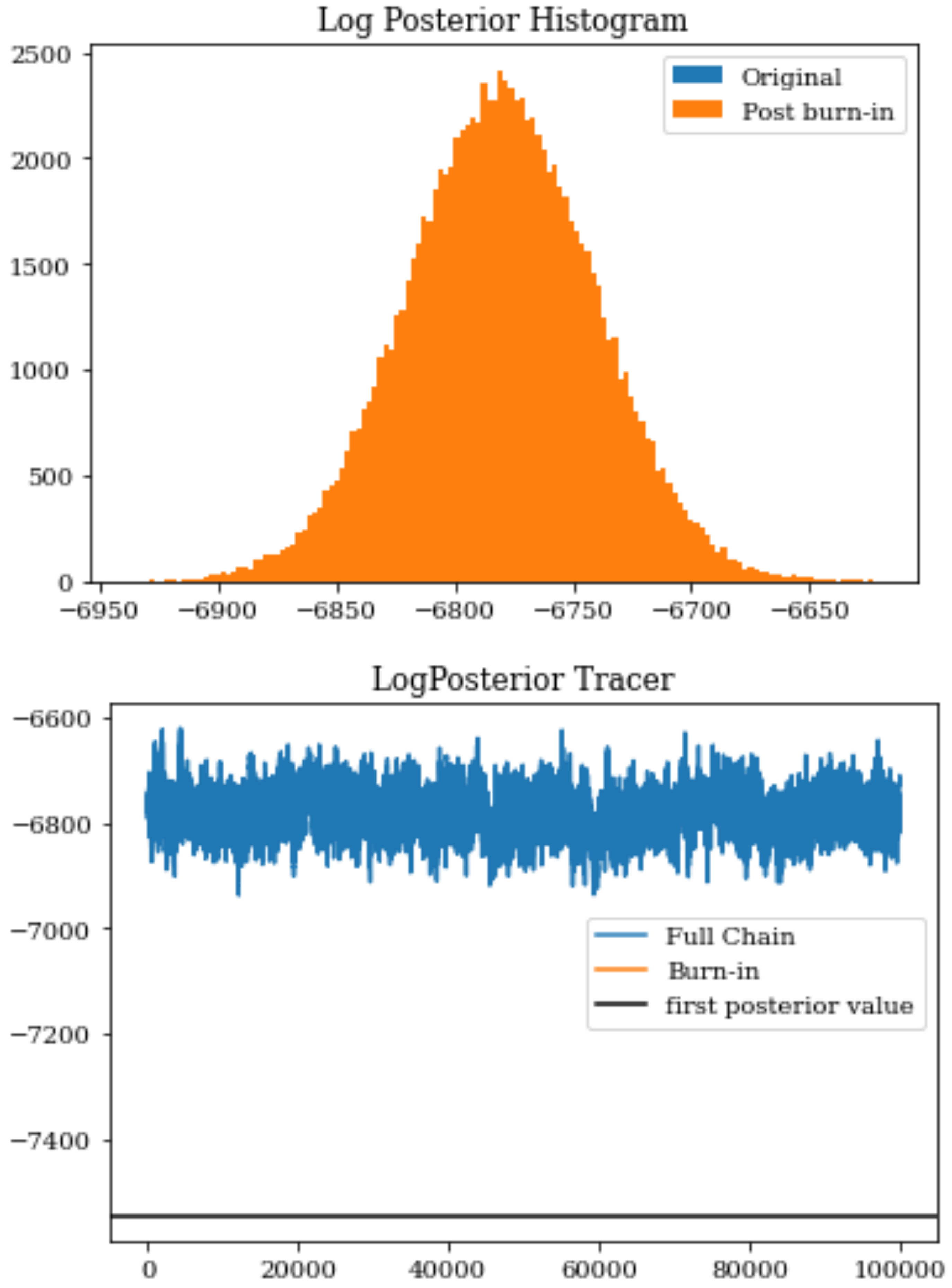

Cholesky: K_{ij} & $x_{\ell m} = L^{-1}\, a_{\ell m}$

Tuned HMC

Three phase tuning

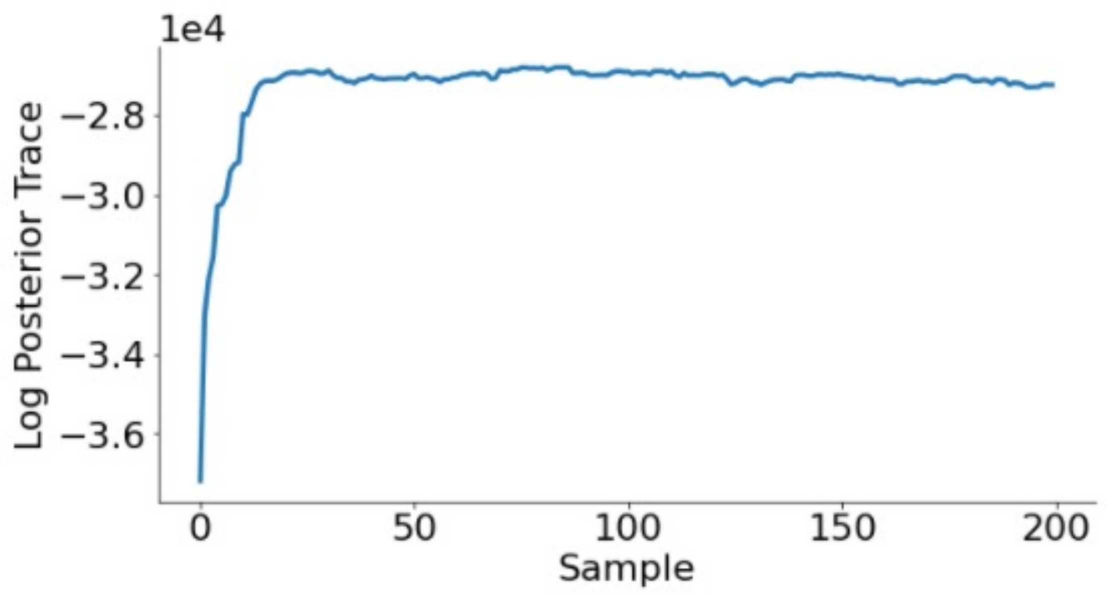

Burn in

Hessian as Step-Sizes

$$\mathcal{E} = \eta \left(\frac{\partial^2 \psi}{\partial \mathbf{x}^2}\right)^{-1/2}$$

Loureiro et al., OJA, 2023 (ArXiv:2210.13260), Sellentin, Loureiro et al. *in prep*

Tuned HMC

Three phase tuning

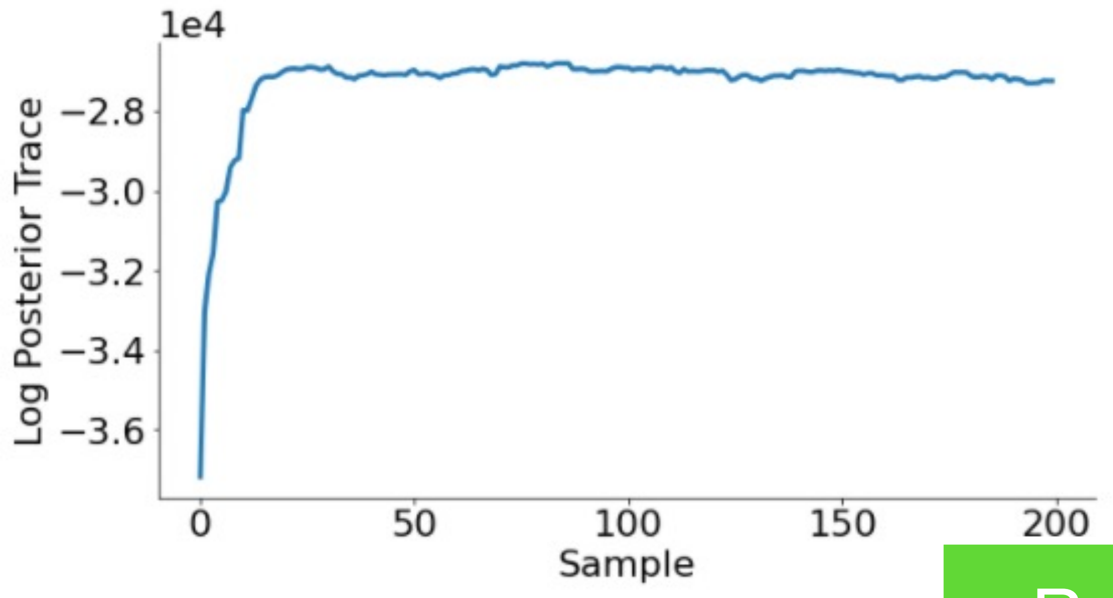

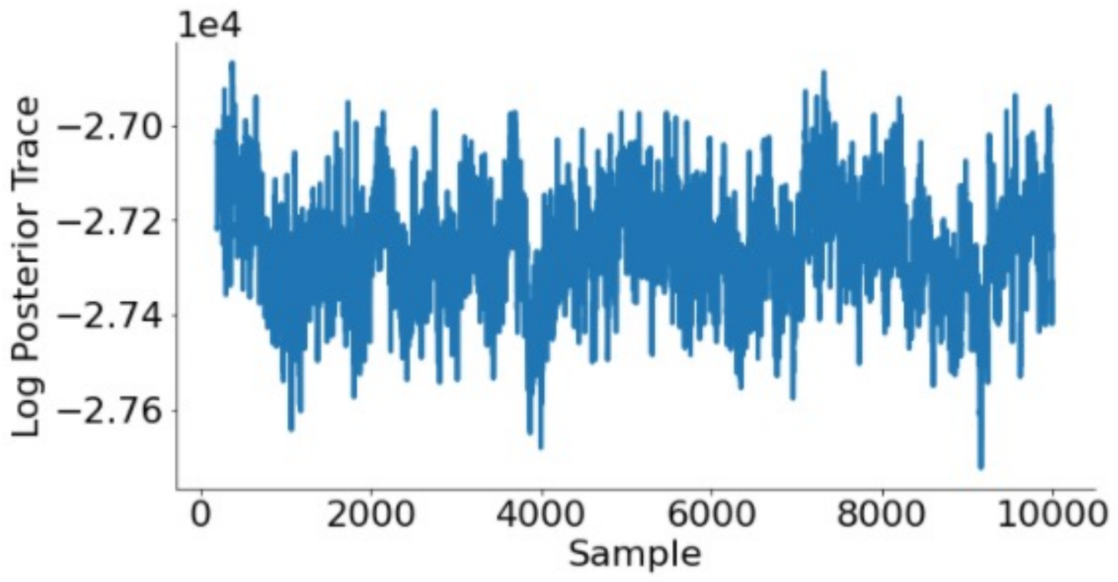

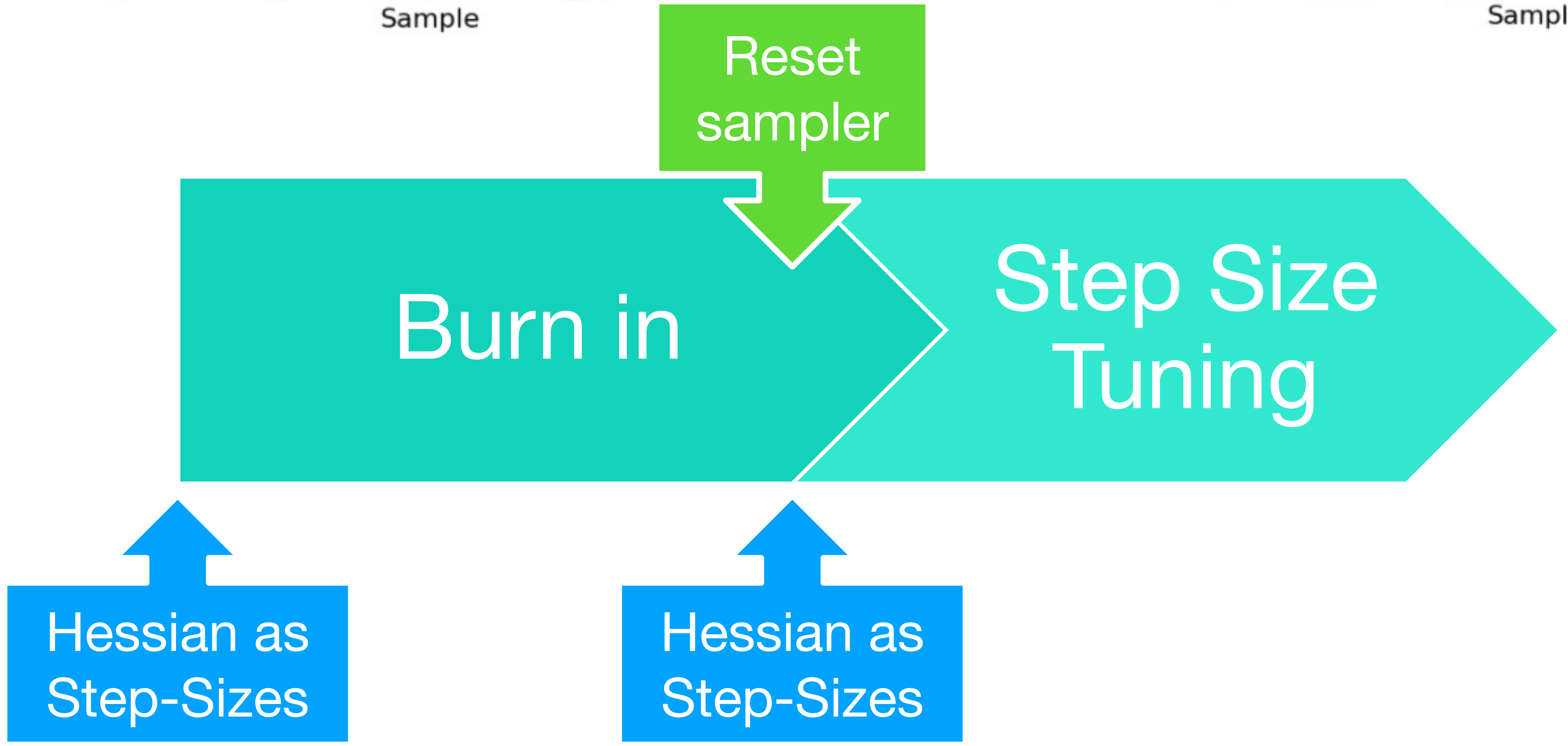

$$\mathcal{E} = \eta \left(\frac{\partial^2 \psi}{\partial \mathbf{x}^2} \right)^{-1/2}$$

Loureiro et al., OJA, 2023 (ArXiv:2210.13260), Sellentin, Loureiro et al. *in prep*

Tuned HMC

Three phase tuning

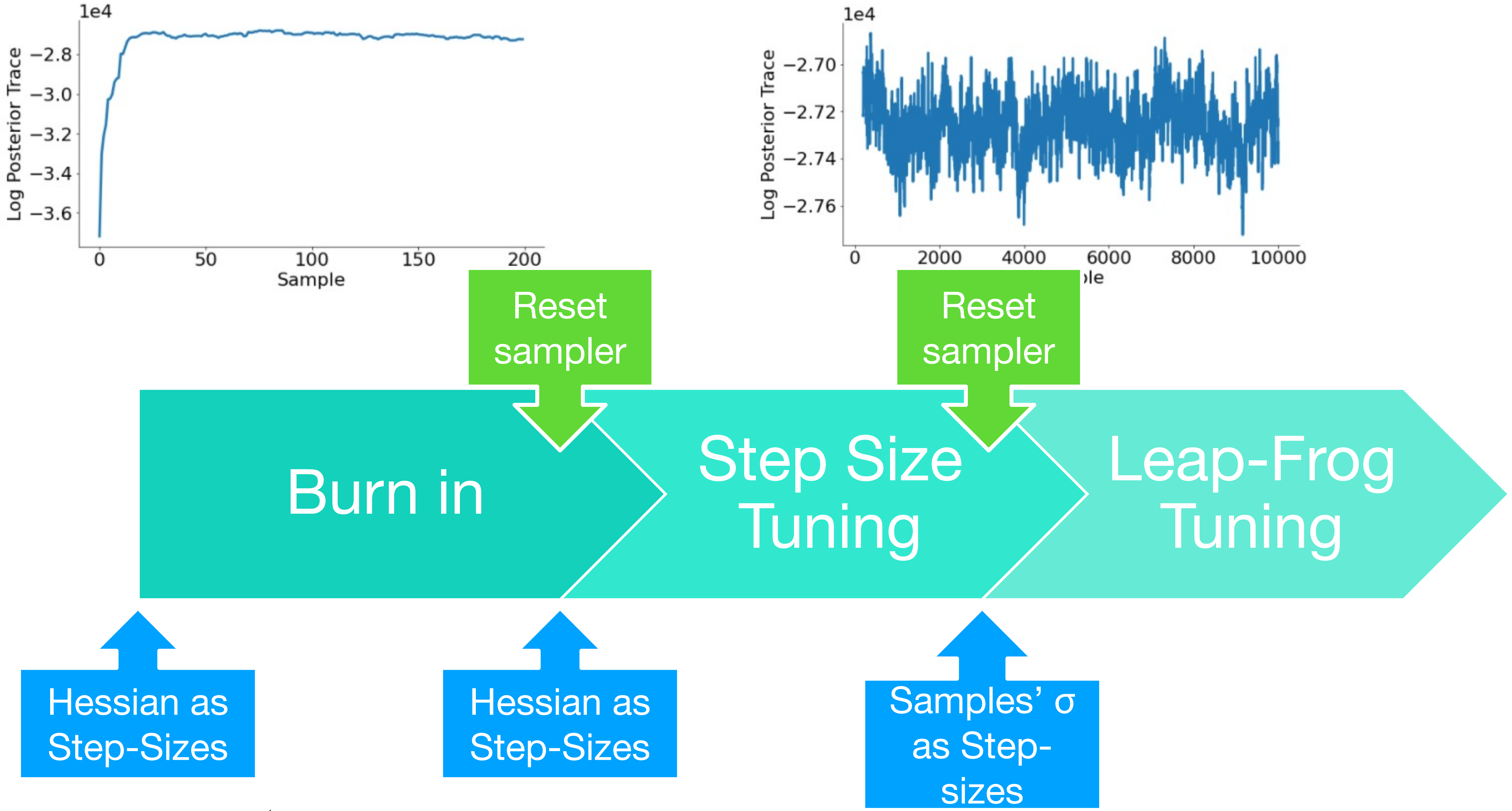

$$\mathcal{E} = \eta \left(\frac{\partial^2 \psi}{\partial \mathbf{x}^2} \right)^{-1/2}$$

Loureiro et al., OJA, 2023 (ArXiv:2210.13260), Sellentin, Loureiro et al. *in prep*

Tuned HMC

Three phase tuning

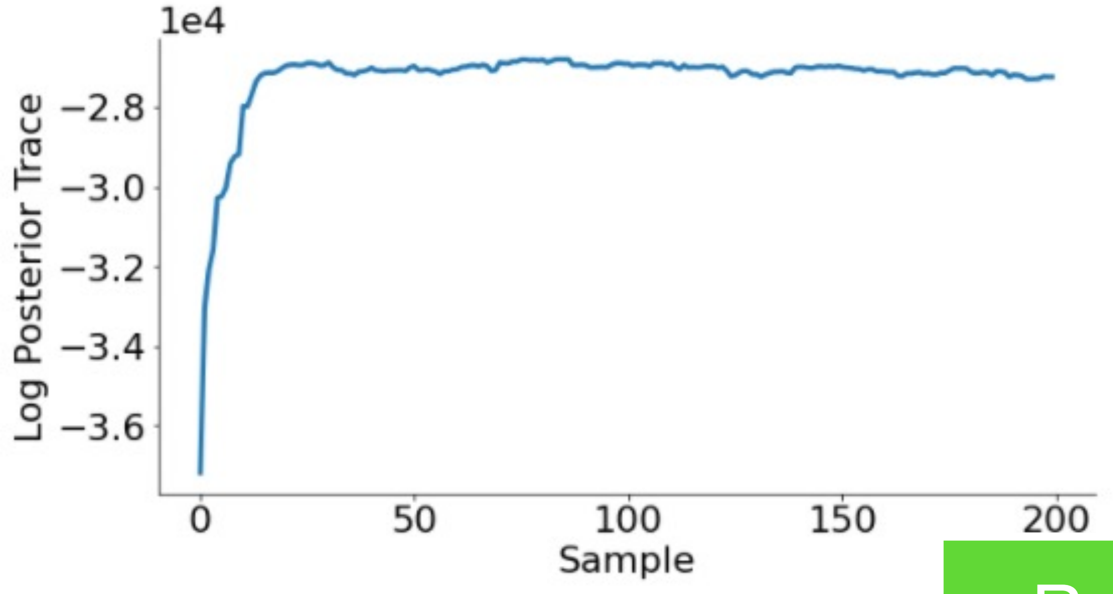

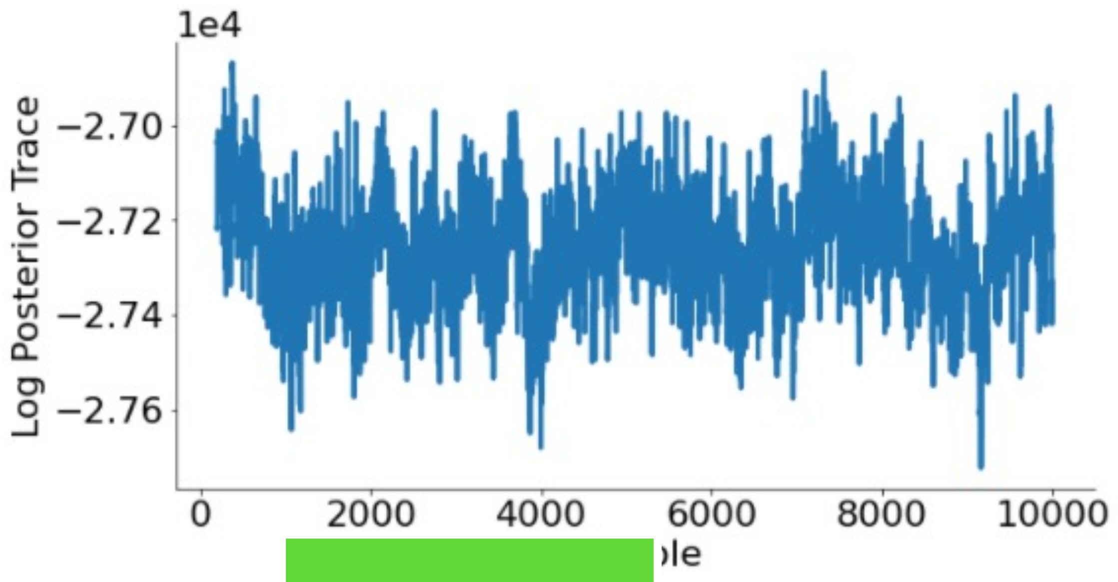

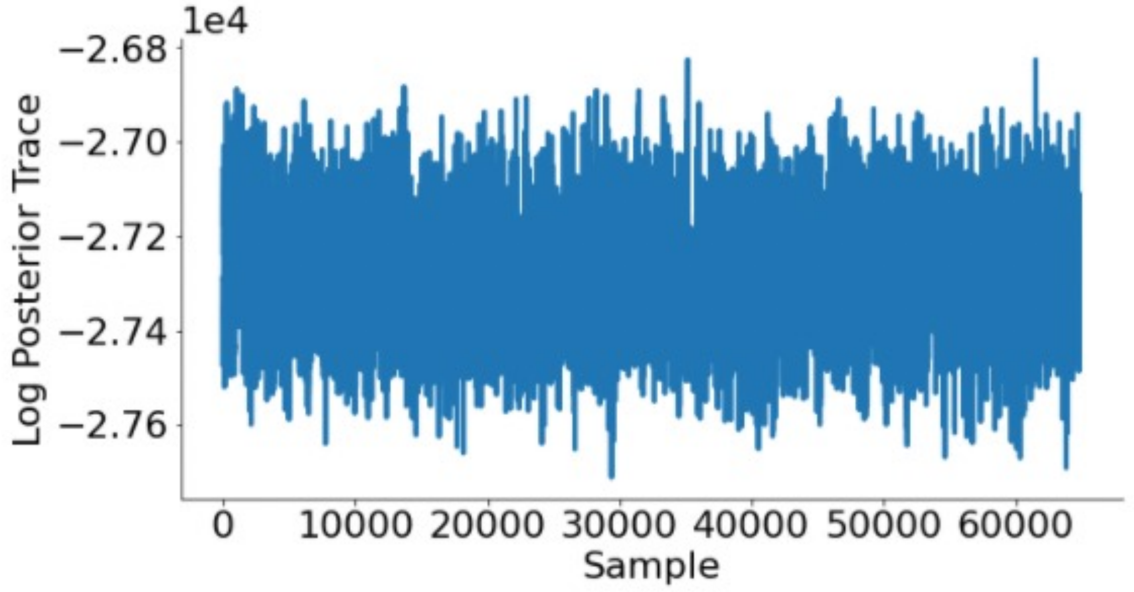

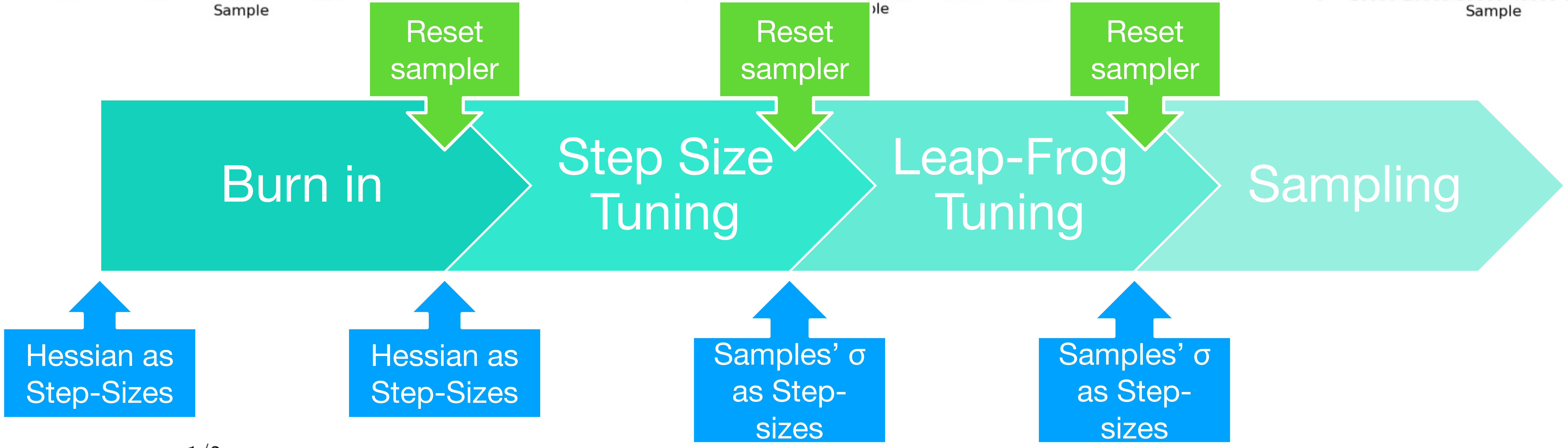

$$\mathcal{E} = \eta \left(\frac{\partial^2 \psi}{\partial \mathbf{x}^2} \right)^{-1/2}$$

Tuned HMC

Three phase tuning

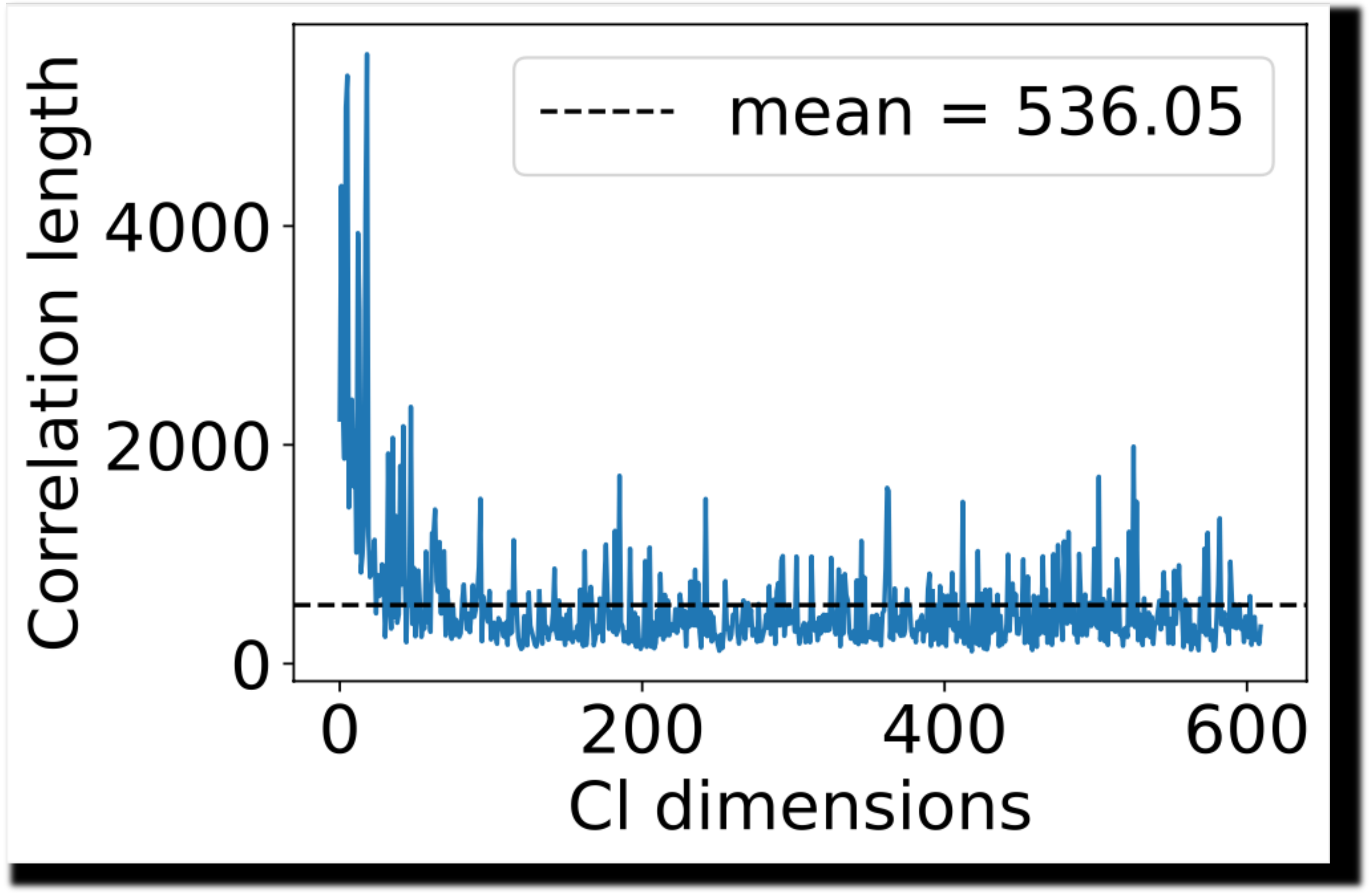

Normal HMC

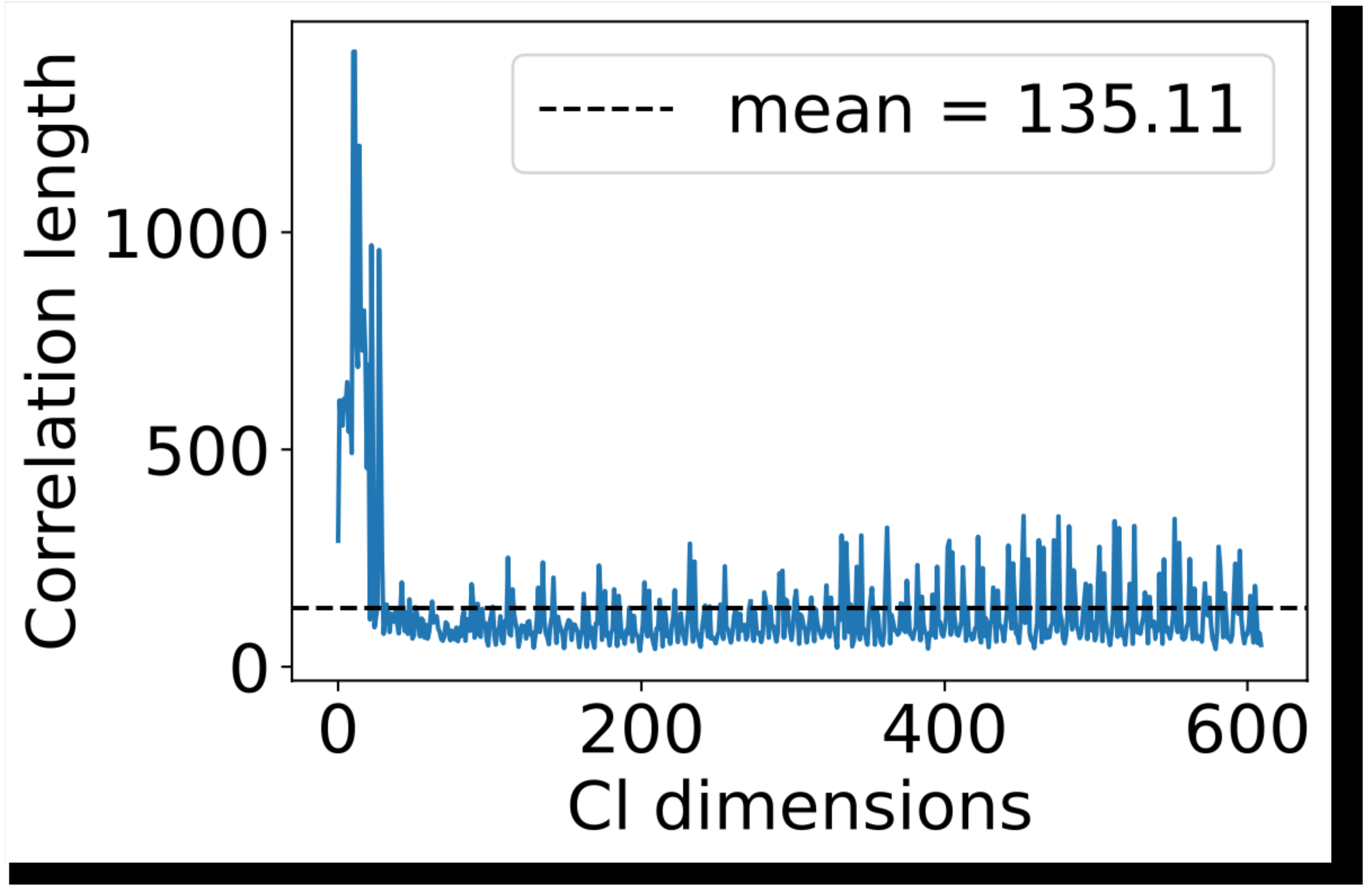

Tuned HMC

Sellentin, Loureiro et al. *in prep*

5. Applications to Weak Lensing

Simulated Euclid-like data

Weak Lensing

Euclid-like case

- Two tomographic bins
- Multipoles: 4, 2048
- Nside = 1024 (12.5M pixels)
- 16.8 Million free parameters; ~20k are C_ℓ
- Noise:
  - 3 gals/arcmin^2/bin
  - $\sigma(e) = 0.28$

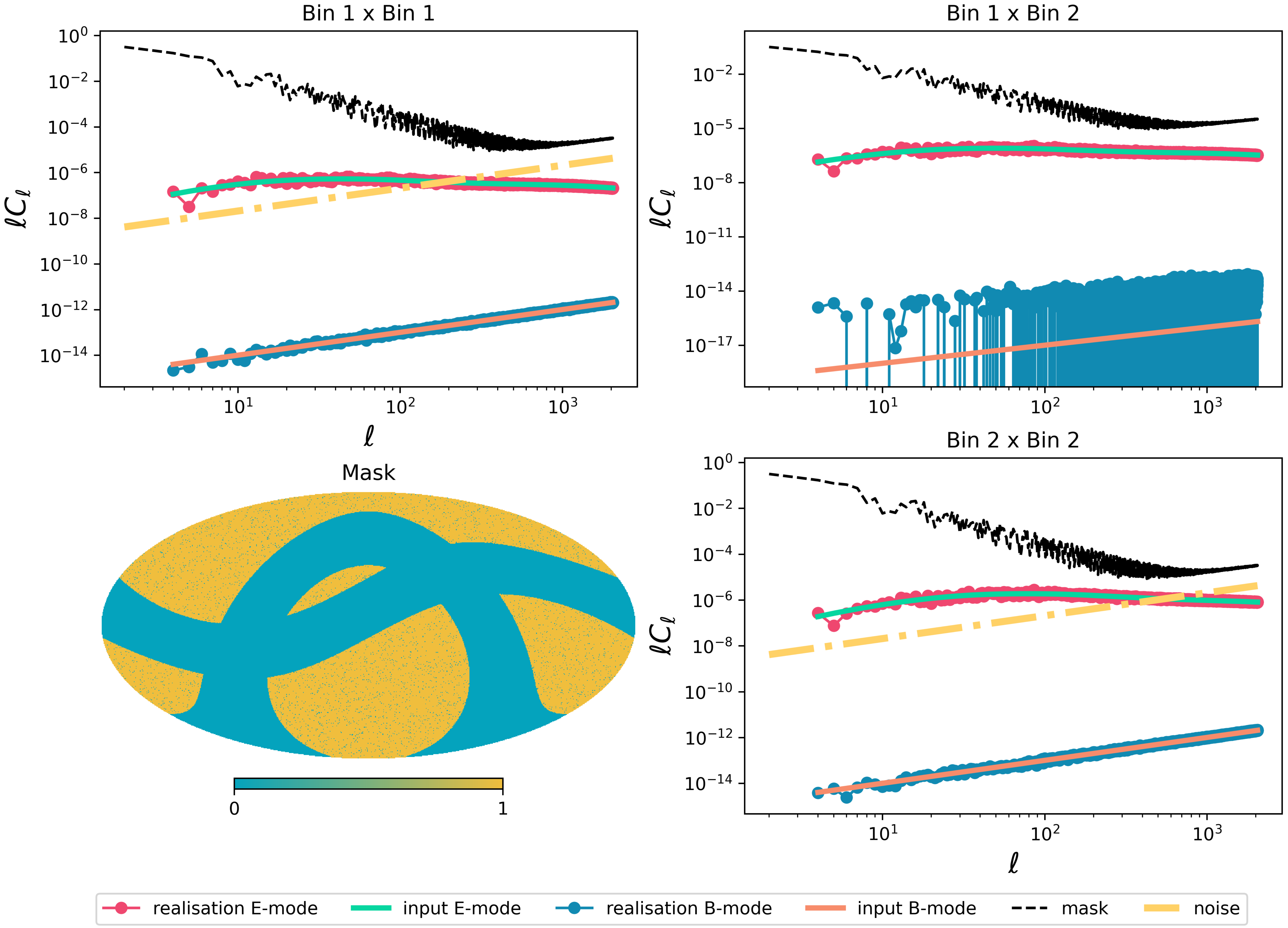

Loureiro et al., OJA,. 2023 (ArXiv:2210.13260)

Weak Lensing

Angular Power Spectra

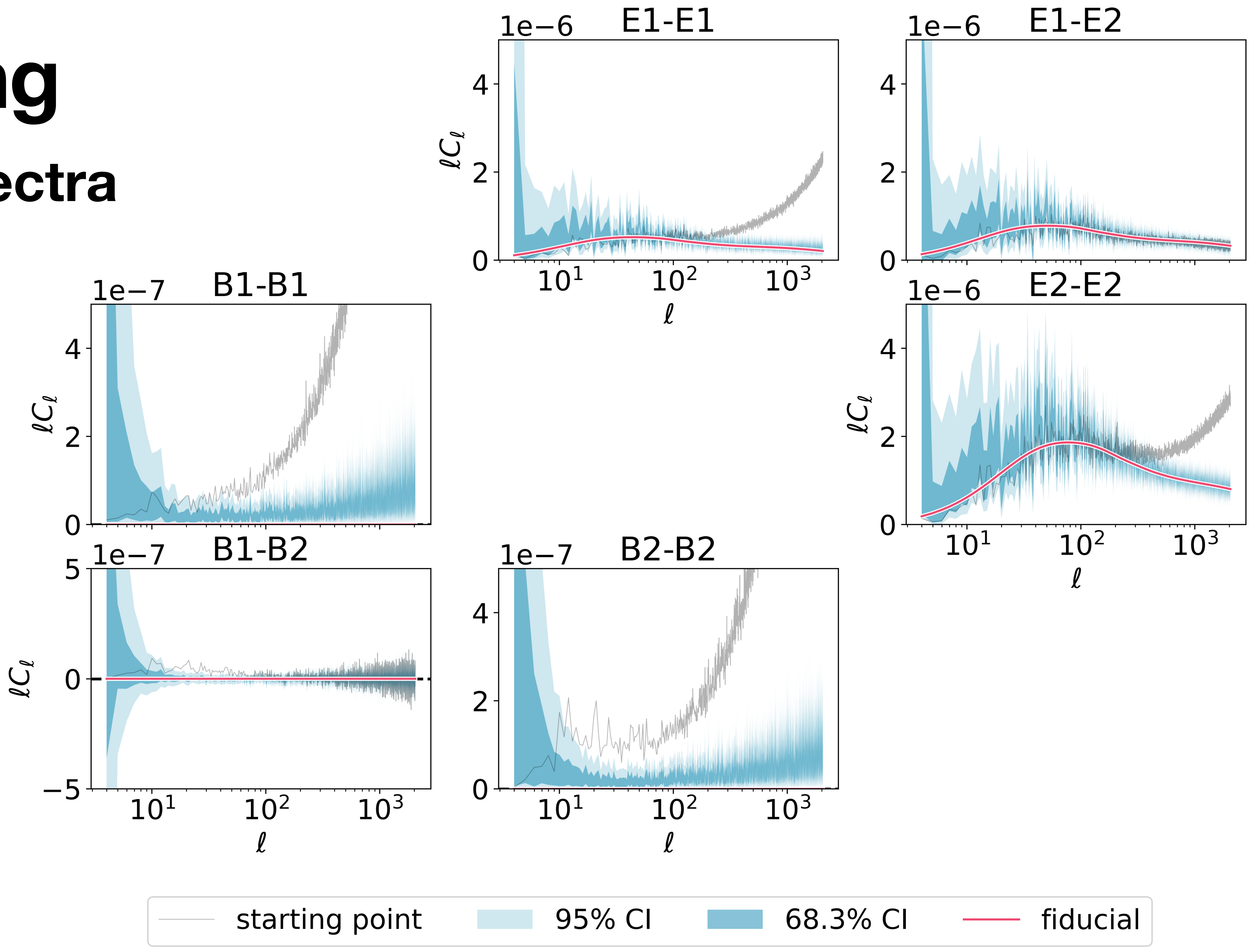

Loureiro et al., OJA,. 2023 (ArXiv:2210.13260)

Weak Lensing

Angular Power Spectra

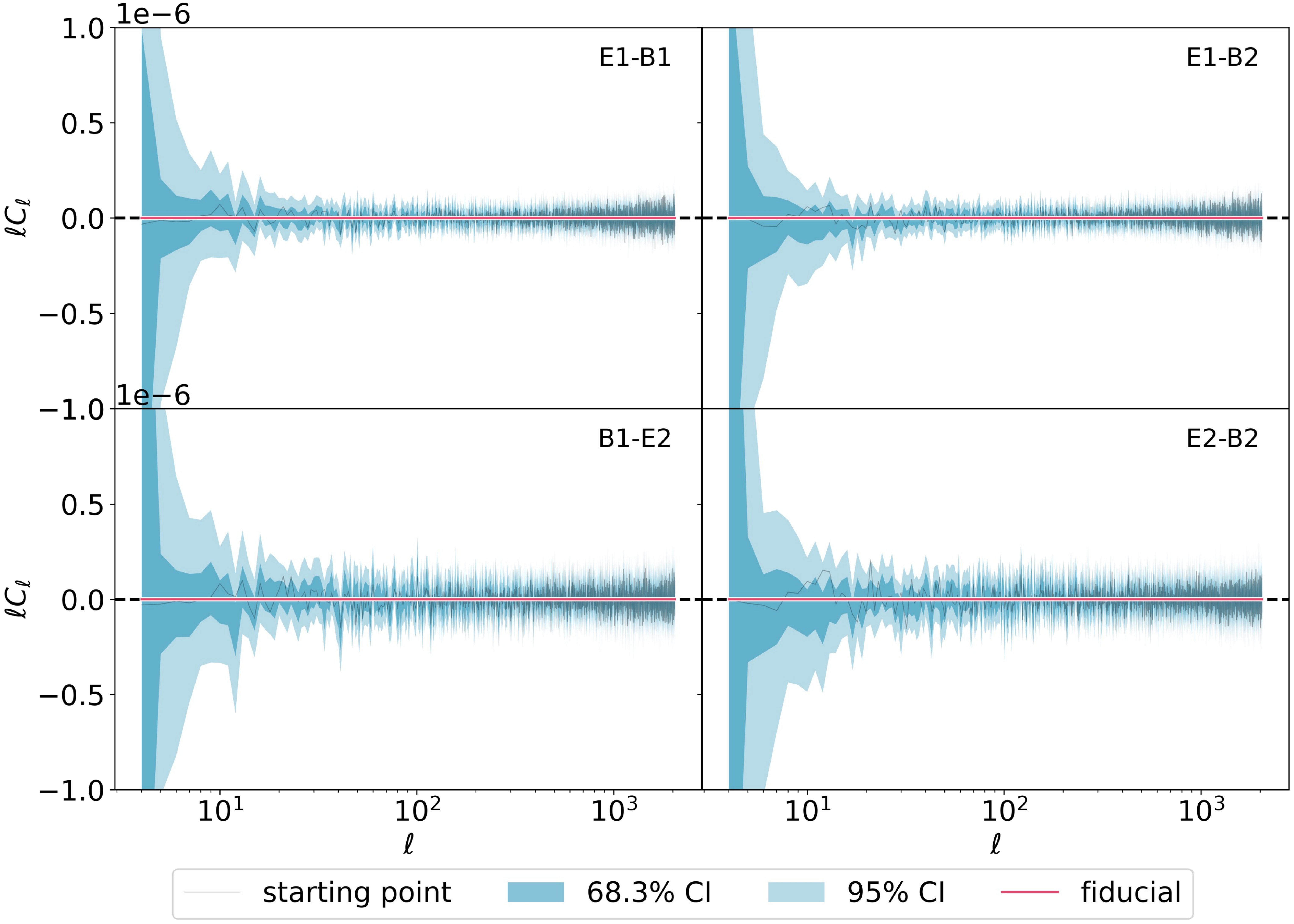

Loureiro et al., OJA,. 2023 (ArXiv:2210.13260)

Weak Lensing

Angular Power Spectra

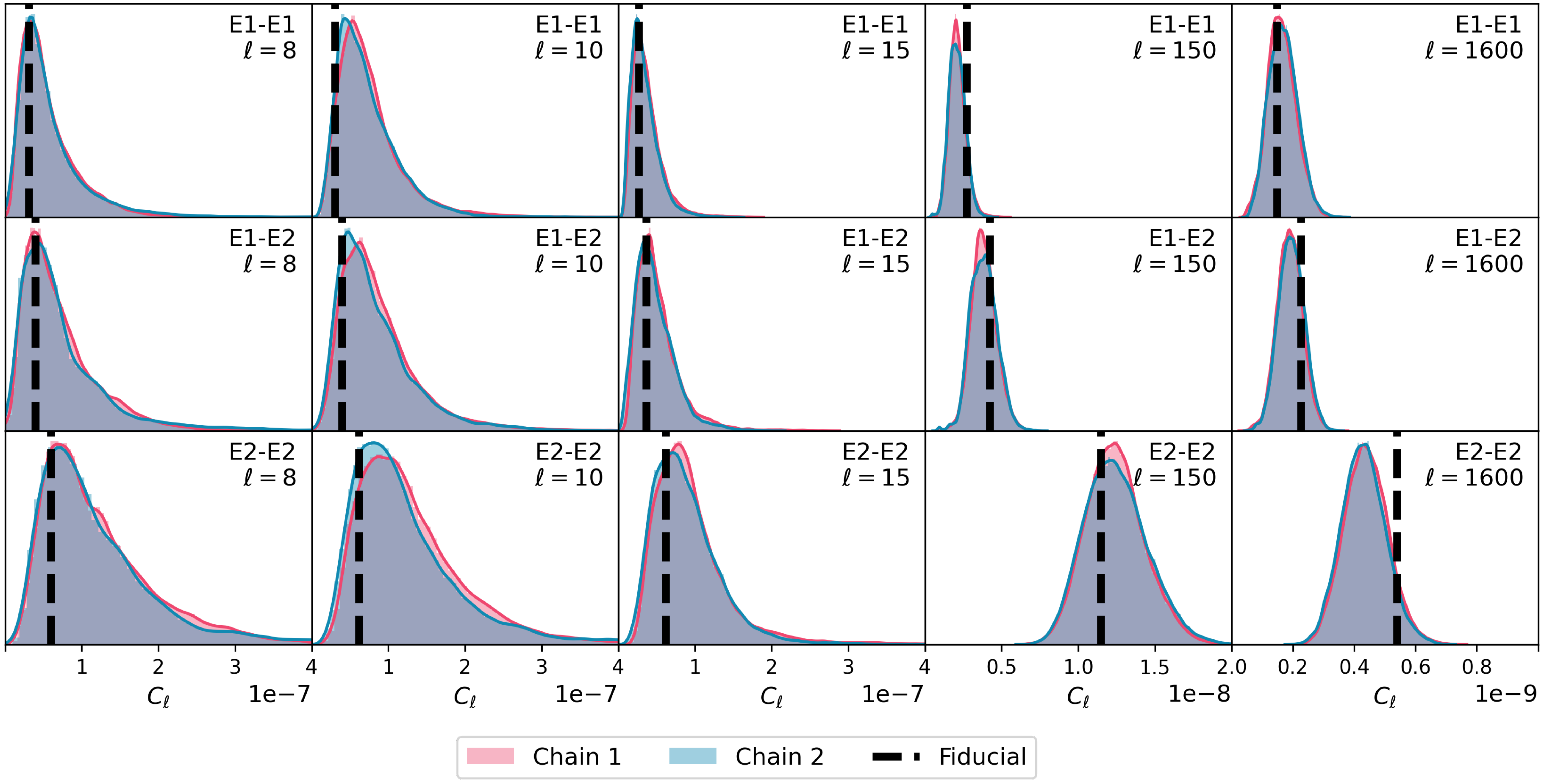

Loureiro et al., OJA,. 2023 (ArXiv:2210.13260)

Weak Lensing

E/B Correlations

Safe to use the point estimates,
no E/B leak detected!

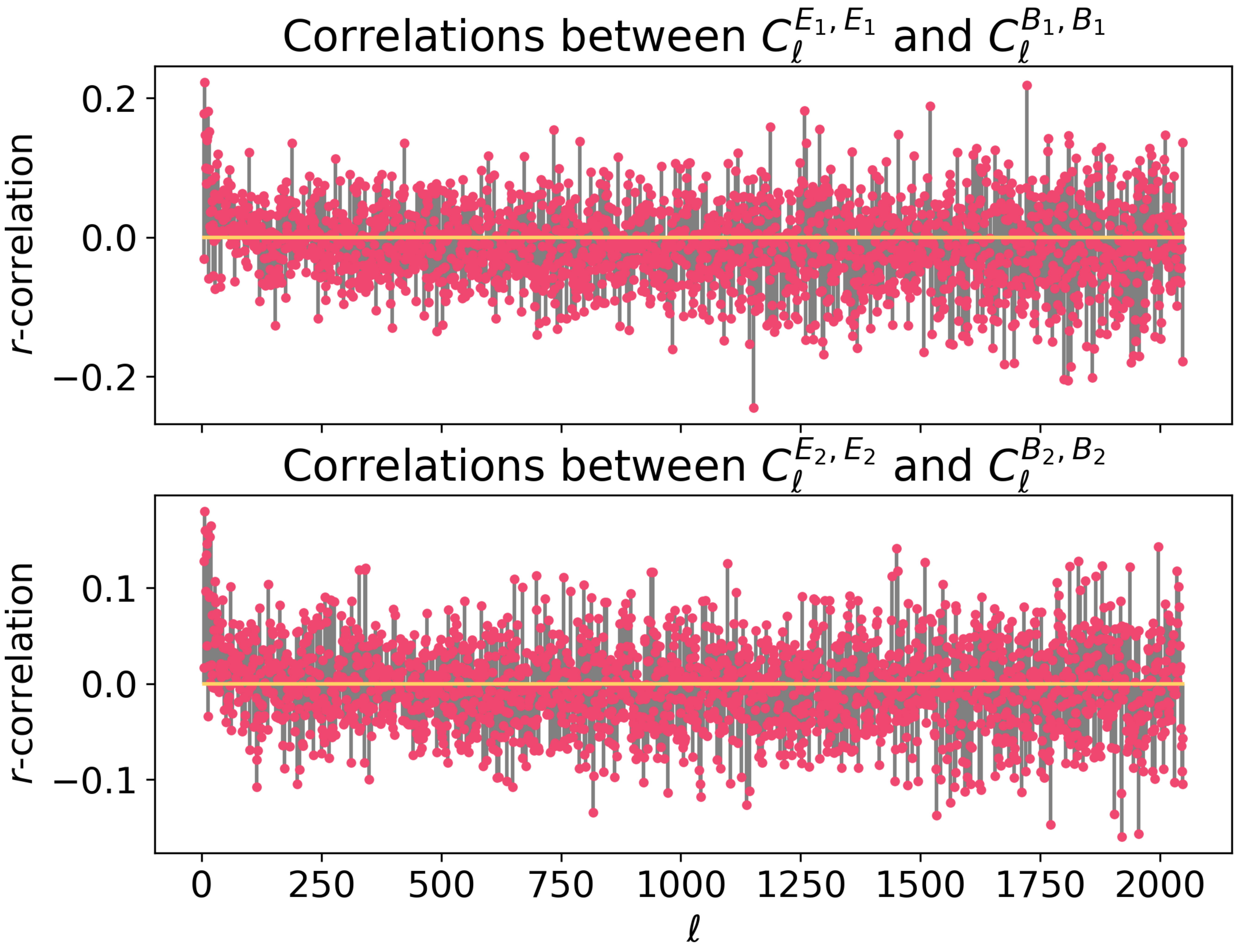

Loureiro et al., OJA,. 2023 (ArXiv:2210.13260)

Weak Lensing

Inferred shear maps

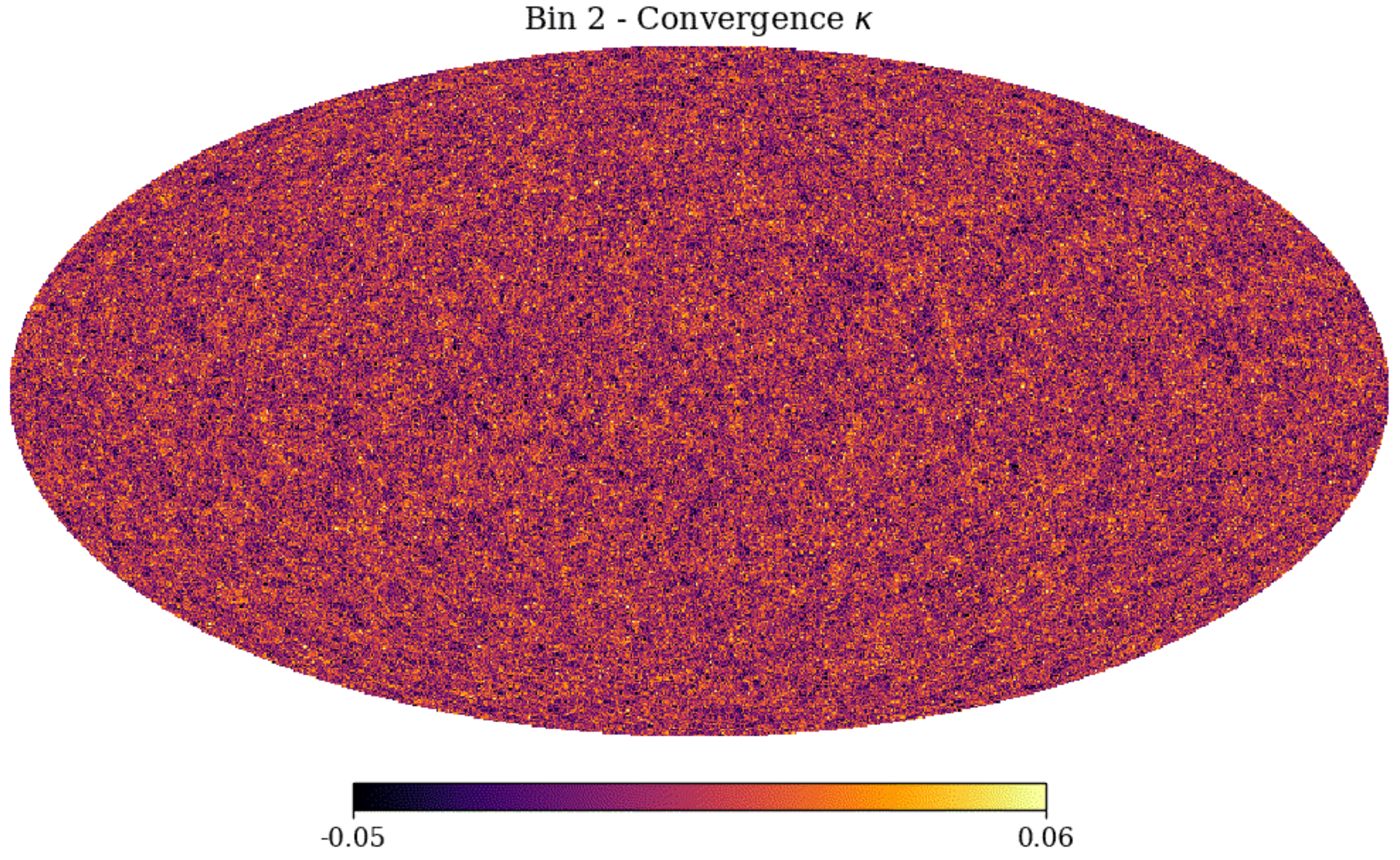

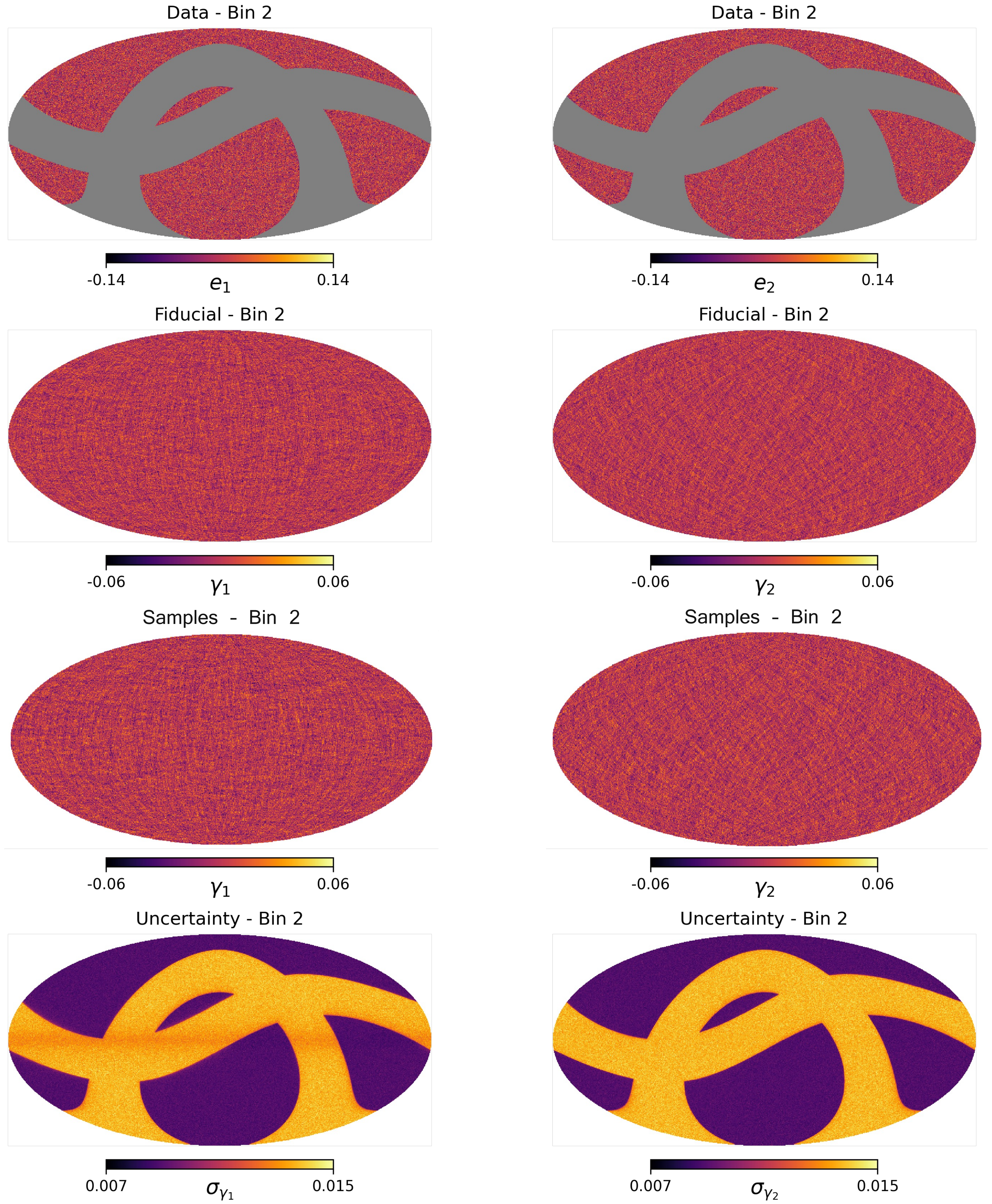

Loureiro et al., OJA,. 2023 (ArXiv:2210.13260)

Weak Lensing

Reconstructed Lensing Potential

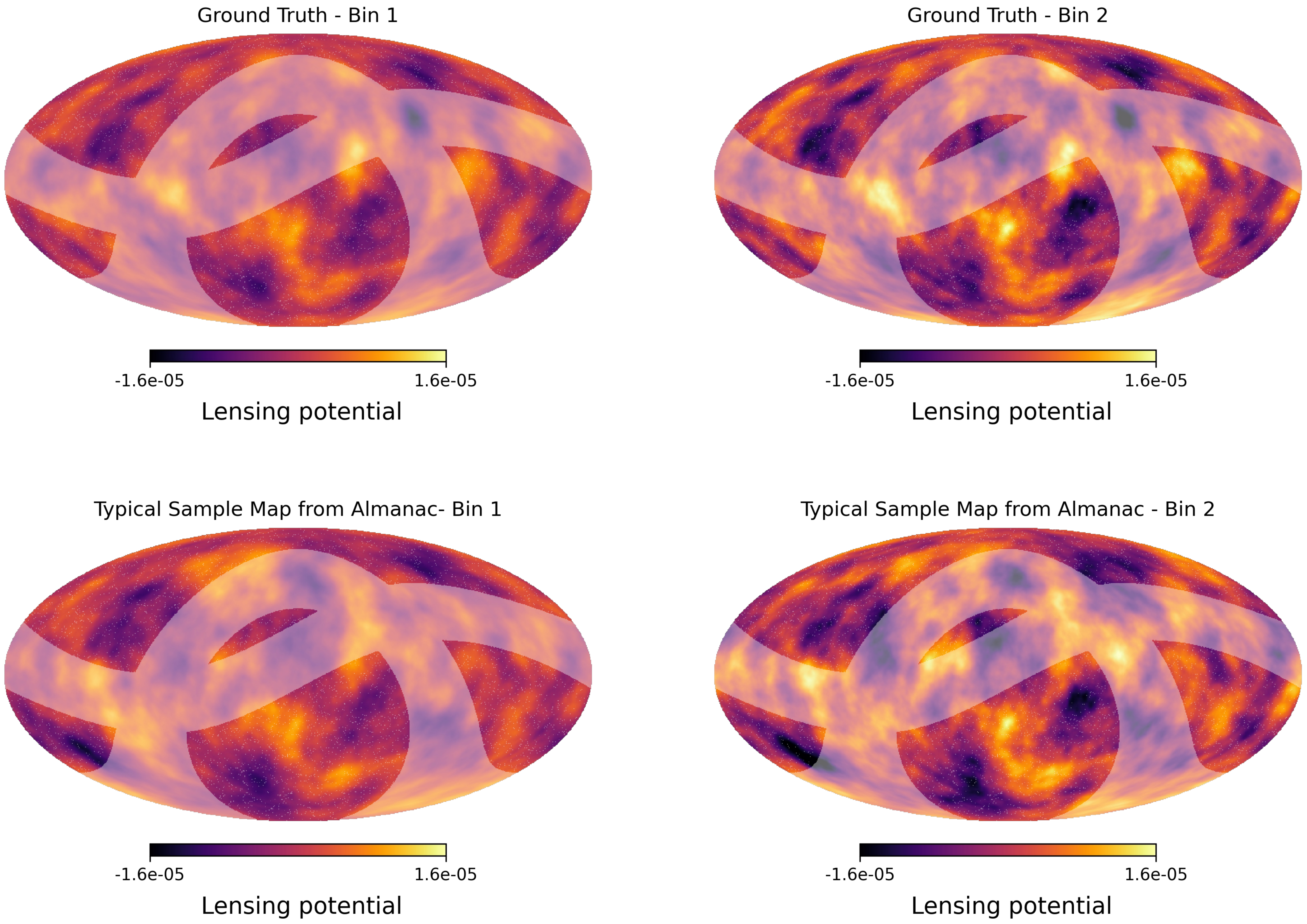

Loureiro et al., OJA,. 2023 (ArXiv:2210.13260)

Weak Lensing

Map consistency check

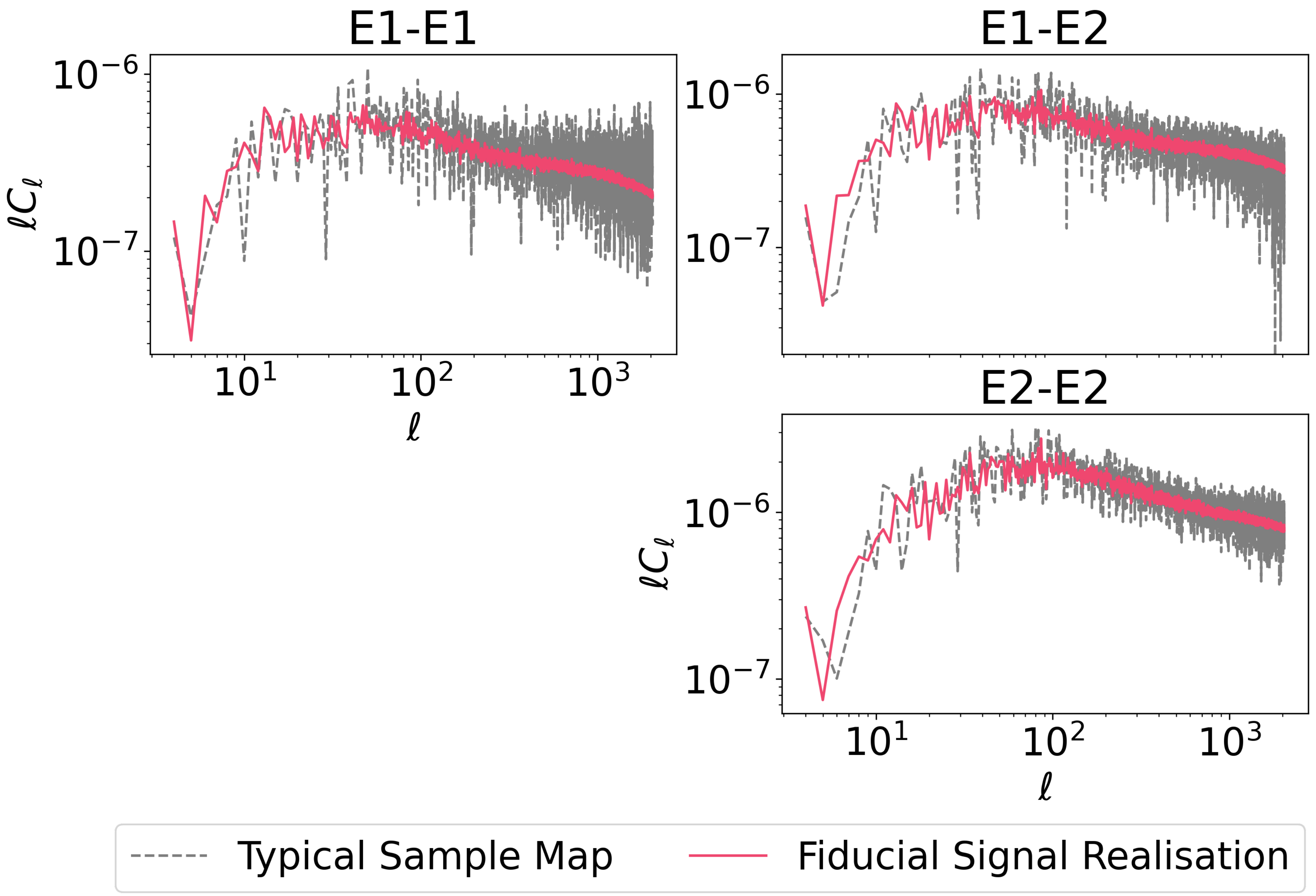

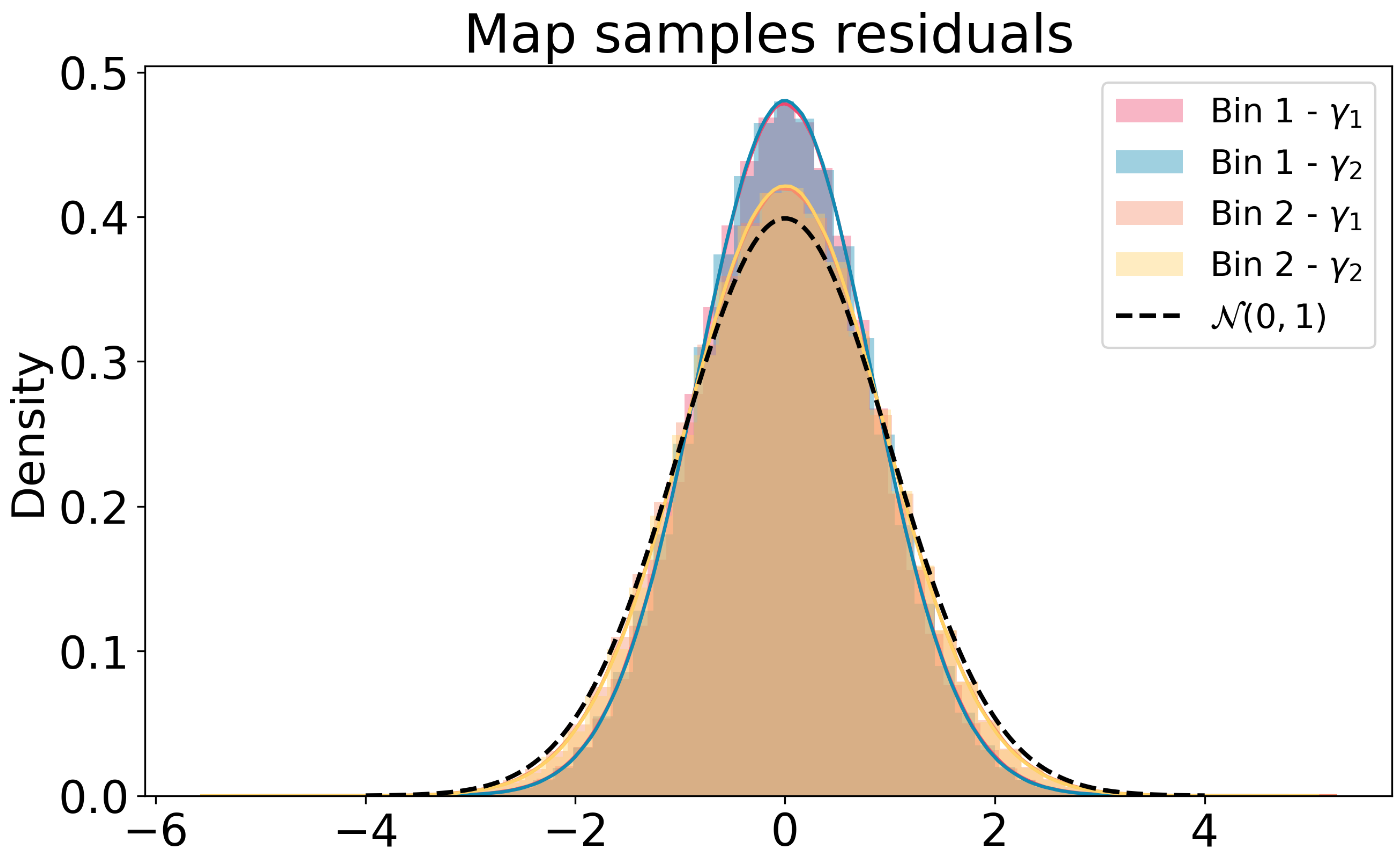

Loureiro et al., OJA,. 2023 (ArXiv:2210.13260)

6. Convergence Testing

All diagnostics we carried out…

Convergence Diagnostics

Posterior Trace Analysis

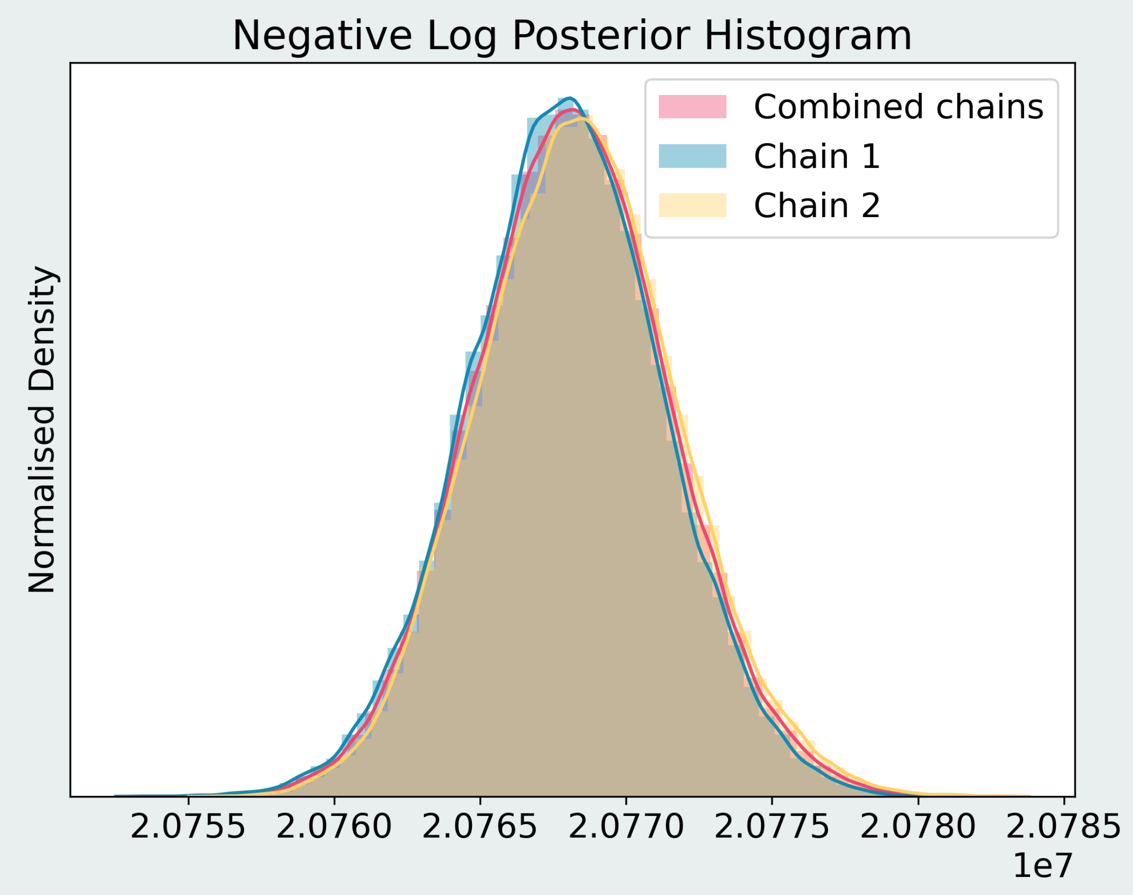

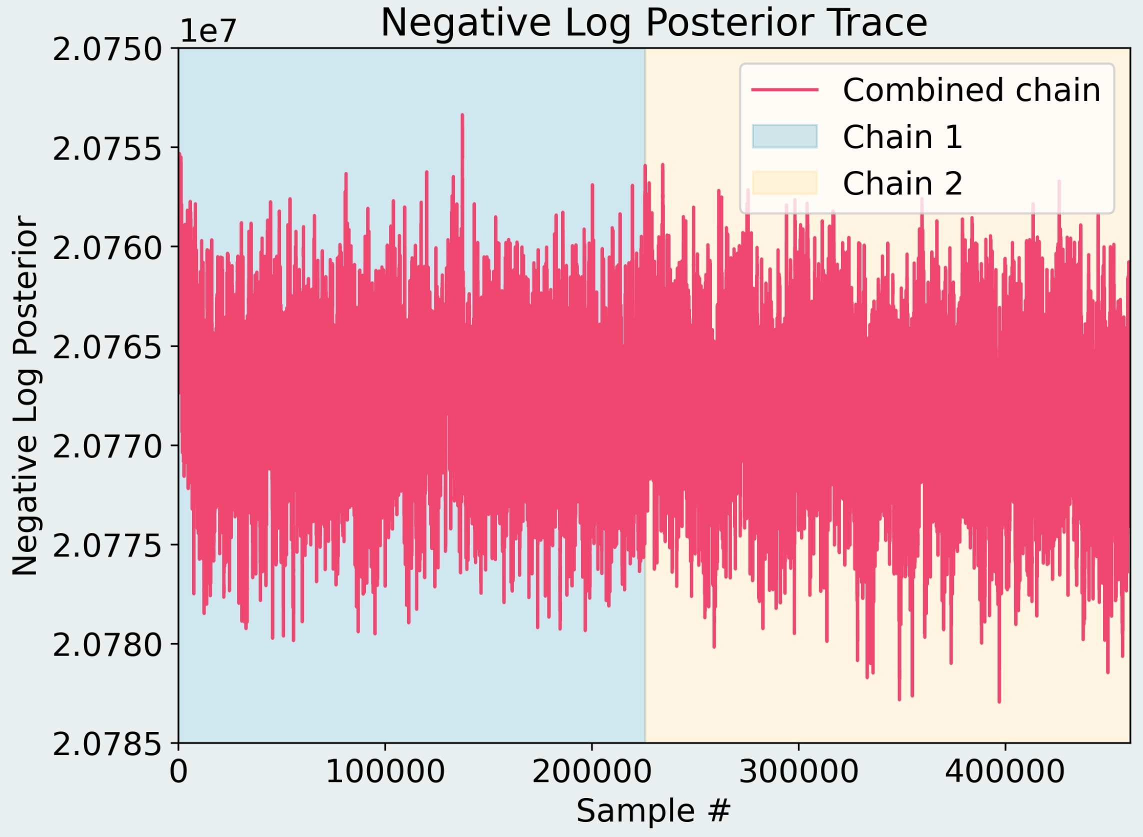

Fraction of Missing Info

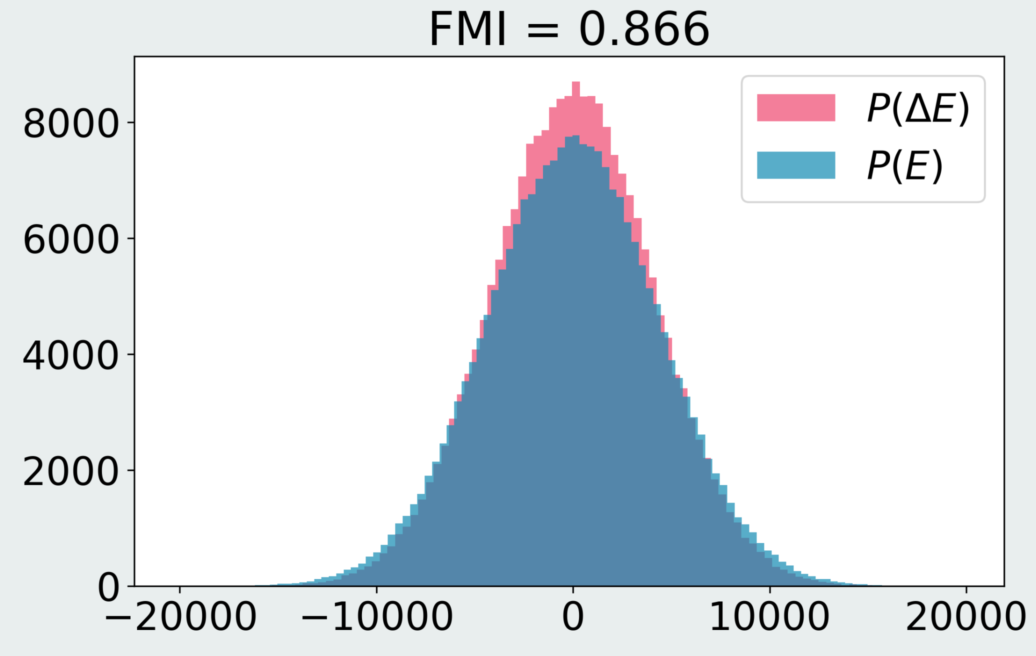

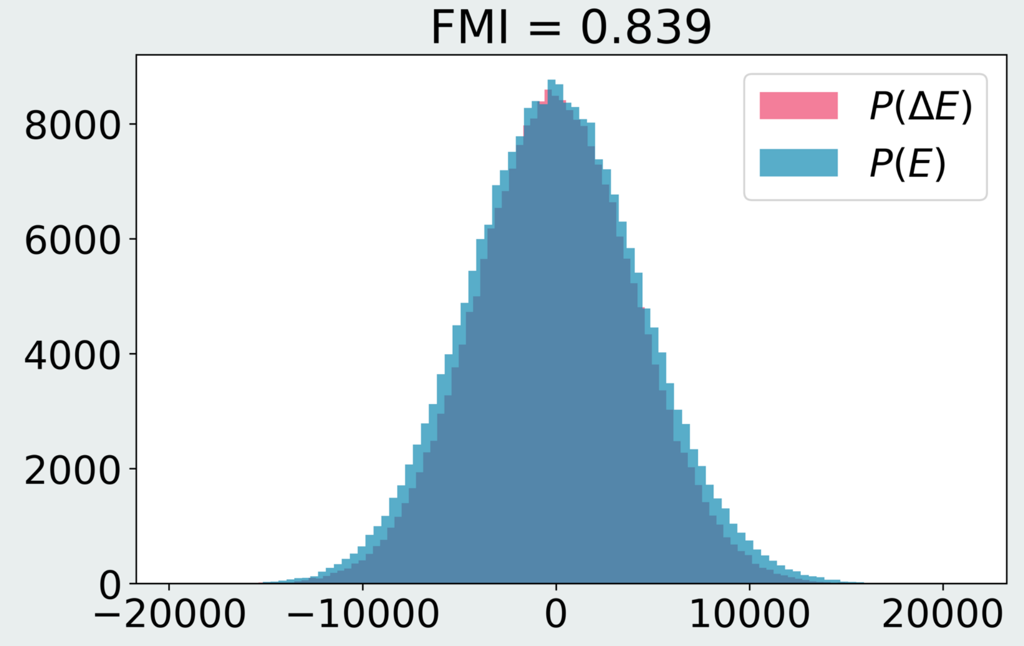

$$\mathrm{FMI} = \frac{\sum_{n=1}^{N}(E_n - E_{n-1})^2}{\sum_{n=0}^{N}(E_n - \bar{E})^2}$$

Hanson Diagnostics

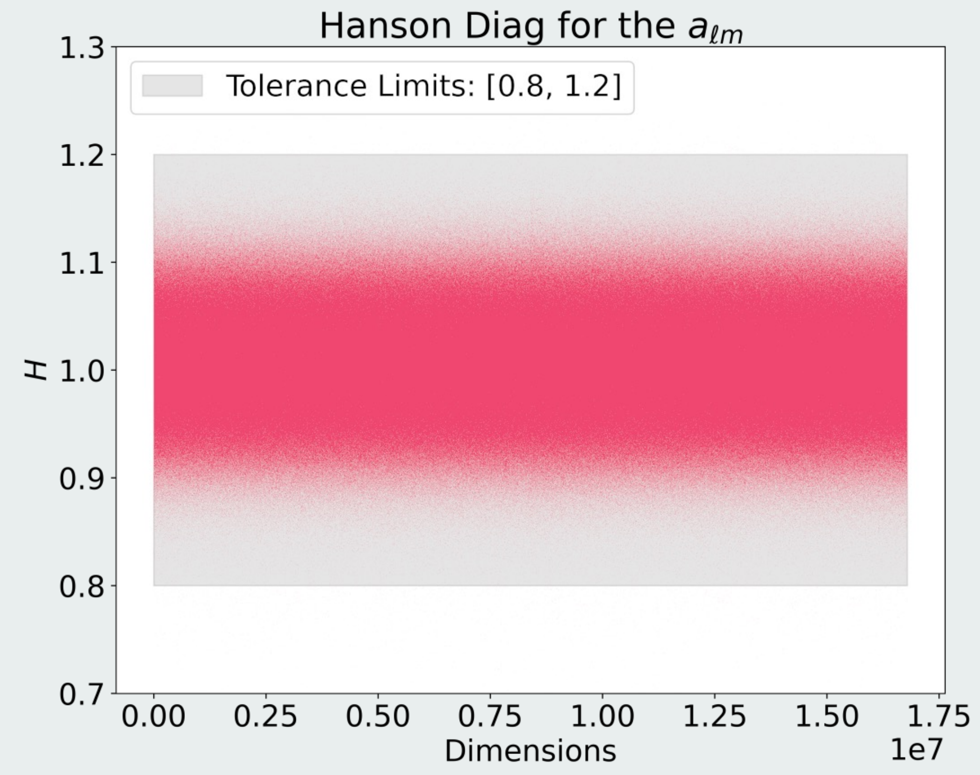

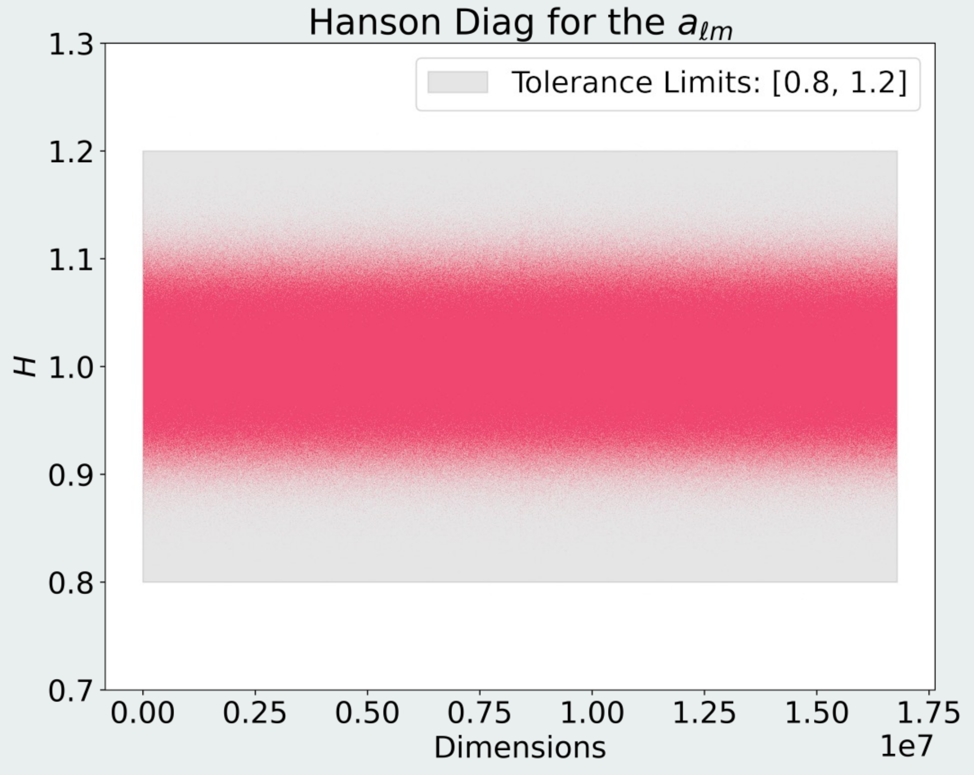

$$\mathcal{H}_i = \frac{\frac{1}{N}\sum_{n=1}^{N}(x_{n,i} - \bar{x}_i)^2}{\frac{1}{3N}\sum_n (x_{n,i} - \bar{x}_i)^3 \nabla_{x_i}\psi}$$

Gelman Rubin Test

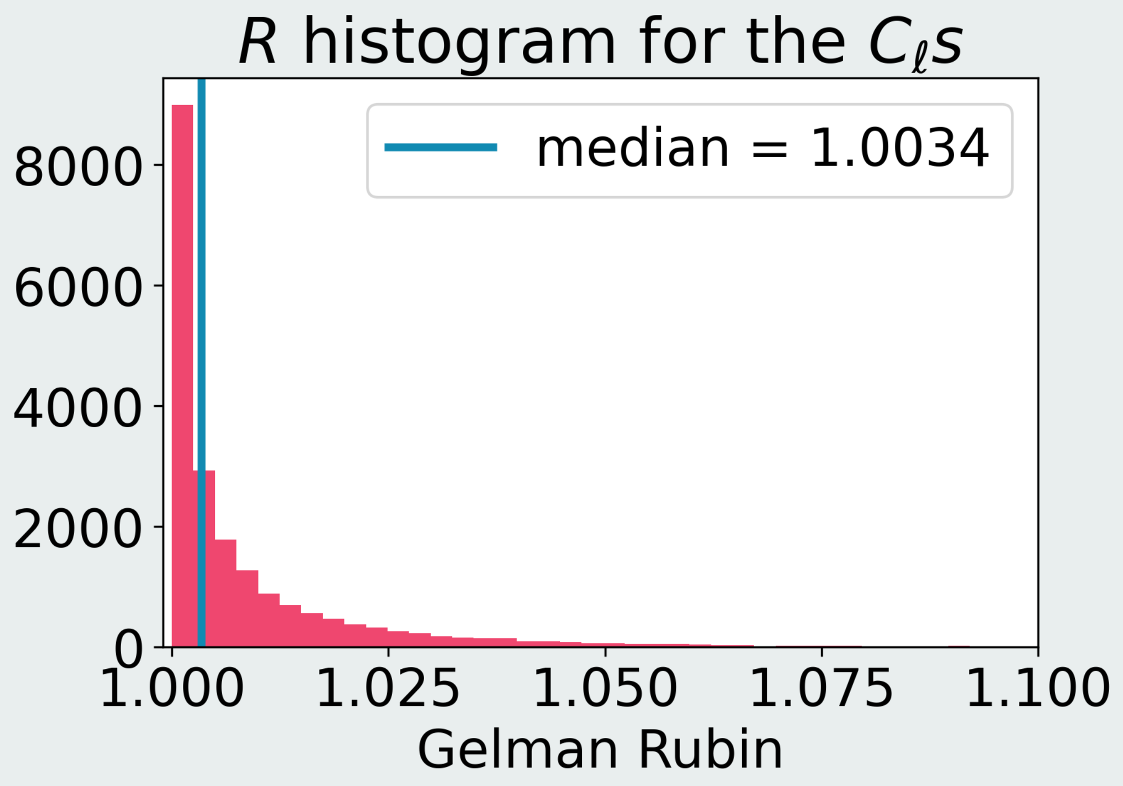

Correlation Length

Chain 1: 3042
Chain 2: 2585
Total samples: 2.25×10^5
Effective sample size: 165

Loureiro et al., OJA,. 2023 (ArXiv:2210.13260)

7. Conclusions & Next Steps

What we achieved and where are we going from here?

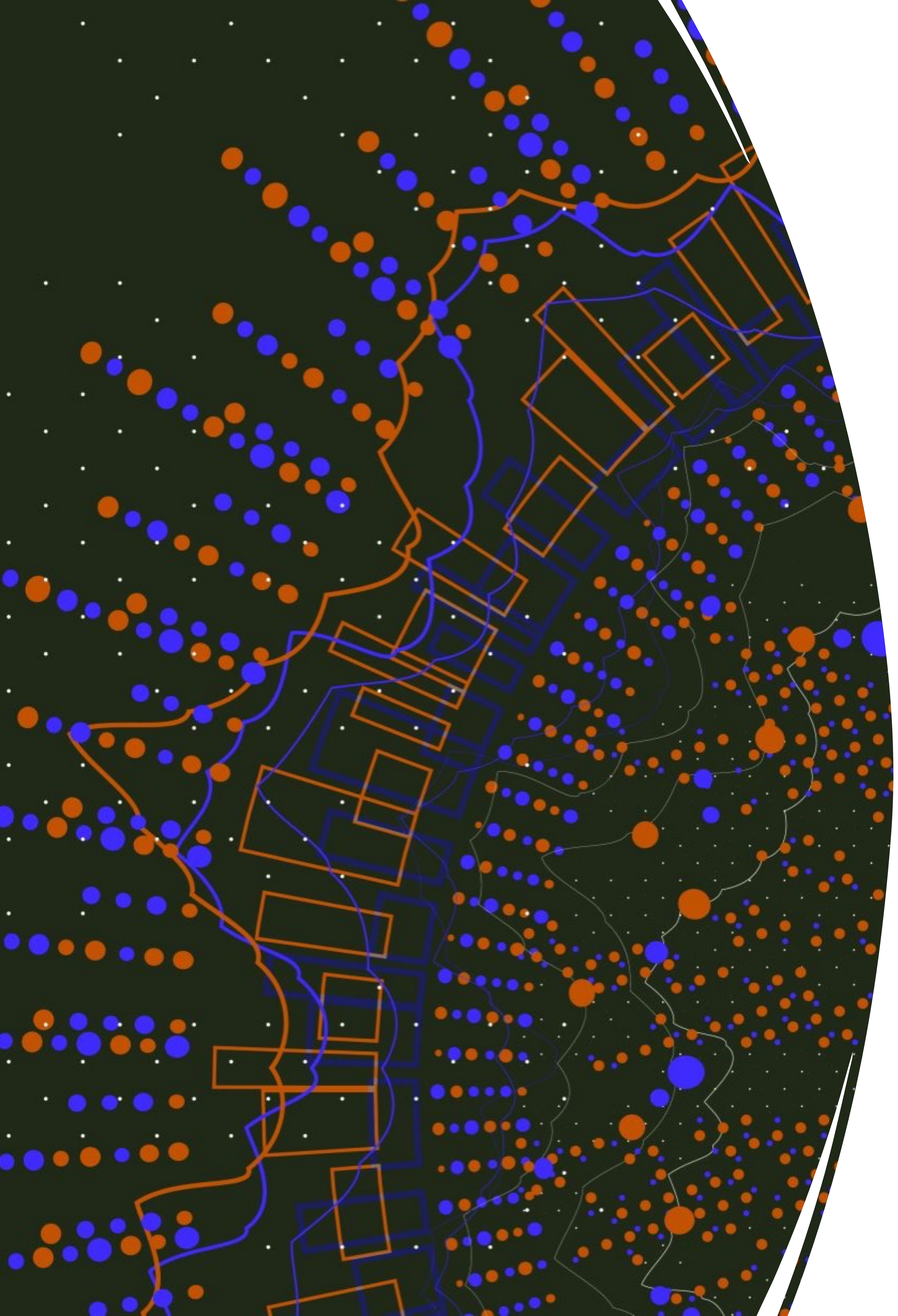

Summary

- Next Gen Surveys require Next Gen Cosmological Analysis
- Field Level Inference is an optimal way to extract cosmological information for upcoming cosmological surveys
- Almanac can recover the full sky posterior of high-resolution maps and angular power spectra (lmax = 2048!)
- We retain the ability to perform systematic contamination checks: EB “leakage”, B-modes, and more
- We can optimally (by construction) infer the largest scales accessible in Euclid/LSST, including their full marginalised posterior
- We can now also infer (aka have an educated guess) mass maps where surveys will not even observe!

Next:

- **A background paper on our new sampler with applications to CMB simulations is on the way.**
- Applications to Stage III Survey Data
- Cosmological analysis from point estimates (by Javier Lafaurie)
- Cosmological analysis using normalising flows
- Primordial non-gaussianities with Weak Lensing Fields

Thanks!

arthur.loureiro@fysik.su.se

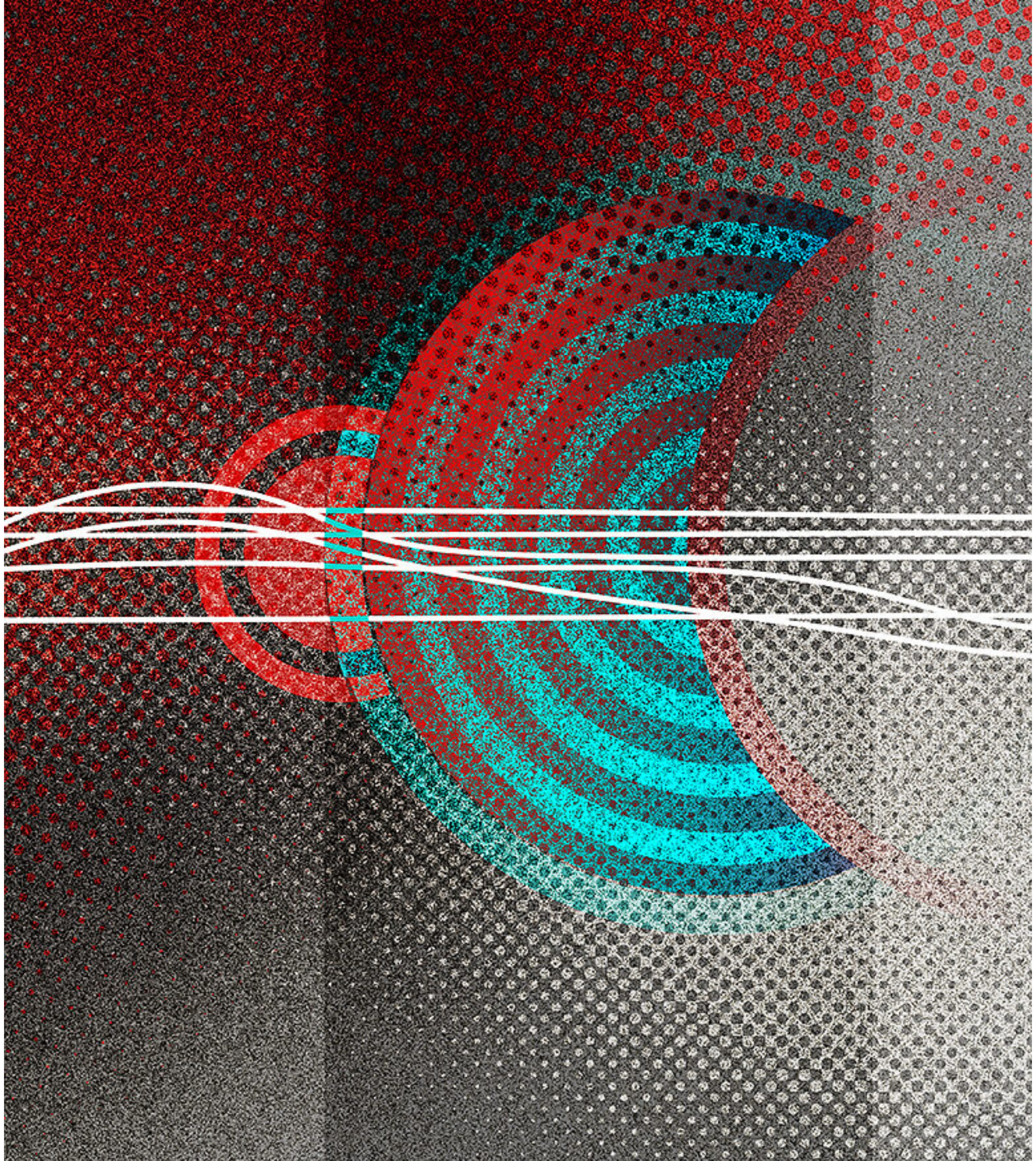

CMB Temperature

Low Signal-to-noise case

- Temperature-only
- Single channel simulation
- Multipole range: 2, 1024
- Nside: 512 (3.14M pixels)
- Noise level: 1e-6 K/pixel
- WMAP-Like Mask

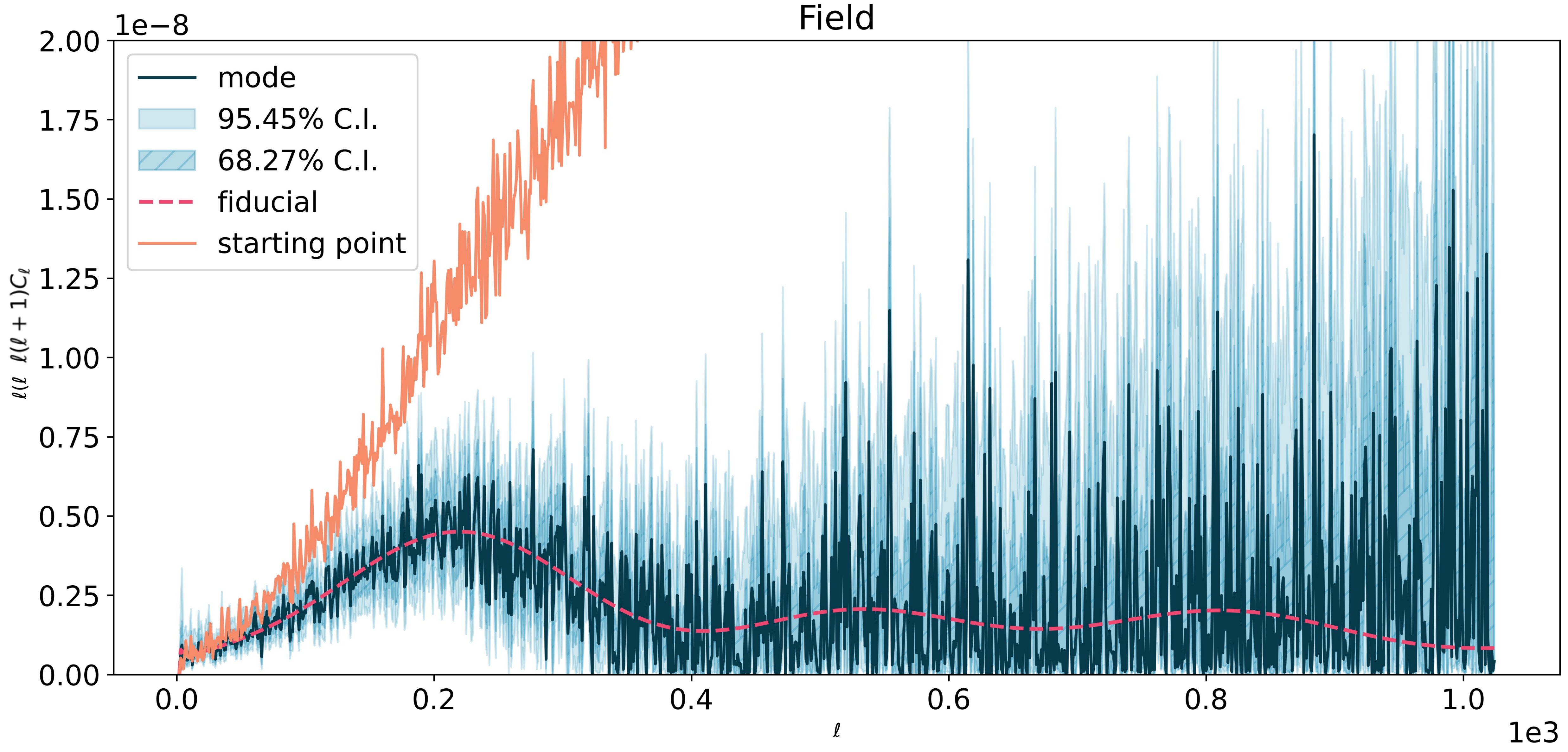

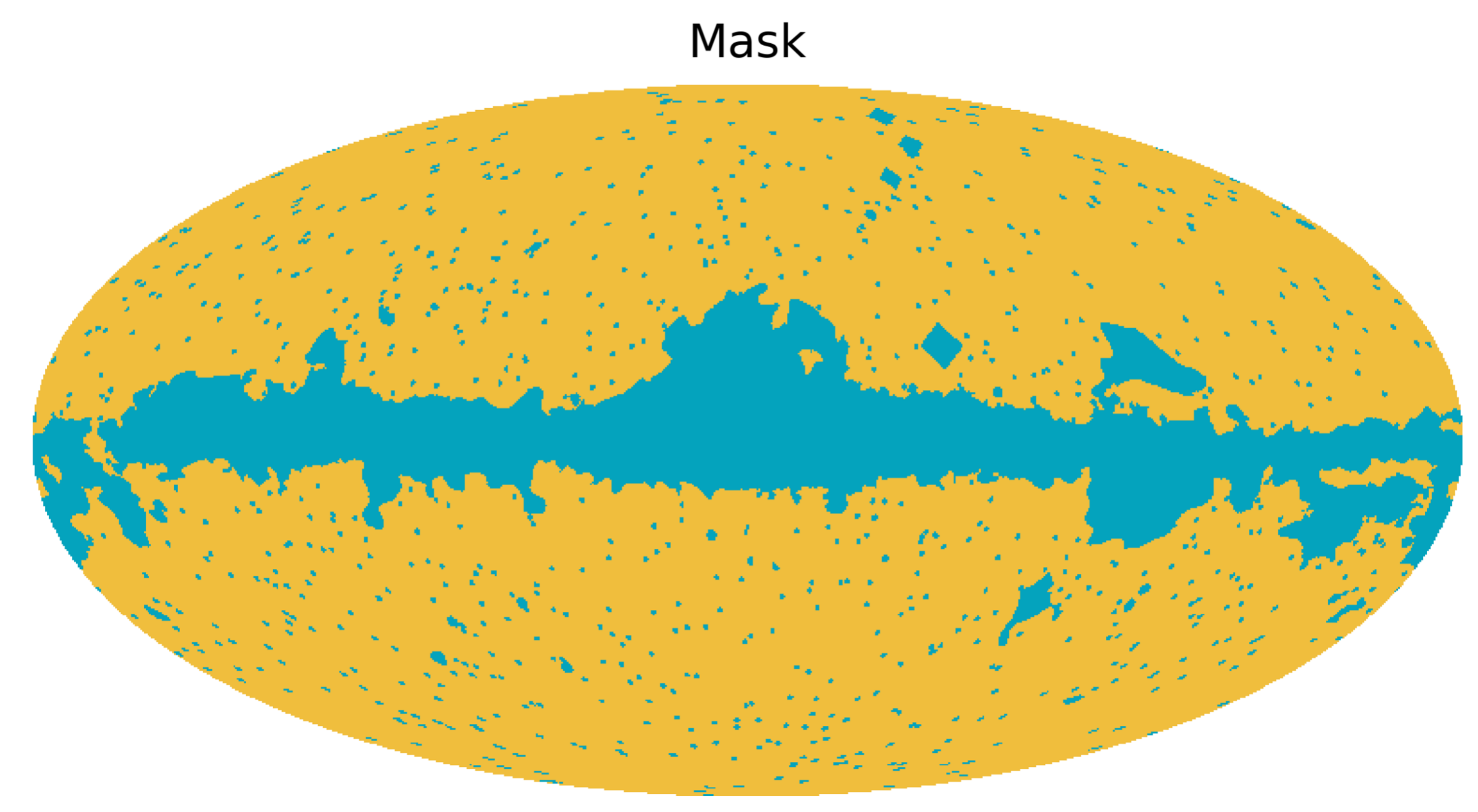

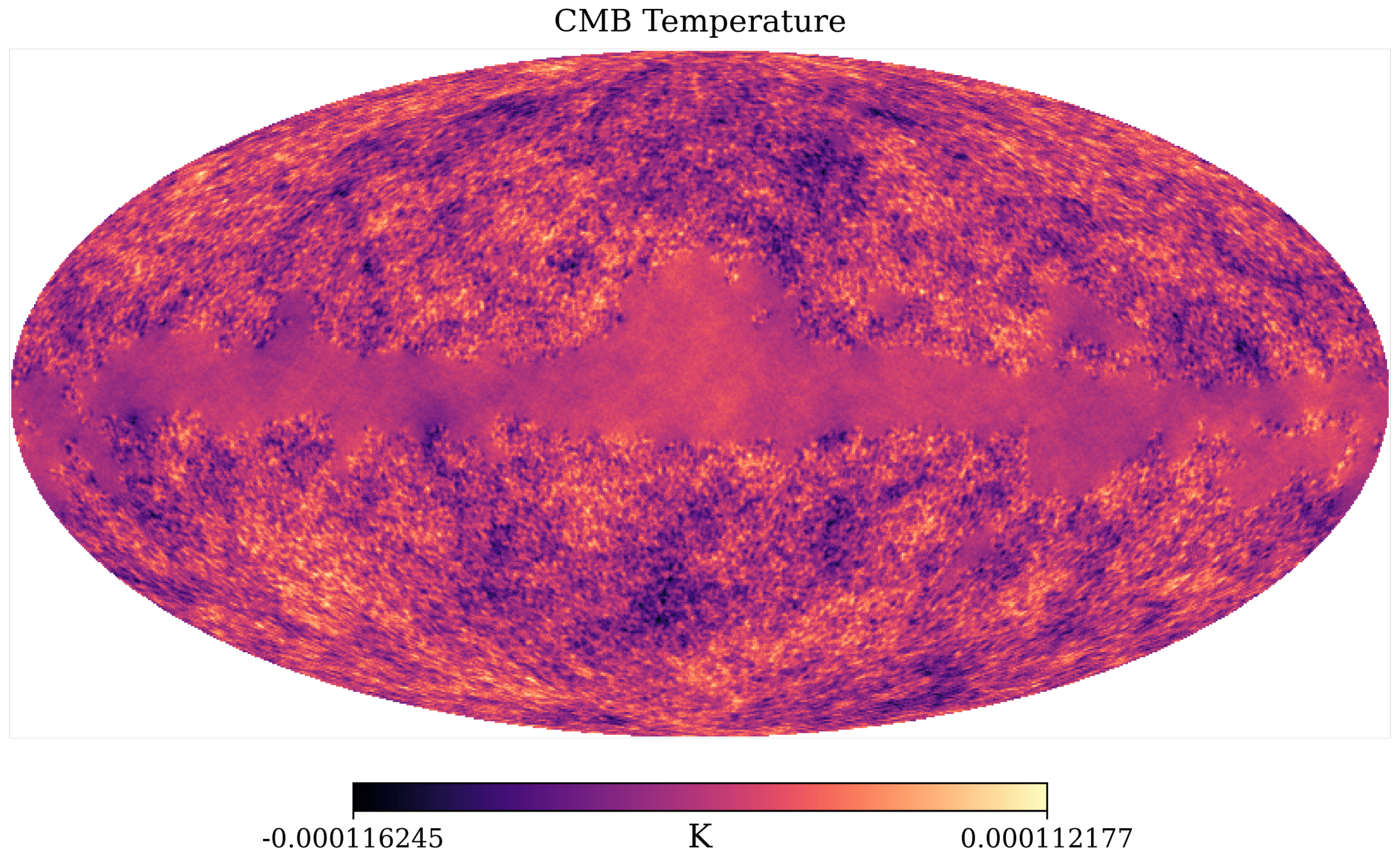

Mean Map from the samples

Sellentin, Loureiro et al. *in prep*

CMB Polarisation

Mid Signal-to-noise

- Polarisation only, no EB-cross
- Single channel simulation
- Multipole range: 2, 1024
- Nside: 512 (3.14M pixels)
- Noise level: 2e-6 K / pixel
- WMAP-Like Mask

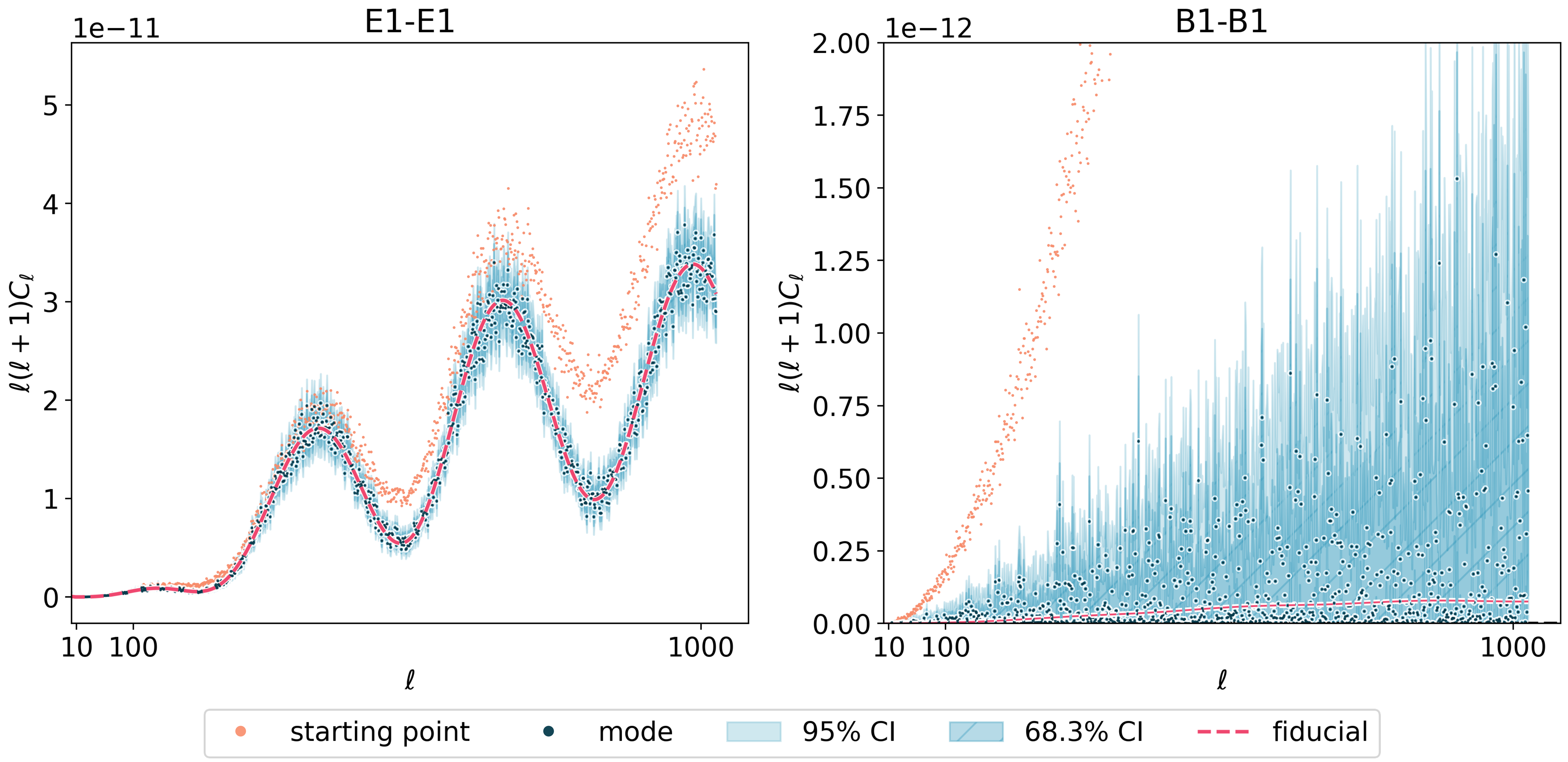

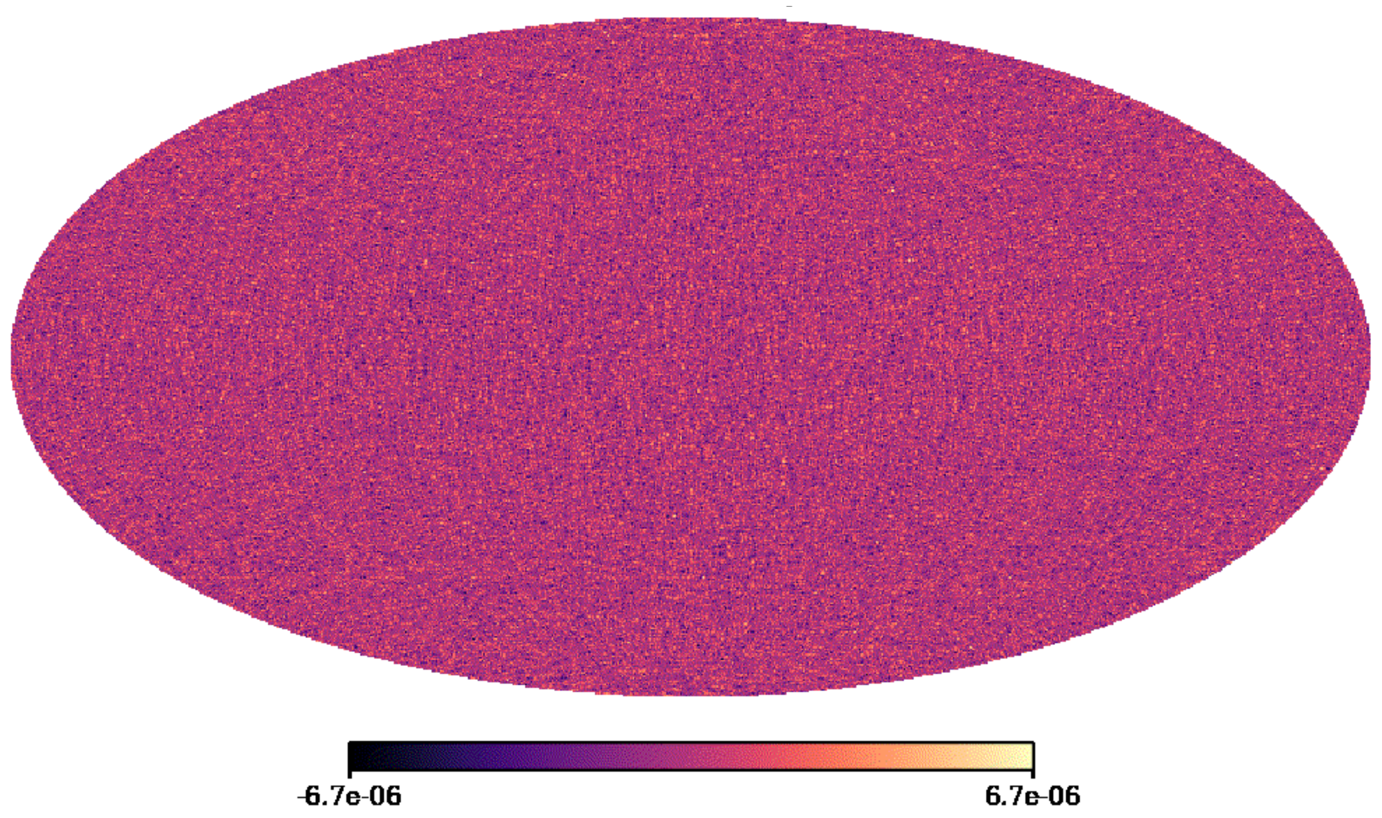

Q

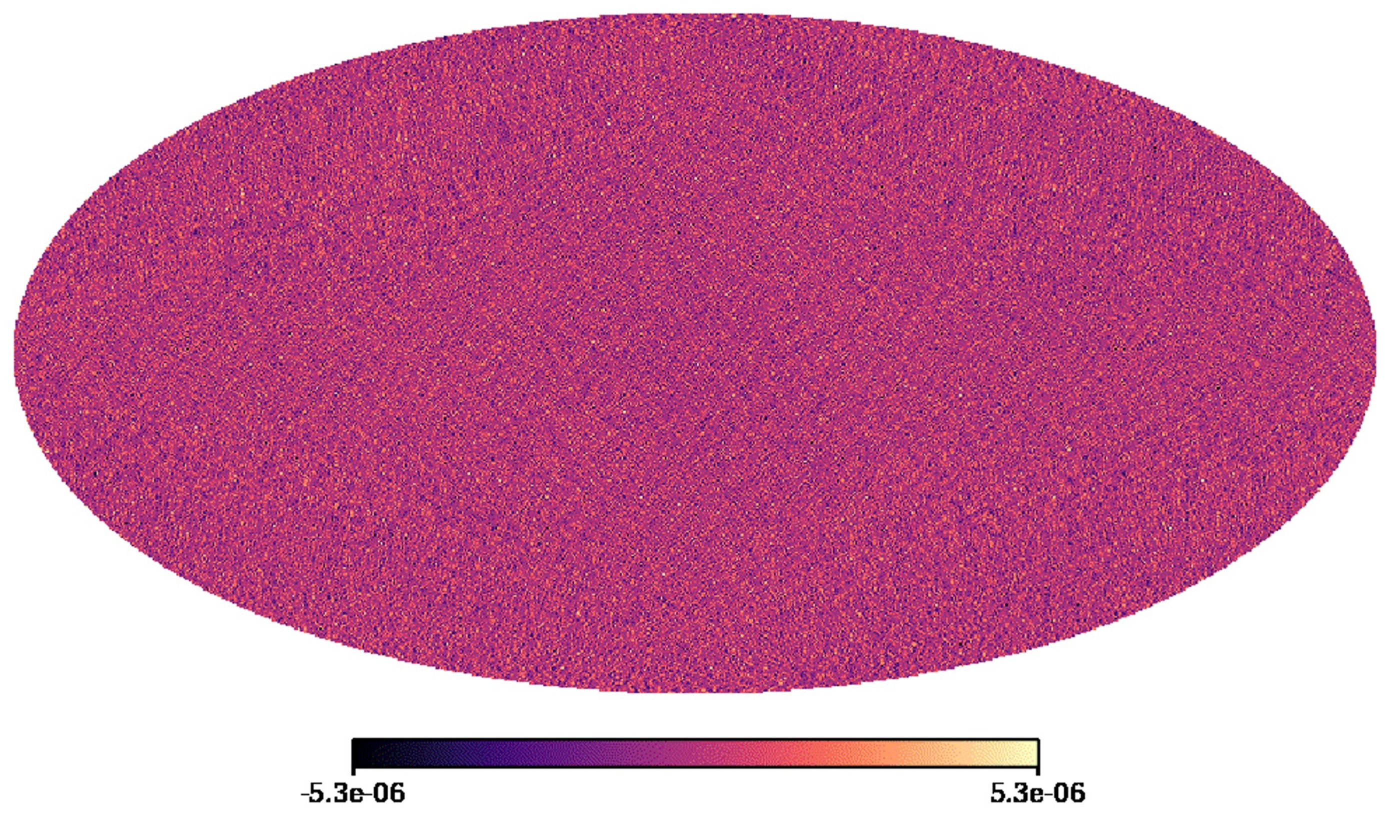

U

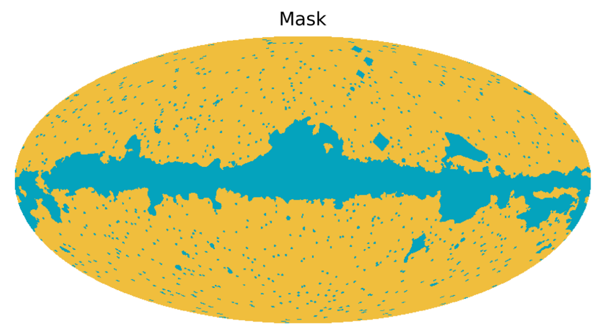

Sellentin, Loureiro et al. *in prep*